Stony Brook University

The DNA Damage Response: p53 Regulation of the CHK1-Suppressed Pathway and Sphingolipid Metabolism

A Dissertation Presented

by

Brittany Carroll

to

The Graduate School

in Partial Fulfillment of the

Requirements

for the Degree of

Doctor of Philosophy

in

Molecular and Cellular Biology

(Concentration – Biochemistry and Molecular Biology)

Stony Brook University

May 2015

Stony Brook University

The Graduate School

Brittany Carroll

We, the dissertation committee for the above candidate for the

Doctor of Philosophy degree, hereby recommend

acceptance of this dissertation.

Lina Obeid, M.D. – Dissertation Advisor
Dean of Research, Professor of Medicine, School of Medicine

Kenneth Shroyer, M.D, Ph.D
Marvin Kushner Professor and Chair, Department of Pathology, School of Medicine

Yusuf Hannun, M.D.
Director of Stony Brook Cancer Center, Vice Dean of Cancer Medicine, Joel Kenny Professor of Medicine, School of Medicine

Michael Frohman, M.D, Ph.D
Director Stony Brook Medical Scientist Training Program, Professor and Chair, Department of Pharmacological Sciences

Sumita Bhaduri-McIntosh, M.D, Ph.D
Associate Professor, Departments of Pediatrics, Molecular Genetics and Microbiology

This dissertation is accepted by the Graduate School
Charles Taber
Dean of the Graduate School

Abstract of the Dissertation

The DNA Damage Response: p53 Regulation of the CHK1-Suppressed Pathway and Sphingolipid Metabolism

by

Brittany Carroll

Doctor of Philosophy

in

Molecular and Cellular Biology

(Concentration – Biochemistry and Molecular Biology)

Stony Brook University

2015

The DNA damage response (DDR) is a complex and interconnected signaling network that dictates whether a cell repairs itself and survives or is damaged beyond repair and eliminated; therefore the proteins in this network must be tightly regulated in order to ensure genomic integrity. Conversely, mutational or epigenetic inactivation of DDR components leads to genomic instability, a hallmark of cancer. Indeed there is a high frequency of DDR defects in human cancers of which mutations in the DDR effector and tumor suppressor protein p53 are the best characterized and occur in greater than 50% of all human cancers. Interestingly, a novel DDR pathway has emerged termed the CHK1-Suppressed (CS) pathway that is activated by inhibition or loss of the cell cycle kinase CHK1, leading to an apoptotic response to DNA damage in the presence of mutant p53 that is mediated by the protease Caspase 2. Although the functions of the CS-pathway have been probed through pharmacological inhibition and siRNA knockdown it remains unclear whether and how CHK1 inhibition can be regulated endogenously. Recently, we characterized the first endogenous activation of the CS-pathway, demonstrating that upon DNA damage wild type p53 acts an endogenous regulator of CHK1

levels that modulates Caspase 2 activation and ultimately controls cell fate. Moreover, we demonstrate that CHK1 levels persist in response to DNA damage in mutant p53 cancer cells, leading to CHK1-mediated activation of the pro-survival transcription factor NF-κB and induction of a pro-inflammatory response that is abrogated by loss or inhibition of CHK1. These data constitute a novel role for CHK1 in response to DNA damage outside of the cell cycle in regulating inflammation. Lastly we identify the lipid kinase Sphingosine Kinase 1 (SK1), whose kinase activity produces the pro-survival lipid mediator Sphingosine 1-Phosphate (S1P) as the first identified effector of the CS-pathway; whereby activation of the CS-pathway leads to SK1 proteolysis and decreases in cellular S1P levels in response to DNA damage. These data have important clinical applications as many CHK1 inhibitors are in clinical trials and our data provide evidence that targeting CHK1 in mutant p53-mediated cancers may abrogate NF-κB and SK1 signaling both of which are associated with increased cellular survival and chemoresistance.

Dedication Page

To my two biggest inspirations, my loving parents. Mom and dad without your never-ending love and support none of this would have been possible. Thank you for always encouraging me to pursue my dreams and believing in me no matter what.

Table of Contents

List of Figures

List of Supplemental Figures

List of Illustrations

List of Tables

List of Abbreviations

AC	Acid Ceramidase
AP	Abasic Site
Apaf-1	Apoptotic Protease Activating Factor 1
ATM	Ataxia Telangiectasia Mutated
ATR	Ataxia Telangiectasia Mutated and Rad3-related Protein
ATRIP	ATR interacting protein
BER	Base Excision Repair
BIFC	Bimolecular Florescence Complementation
BMP4	Bone Morphogenetic protein 4
BRCA1	Breast Cancer 1, Early Onset
BRCA 2	Breast Cancer 2, Early Onset
CARD	Caspase Recruitment Domain
CDase	Ceramidase
Cer	Ceramide
CerS	Ceramide Synthase
CHK1	Checkpoint Kinase 1
CHK2	Checkpoint Kinase 2
CDK	Cyclin-Dependent Kinase
CS-Pathway	CHK1-Suppressed Pathway
DD	Death Domain
DDR	DNA Damage Response
DSB	Double-Strand Breaks
DSBR	Double-Strand Break Repair
GG-NER	Global-Genome Nucleotide Excision Repair
HR	Homologous Recombination
IL6	Interleukin 6
IL8	Interleukin 8
MDM2	Mouse Double Minute 2

MRN	MRE11-RAD50-NBS1
NC	Neutral Ceramidase
NER	Nucleotide Excision Repair
NEMO	NF-κB Essential Modulator
NF-κB	Nuclear Factor Kappa-Light-Chain-Enhancer of Activated B Cells
NHEJ	Non-Homologous End Joining
p53AIP1	P53-Regulated Apoptosis-Inducing Factor
PIDD	P53-Induced Protein with a Death Domain
PUMA	P53 Upregulated Modulator of Apoptosis
RAIDD	RIP Associated Ich-1/CED Homologous Protein with Death Domain
ROS	Reactive Oxygen Species
RPA	Replication Protein A
S1P	Sphingosine 1-Phosphate
S1PL	Sphingosine 1-Phosphate Lyase
SK1	Sphingosine Kinase 1
SK2	Sphingosine Kinase 2
SM	Sphingomyelin
SM1	Small Molecule Inhibitor
Smase	Sphingomyelinase
Sph	Sphingosine
SL	Sphingolipid
SPPase	Sphingosine 1-Phosphate Phosphatase
SSB	Single-Strand Breaks
ssDNA	Single-Strand DNA
TC-NER	Transcription-Coupled Nucleotide Excision Repair
TMV	Tumor-derived Microvesicles
TNBC	Triple Negative Breast Cancers
TNFR	Tumor Necrosis Factor Receptor
UV	Ultraviolet Light
VEGF	Vascular Endothelial Growth Factor
XP	Xeroderma Pigmentosum

Acknowledgments

This body of work would not have been possible without the support of so many individuals. I would like to take this opportunity to acknowledge and thank this special group of people.

First and foremost, I would like to thank my family, who have been my biggest supporters and inspiration throughout my life and graduate school. Thank you mom and dad for instilling the importance of education and hard work at a very young age and for being my biggest fans throughout all my endeavors. To my sisters, Madeline and Sarah Margaret, thank you for always being a phone call away whenever I need to talk. You two are such inspiring role models that I am so thankful for. To my sweet nephews and nieces thank you for being so adorable and always putting a smile on my face. To my sweet Kelsie, our long walks are one reason I made it through graduate school. You truly are a great companion. All my accomplishments are possible because of the love and support from all of you.

Second I would like to thank my mentor Dr. Obeid. I knew as soon as I met you I wanted to join your lab and I have never once regretted that. You are an amazing role model and embody what a true mentor and scientist should be. You always pushed me to be the best I could be and for that I will be forever grateful. You are not only a great mentor but an amazing friend who has given me great advice about life and who I knew I could always count on no matter what. I am truly grateful to have you in my life as a mentor, friend and role model. During graduate school, I was lucky enough to have not one amazing mentor but two. Thank you Dr. Hannun for always inspiring and pushing me to be the best scientist I could be. I admire your passion for science and discovery and for always making time for students even with a hectic schedule.

Next I would like to thank my amazing friends. Thank you Megan and Ashley for being the best two friends a girl could ask for and for always being there no matter what. Love you to the moon and back. Thank you Adada, Mel Pilar and Justin for all the amazing adventures. My life would not be the same without you three. Thanks Cat and MPG for always being up for wine down Wednesdays. Thank you Ashley and Justin for being amazing friends and making

delicious wine and night caps. Thank you Janet for everything you do and for always being there when I needed to talk. Ana, Megan, Rose and Kelly, my bookclub girls, I am so thankful I meet you all. You four are amazing and inspiring women and I happy to call you friends. Thank you for making my transition to New York that much easier.

I would also like to thank all the members of Dr. Obeid and Dr. Hannun's lab. Thank you all for help, support and guidance over the years.

Last but not least, I would like to thank my committee members. First, thank you all so much for dedicating your time to be apart of my PhD despite very busy schedules. Second, I am very grateful for all your guidance and support over the past couple of years. I am very lucky to be surrounded by such an inspiring and accomplished group of people. Thank you all for believing in me.

Vita, Publications and/or Fields of Study

Brittany L. Carroll
5-4A President's Drive
Port Jefferson, NY 11777
910-591-9928
brittany.carroll@stonybrook.edu

Education

07/2012-present **Stony Brook University** Stony Brook, NY
Doctoral Degree
Molecular and Cellular Biology
Lina Obeid, M.D.

08/2010-06/2012 **Medical University of South Carolina** Charleston, SC
Doctoral Degree (transferred)
Biochemistry and Molecular Biology
Lina Obeid, M.D.

07/2005-12/2007 **East Carolina University** Greenville, NC
Bachelors of Science in Biology, Graduated *cum laude*

08/2003-06/2005 **Presbyterian College** Clinton, SC
Bachelors of Science in Biology (transferred)

Research Experience

07/2012-present **Stony Brook University** Stony Brook, NY
Predoctoral Researcher, Department of Molecular and Cellular Biology
"Sphingolipids Role in Cancer Biology"

08/2010-06/2012 **Medical University of South Carolina** Charleston, SC
Predoctoral Researcher, Department of Biochemistry and Cellular Biology
"Sphingolipids Role in Cancer Biology"

07/2009-08/2010 **Medical University of South Carolina** Charleston, SC
Research Specialist, Department of Craniofacial Biology
"Regulation of mRNA stability mechanisms in oral cancer progression"

01/2008-07/2009 **East Carolina University** Greenville, NC
Research Specialist, Department of Microbiology and Immunology
"Optimization of rapid detection systems to combat biological warfare"

01/2007-01/2008 **East Carolina University** Greenville, NC
Honors Undergraduate Internship, Department of Microbiology and Immunology
"Identification of novel small non-coding RNAs in *brucella abortus"*

Awards

Best Presentation Award recipient
International Ceramide Conference/Sphingolipid Club, 2015

Ruth L. Kirschstein National Research Service Award (F31) recipient
National Institutes of Health (National Cancer Institute), 2014
Amount awarded $68,370

Sangtosh Nigam Outstanding Young Scientist Award Finalist
Bioactive Lipids in Cancer, Inflammation and Related Disease, 2013

Travel award recipient
International Ceramide Conference, 2013

Ralph H. Johnson VAMC Student Research Award, Charleston Research Institute, 2011

Graduate Assistance in Areas of National Need (GAANN) Fellowship Recipient
MUSC, 2011

Travel Award Recipient
Charleston Ceramide Conference, 2011

Dean's Scholarship Recipient
MUSC, 2010

Activities

President, Graduate Career Association, Stony Brook University, 2014-2015

Executive Committee Member, Graduate Career Association
Stony Brook University, 2013

Judge, Long Island Science and Engineering Fair
Westbury, NY, 2013-2014

Publications

Carroll B, Shamseddine A, M, Hannun YA, Obeid LM
Caspase 2 is Required for Sphingosine Kinase 1 Proteolysis: Implications to the CHK1-Suppressed Pathway. Submitted and in revision

Carroll B, Polouski-Gross M, Donaldson J, Hannun YA, Obeid LM

Defining a novel role for Checkpoint Point Kinase 1 in Inflammation. In Preparation.

Achraf A. Shamseddine, Christopher J. Clarke, **Brittany Carroll**, Michael V. Airola, Antonella Rella, Lina M. Obeid, Yusuf A. Hannun
Neutral sphingomyelinase-2 is the primary neutral sphingomyelinase activated by Doxorubicin via a p53-dependent mechanism. In Preperation

Salama MF, **Carroll B**, Adada M, Pulkoski-Gross M, Hannun YA, Obeid LM.
A Novel Role of Sphingosine Kinase-1 in the Invasion and Angiogenesis of VHL Mutant Clear Cell Renal Cell Carcinoma. FASEB J. 2015 Mar 24.

Carroll B, Donaldson J, Obeid, LM
Sphingolipids in the DNA Damage Response. Adv Biol Regul. 2014 Nov 18.

Orr Gandy KA, Adada M, Canals D, **Carroll B**, Roddy P, Hannun YA, Obeid LM. *Epidermal growth factor-induced cellular invasion requires sphingosine-1-phosphate/sphingosine-1-phosphate 2 receptor-mediated ezrin activation.* FASEB J. 2013 Apr 29.

Talwar S, Jin J, **Carroll B**, Liu A, Gillespie BM, Palanisamy V.
Caspase-mediated cleavage of RNA-binding protein HuR regulates c-Myc expression after hypoxic stress. J. Biol. Chem. 2011 Jul 27.

Selected Meetings
And Presentations

International Ceramide Conference, Montauk, New York, **October 2013**
REGULATION OF SPHINGOSINE KINASE 1 BY P53 AND CASPASE 2 (oral)

Southeastern Lipid Conference, Cashiers, North Carolina, **October 2012**
P53 REGULATION OF SPHINGOSINE KINASE 1 (oral)

FEBS Advanced Course in Lipid Signaling and Cancer, Vico Equense, Italy, **October 2012**
P53 REGULATION OF SPHINGOSINE KINASE 1 (poster)

Charleston Ceramide Conference, Villars, Switzerland, **March 2011**
REGULATION OF SPHINGOSINE KINASE 1 BY P53-DEPENDENT PROTEOLYSIS (poster)

RNA Stability Meeting, Montreal, Canada, **October 2010**
CASPASE-MEDIATED CLEAVAGE OF RNA-BINDING PROTEIN HUR REGULATES C-MYC EXPRESSION AFTER HYPOXIC STRESS (poster)

Mid-Atlantic Microbial Pathogenesis Meeting, Wintergreen, Virginia, **February 2009**
IDENTIFICATION OF A POTENTIAL HOMOLOG OF THE SMALL REGULATORY RNA RYHB IN *Brucella abortus* 2308 (poster)

Wind River Conference on Prokaryotic Biology, Estes Park, Colorado, **June 2009**
IDENTIFICATION OF A POTENTIAL HOMOLOG OF THE IRON-RESPONSIVE SMALL REGULATORY RNA RYHB IN *Brucella abortus* 2308 (poster)

East Carolina University's, Brody School of Medicine, Microbiology Immunology Forum, Greenville, North Carolina, April 2008
BIOINFORMATICS APPROACH IN THE IDENTIFICATION OF A PUTATIVE SMALL RNA IN *Brucella Abortus* 2308 THAT POTENTIALLY REGULATES EXPRESSION OF A GENE ENCODING A COMPONENT OF THE TYPE IV SECRETION MACHINERY (poster)

Chapter 1

The DNA Damage Response: A Review

Abstract

Even though over half a century has passed since the DNA structure was discovered, our understanding of the mechanisms responsible for preserving genome integrity and ultimately ensuring faithful transmission of genetic material across generations is still incomplete. DNA is constantly exposed to insults from environmental agents such as ultraviolet radiation as well as endogenous insults that are generated during normal cellular metabolism; and therefore the cell must have an effective and efficient process of sensing and repairing this damage in order to preserve genomic integrity. The DNA damage response (DDR) is an intricate and highly orchestrated signal transduction pathway that has evolved to sense DNA damage and initiate the appropriate repair pathway in order resolve the damage in coordination with ongoing cellular physiology. Numerous enzymes that chemically modify DNA to repair the lesion execute the DDR. These repair tools must be precisely regulated as misuse or incorrect timing or localization of DDR enzymes may result in genomic instability. Consequently eukaryotic cells have developed strategies to recruit and activate the appropriate proteins in both space and time according to the type and severity of the lesion. This chapter will provide an overview of the DDR including DNA damage sensing, signaling, repair and the biological consequences.

1.1 Introduction

The survival of any organism is contingent upon the ability of that organism to deliver intact and accurate genetic material to subsequent generations. The accurate transmission of genetic material from one cell to its daughters is a complex process that must be achieved despite constant insults of both environmental and endogenous agents on the DNA; therefore this process requires not only accurate DNA replication and chromosome distribution but also an ability to survive and repair spontaneous and induced DNA damage to minimize the number of inheritable mutations, thus preserving the genome [1].

The preservation of genomic integrity is no small task. There are approximately 10^{13} cells in the human body that are subjected to tens of thousands to millions of DNA lesions per day [2]. These genomic insults can arise form either endogenous sources such as the generation of reactive oxygen species (ROS), a by-product of oxidative phosphorylation or exogenous sources like exposure to chemicals or ultraviolet light (UV) [3]. Consequently, to deal with this myriad of insults eukaryotes have evolved the DNA damage response (DDR). The DDR is an intricate signal transduction pathway consisting of numerous proteins that sense DNA damage and transduce this information to effector proteins which then go on to mediate an appropriate response to the damage within the cell [1]. Although the proteins involved and the response elicited differ according to DNA lesions, they usually occur by a common general program **(Scheme 1).**

Genomic instability is a hallmark of cancer [4]. Given the importance of the DDR in genome preservation it is now widely accepted that the DDR acts as an "anti-cancer barrier." Breaches of this barrier in the form of mutational or epigenetic inactivation of DDR components may allow for malignant progression and indeed there is a high frequency of DDR defects in human cancers [5].

This chapter will provide an overview of DNA damage repair mechanisms and signaling networks and also provide background on the intimate relationship between the DDR and cancer.

1.2. DNA Damage Repair Mechanisms

There are a variety of DNA damage repair mechanisms that are initiated according to specific DNA lesions and collectively are capable of protecting cells against most genomic injuries. In mammals, cells mostly encounter DNA damage in the form of bulky adducts, base mismatch, insertions or deletions, DNA single strand breaks (SSBs) or double strand breaks (DSBs). A brief description of the proteins involved in DNA damage sensing and the main pathways employed to repair SSBs and DSBs is outlined below.

1.2.1. Base Excision Repair

Most subtle changes to DNA such as small base adducts and SSBs that do not strongly disturb the DNA double-helix are repaired through a series of reactions collectively termed base excision repair (BER) [6]. BER is initiated by lesion-specific DNA glycosylases, which specifically recognize and excise damaged or inappropriate bases from the DNA backbone, resulting in the formation of an abasic (AP) site. The AP site is then cleaved by the action of AP-endonucleases resulting in a SSB that can then be processed by short-patch BER where a single nucleotide is replaced or long-patch BER where 2-10 new nucleotides are synthesized [7, 8]

1.2.2. Nucleotide Excision Repair

Nucleotide excision repair (NER) is responsible for the removal of numerous single-strand lesions including those caused by UV light resulting in bulky adducts that distort the DNA helical structure [9]. NER is a complex and multi-step process that is characterized by two different modes of DNA damage detection and is therefore often divided into two subclasses: transcription-coupled NER (TC-NER) and global genome NER (GG-NER). TC-NER detects and repairs transcriptional-stalling lesions, allowing for rapid resumption of transcription [10, 11], while GG-NER detects lesions anywhere in the genome not just as part of a blocked transcription process but because the lesion disrupts base pairing and distorts the DNA helix [11]. Although these processes detect lesions via distinct mechanisms, they repair the damage in a similar way, sharing the same process for lesion incision, repair and ligation. In short, upon recognition of the lesion a bi-directional helicase opens up the damaged DNA segment encompassing approximately 30 nucleotides [12]. The unwound DNA is stabilized by the DNA-

binding proteins XPA and RPA (Replication Protein A) [13]. In addition to stabilizing the unwound DNA, XPA and RPA are also responsible for orienting the two structure-specific endonucleases XPG and ERCC1-XPF which incise the damaged strand 3' and 5' with respect to the lesion, leaving the undamaged single-stranded DNA (ssDNA) [13-15]. DNA polymerase and other DNA replication proteins such as PCNA and RPA bind to and use this undamaged ssDNA as a template to synthesize a short complimentary sequence [16]. In the final step the gap is sealed by DNA ligase I or III, depending on the proliferation status of the cell [17].

1.2.3. DNA Double Strand Break Repair (DSBR)

DNA damage caused by ionizing radiation or from replication fork collapse for example result in DSBs, in which both strands of the DNA double helix are severed. This type of lesion is especially hazardous to the cell because they are difficult to repair as the cell cannot rely on copying the genetic information from the undamaged strand and therefore can lead to loss or rearrangement of genomic sequences.

The cell employs two principal mechanisms for repair of DSBs that are determined by the phase of the cell cycle: homologous recombination (HR) and non-homologous end joining (NHEJ). HR is a conservative process that restores the original DNA sequence to the site of damage and as it name implies requires a homologous sister chromatid. HR acts exclusively in the S- and G2-phase of the cell cycle and is usually initiated as a result of replication fork collapse [18]. HR is always initiated by the binding of the MRE11-RAD50-NBS1 (MRN) complex to a DSB. The function of the MRN complex is to hold the lesion together and provide the structural bases for the CtIP nuclease [19]. The MRN-CtIP complex in coordination exonuclease I (EXOI) catalyzes DNA end resection at the 5' end of the DNA break [20, 21]. The newly created single-strand region is coated by RPA and exchanged into a RAD51 nucleo-protein filament. The 3' end of this filament then goes on to invade the homologous sister chromatid which is then used as a template for the synthesis of new DNA at the DSB site [22].

On the other hand NHEJ can occur throughout the cell cycle and in post-mitotic cells and does not require a homologous template as break ends are directly ligated [23]. During NHEJ DSBs are recognized by the Ku70/Ku80 hetero-dimer that binds the DNA and subsequently

activates the protein kinase DNA-PKcs. Activation of DNA-PKcs leads to the recruitment of the MRN complex that is involved in DNA end-processing followed by ligation of the two ends by the XRCC4/LigaseIV complex [24-26]. NHEJ is inherently mutagenic as DNA end-processing can cause deletions or mutations of DNA sequences at or around the DSB site.

1.3. DNA Damage Signaling

The detection of DNA damage (outlined above) is linked to a highly orchestrated signaling cascade that consists of transducers that relay a signal normally via phosphorylation events to effector proteins that elicit an appropriate biological response according to the type and severity of the DNA damage detected. To ensure completion of lesion removal before replication or cell division the cell cycle can be arrested at the G1/S transition, within the S-phase or at the G2/M transition depending on the nature of the injury and the phase of the cell cycle in which the lesion was detected [27]. Alternatively, if the DNA damage is too severe or many lesions are sensed, apoptosis can be triggered in order to rid the body of potentially harmful cells [28].

1.3.1 Proximal Transducers

The two related serine/threonine protein kinases ATM (ataxia telangiectasia mutated) and ATR (ataxia telangiectasia mutated and Rad3-related protein) are central components of the DDR [29]. Both proteins are recruited to and activated by sites of DNA damage and subsequently phosphorylate several key proteins that then act to initiate DNA damage checkpoints resulting in cell cycle arrest, DNA repair or apoptosis [30].

ATM, which is normally found within the cell as inactive dimers, is recruited to and activated by DSBs. More specifically the MRN complex at DSBs directly activates ATM via an interaction with the NBS1 subunit and subsequently a functional MRN complex is required for ATM activation [31, 32]. Once activated ATM can then go on to phosphorylate a number of downstream targets including other transducers of the DDR as well as DDR effectors. ATM-mediated phosphorylation may enhance or repress the activity of the target protein [33]. Interestingly, ATM deficiency (lost or inactive) leads to the genomic instability disorder ataxia-

telangiectasia that is characterized by neurodegeneration, radiation sensitivity, and cancer predisposition [34].

On the other hand, ATR is activated in response to persistent RPA-coated ssDNA that is common at stalled replication forks and also as an intermediate in NER and HR. ATR works in concert with a partner protein ATRIP (ATR interacting protein) which also recognizes RPA-coated ssDNA. Once activated ATR like ATM then phosphorylates downstream targets to modulate their activity [35]. Interestingly, ATR knockout mice are embryonic lethal and thus far there are no mutations in ATR associated with any human disease suggesting that ATR has a constitutive function during the normal cell cycle [36, 37].

1.3.2. Distal Transducers

Although ATM and ATR can directly phosphorylate effectors of the DDR to elicit a biological response, they also phosphorylate and activate other transducers, allowing for enhancement or redirection of the ATM-ATR response. Of these distal transducers, the cell cycle proteins CHK1 (checkpoint kinase 1) and CHK2 (checkpoint kinase 2) are the best characterized. CHK1 and CHK2 are serine/threonine kinases that although are unrelated structurally do have some overlapping substrate specificity [38].

Although CHK1 has a physiological role, monitoring DNA replication during normal cell cycles, it also becomes activated in response to DNA damage. Upon recognition of ssDNA breaks, ATR activates and regulates CHK1 via phosphorylation events at conserved residues Ser-317, Ser-345 and to a lesser extent Ser-366. There is also an auto-phosphorylation site present at Ser-296 that becomes phosphorylated after ATR phosphorylation [39]. Owing to the role CHK1 plays in normal cell homeostasis, CHK1 is essential for mammalian development and viability as CHK1 knock-out mice are embryonic lethal [40, 41]

Unlike CHK1, under normal conditions CHK2 is present in the nucleus in an inactive monomeric form. In response to DNA damage (mostly DSBs), CHK2 becomes phosphorylated by ATM on residue T68 as well as other residues at the N-terminus, a region rich in serine-glutamine and threonine-glutamine pairs that are known motifs of ATM and ATR [42].

Interestingly, several mutations have been identified within CHK2 that result in decreased DNA repair ability and subsequently predisposition to cancer [43, 44].

Once activated by DNA damage, CHK1 and CHK2 phosphorylate effector proteins that are responsible for the execution of DDR functions such as cell cycle arrest to allow for DNA damage repair or apoptosis. Although these two kinases have considerable overlap of substrate specificities, they do not seem to play redundant roles within the cell as CHK2 cannot compensate for loss of CHK1 which is embryonic lethal in mice. Also of note, although in the past ATR was thought to exclusively phosphorylate CHK1 and ATM exclusively CHK2, recently considerable crosstalk among these kinases has been described exemplified by ATM phosphorylation and activation of CHK1 in response to ionizing radiation [45, 46].

1.3.3. Effectors

In the final arm of the DDR, upstream signals from transducers converge on downstream effectors that are responsible for executing an appropriate biological response. Of all the effectors identified thus far, the tumor suppressor p53 appears to be the central regulator of the cell's response to DNA damage. Consequently p53 is commonly referred to as the "guardian of the genome" [47]. P53 is a transcription factor that directly activates (or sometimes represses) the expression of a plethora of genes involved in cell cycle arrest, DNA damage repair and apoptosis through binding of specific p53-binding motifs within the target gene [48]. In fact over 4,000 genes have been identified that contain at least one p53 consensus binding sequence within their regulatory region [49].

In unstressed cells p53 is maintained at very low levels as a consequence of its rate of degradation rather than by translation from mRNA. P53 degradation is mediated by ubiquitin ligases, of which MDM2 (mouse double minute 2) is the best studied. MDM2 is an E3 ubiquitin ligase that directly ubiquitinates p53 and targets it for proteosomal degradation [50]. The mechanism of p53 stabilization and activation is complex but in all cases involves a series of post-translational modifications of which phosphorylation dominates. Phosphorylation of p53 by DDR transducers, ATM, ATR, CHK1 and CHK2 on different residues results in p53 stabilization mainly by disrupting the interaction between p53 and MDM2 [51, 52].

For the most part, the first effect of p53 expression in mammalian cells is on the cell cycle. P53 can directly bind and stimulate the expression of $p21^{WAF1/CIP1}$, an inhibitor of the cyclin-dependent kinases (CDKs). CDKs are responsible for ensuring smooth progression through the cell cycle and therefore are tightly regulated. When activated, CDKs form complexes with a family of regulator proteins called cyclins [53]. In response to DNA damage and following induction by p53, $p21^{WAF1/CIP1}$ binds to and inhibits the activity of these complexes including, cylcin-CDK2, -CDK1 and –CDK4/6 to halt cell cycle progression at the G1-to-S and G2-to-M transitions [47]. Interestingly, p21-deficient cells have a defect in p53-induced cell cycle arrest, suggesting that P53 induction of p21 is a critical target and effector of p53-mediated cell cycle arrest [54, 55]. P53 can also induce the expression of the proteins 14-3-3σ and GADD45, both of which promote G2/M checkpoint arrest via interactions with the Cyclin B1-CDK1 complex.

In addition to cell cycle responsibilities, the role of p53 in apoptosis has been intensely studied both *in vitro* and *in vivo* and was firmly established by a group of studies demonstrating that thymocytes, pre-B cells, mature B and T cells and intestinal stem cells from p53 knockout mice are resistant to death induced by a number of different DNA damaging agents [56-59]. Importantly, p53 regulates genes in both the extrinsic (death receptor) and intrinsic (mitochondrial) cell death pathways. Activation of the extrinsic cell death pathway is initiated by binding of death ligands to death receptors at the cell membrane and is tightly regulated by both death inhibitors and the compositions and levels of proteins within the cell at the cell membrane. P53 directly activates two pro-apoptotic members of the tumor necrosis factor receptor (TNFR) superfamily, Fas/Apo1 and Killer/DR5 that are then involved in the activation of the extrinsic death pathway that ultimately leads to caspase activation and cell death [60, 61]. Caspases are the main executioners of apoptosis and are a family of highly conserved cysteine-dependent aspartate-specific proteases that can proteolytically degrade a number of intracellular proteins to carry out cell death [62]. In addition, the intrinsic cell death pathway, initiated by mitochondrial dysfunctions appears to be vital for p53-dependent apoptosis. Of the p53-inducible proteins involved in induction of intrinsic apoptosis, Bax a pro-apoptotic member of the Bcl-2 family is one of the best characterized. Following p53 induction, Bax binds to the anti-apoptotic Bcl-2 family members, Bcl-2 and $Bcl\text{-}X_l$, promoting a shift from survival to apoptosis

[63, 64]. P53 also modulates the levels of other members of the Bcl-2 family including the two pro-apoptotic proteins PUMA (p53 upregulated modulator of apoptosis) and Noxa. PUMA is a BH-3-only member of the Bcl-2 family that initiates cell death via interactions with both Bcl-2 and Bcl-X_L. Depletion of PUMA by siRNA attenuates p53-mediated apoptotic response; and therefore PUMA appears to be a major effector of p53-induced apoptosis [65, 66]. Another BH-3-only member of the pro-apoptotic Bcl-2 family, Noxa is also induced by p53 and interacts with pro-survival Bcl-2 family members to initiate mitochondrial permeability changes [67]. Similarly, p53-induction of the protein p53AIP1 (p53-regulated apoptosis-inducing factor) at the mitochondria initiates mitochondrial membrane dysfunction leading to apoptosis [68].

P53 is also involved in the regulation of the family of proteases, caspases via direct and indirect mechanisms. For example, p53 regulates the expression of PIDD (p53-induced protein with a death domain) in response to DNA damage. PIDD can then go on to activate Caspase 2 through formation of the Caspase 2 activation platform, the PIDDosome [69, 70]. Similarly, the apoptotic protease activating factor 1 (Apaf-1) is a target of p53 and together with cyotochrome c and caspase-9 forms a ternary complex, the apoptosome which acts to process caspase-9 and in turn activates caspase-3 leading to cell death [71, 72]. P53 can also directly induce the expression of the executioner caspase, caspase-6 [73].

Although p53 is the main effector of the DDR, there are other important effector proteins. For instance, CHK1 and CHK2 can phosphorylate the protein phosphatase Cdc25 and protein kinase Wee1. Phosphorylation of Cdc25 promotes its proteosomal degradation, leading to inhibition of the CDK-cyclin complexes and cell cycle arrest [40]. Similarly, phosphorylation of Wee1 inhibits CDK1 activity, resulting in cell cycle arrest at the G2 phase [74].

1.4. Targeting the DDR for Cancer Therapy

As highlighted throughout this chapter, many human cancers harbor defects in DDR proteins leading to genomic stability. In addition, during tumorigenesis cancer cells frequently acquire defects in certain DNA damage repair pathways and subsequently rely on a compensatory mechanism to survive. For instance, cancers cells with mutations in p53 can no longer rely on p53 to function in promoting cell cycle arrest; therefore these cells become

dependent on other cell cycle arrest mechanisms such as CHK1 phosphorylation of CDC25 [75]. A cancer cell's ability to arrest the cell cycle and repair damaged DNA in response to chemotherapeutics is essential for its survival and results in decreased efficacy of cancer treatments; therefore targeting the "back-up" mechanism, especially in mutant p53 cancers cells has the potential to kill the cancer cells but spare their normal counterparts when in combination with DNA damage.

Indeed many small molecule inhibitors (SMI) have been developed to target several different DDR proteins. Pharmacological inhibition of the upstream transducers ATM and ATR has proven therapeutically beneficial. For instance, the ATP-competitive SMI of ATM, KU-60019 (AstraZeneca) was shown to radio-sensitize glioma cells [76]. Similarly, the ATR inhibitor VE-821 (Vertex Pharmaceuticals) was demonstrated to chemo- and radio-sensitize pancreatic cells in preclinical studies [77, 78].

Downstream of ATM and ATR are the two distal DDR transducers CHK1 and CHK2, that have proven to be viable targets and currently there are many SMIs of these two kinases in both preclinical and clinical stages as a combination therapy for many different human cancers [79, 80]. One of the first SMIs, UCN-01 is a staurosporine derivative isolated from a *Streptomyces* strain [81]. UCN-01 is a protein kinase antagonist that displays cytotoxic effects and was only later shown to be a potent inhibitor of CHK1 through ATP-binding pocket interactions [82, 83]. Six phase II clinical trials have been completed using UCN-01 either as a single agent or in combination with other drugs in patients with different types of advanced cancers. Consequently, a number of novel CHK1 inhibitors have been developed including GDC-0425 (Genentech), MK-8776 (Merck), LY-2606368 (Eli Lilly) and AZD-7762 (AstraZeneca) that have entered Phase I and II clinical trials either as single agents or in combination with several different chemotherapeutics [84-87].

Recently, the tyrosine kinase inhibitor, MK-1775, was discovered through a chemical library screen and was found to inhibit the DDR effector Wee1 kinase [88]. Currently, MK-1775 is in Phase II clinical trial in combination with carboplatin to treat patients with p53-mutated epithelial ovarian cancer.

In summary, pharmacological inhibition of proteins that execute checkpoint activation shows great promise as a viable therapy that could eventually be used as chemo- or radio-sensitizers as well as monotherapeutic agents in cancer treatment. Nevertheless, many of the SMIs developed thus far lack specificity and display off-target effects; therefore the safety, tolerability and efficacy of these drugs used alone and in combination has to be further investigated. Also the need for the development of more potent and specific inhibitors is critical.

1.5. An Emerging DDR Pathway: CHK1-Suppressed Pathway

Recently, the use of CHK1 inhibitors to sensitize mutant p53 cancer cells to DNA damage has been an intense area of research. Currently many CHK1 inhibitors are being tested in both the preclinical and clinical stages in combination with several chemotherapeutics to treat mutant p53 triple negative breast cancers (TNBCs) and mutant p53 ovarian cancers, just to name a few [75, 89-92]. Defects in p53 function render cells dependent on CHK1 to activate cell cycle checkpoints in response to DNA damage; therefore inhibition of CHK1 in combination with DNA damage abrogates checkpoint surveillance leading to "mitotic catastrophe" a form of cell death effecting p53-deficient cells while sparing p53-proficient cells that still have intact checkpoints [75]. Mitotic catastrophe results from a combination of deficient cell cycle checkpoints and cellular damage. Failure to arrest the cell cycle at or before mitosis results in an attempt of abnormal chromosome segregation, which in turn leads to the death of the cell via mitotic catastrophe [93].

Recently, in an attempt to identify p53-independent DDR pathways, p53 mutant zebrafish lines were used for a whole organism-based modifier genetic screen. The goal of this study was to identify DDR kinases whose lose could potentiate radio-sensitivity to mutant p53 zebrafish. Interestingly, it was demonstrated that radiation-induced apoptosis could be restored by depletion or inhibition of CHK1 through a Caspase 2-dependent apoptotic pathway. This novel cell death pathway was conserved in human cancer cell lines and was subsequently termed the "CHK1-Suppressed" (CS) pathway [94] and is depicted in **Scheme 2**. The caspase 2 activation platform the PIDDosome was found to be required for the CS-pathway. The PIDDosome is comprised of three proteins, PIDD (p53-induced death domain protein) and RAIDD (RIP associated Ich-1/CED homologous protein with death domain) that interact through Death Domains (DD)

existing in both proteins and Caspase 2 which is recruited to RAIDD via the caspase recruitment domain (CARD) present in both. Briefly, it was found that ATM phosphorylates PIDD on threonine 78 upon DNA damage only in the absence of CHK1. This phosphorylation is required for PIDD interaction with RAIDD and subsequent caspase 2 activation. Importantly, characterization of the CS-pathway provides evidence of a novel apoptotic pathway in addition to mitotic catastrophe that is activated upon CHK1 inhibition. Identifying the mechanisms behind CHK1 inhibitor sensitivity is essential for the advancement of CHK1 inhibitor therapy. For instance, characterization of effectors of the CS-pathway (ie. Substrates of Caspase 2) could led to the identification of new therapeutic targets that could restore sensitivity to mutant p53 cancer cells.

1.6. Conclusion

Although much progress has been made towards understanding the DDR, much remains to be learned about this complex and important signal transduction pathway. A major challenge is to understand in more detail how DDR proteins are regulated and conversely the biological implications when these proteins are deregulated, such as in cancer. As the concept of personalized medicine emerges, tumor-specific defects of DDR proteins constitute a promising therapeutic avenue to be exploited for the selective elimination of cancer cells.

Chapter 2

Sphingolipids and the DNA Damage Response

Abstract

Recently, sphingolipid metabolizing enzymes have emerged as important targets of many chemotherapeutics and DNA damaging agents and therefore play significant roles in mediating the physiological response of the cell to DNA damage. In this chapter we will highlight points of connection between the DNA damage response (DDR) and sphingolipid metabolism; specifically how certain sphingolipid enzymes are regulated in response to DNA damage and how the bioactive lipids produced by these enzymes affect cell fate.

2.1 Introduction

It is becoming increasingly evident in the literature that sphingolipid metabolizing enzymes are important targets of many chemotherapeutics and DNA damaging agents and therefore play significant roles in mediating the physiological response of the cell to DNA damage. Sphingolipid metabolites, including ceramide, sphingosine, and sphingosine 1-phosphate (S1P), are established bioactive lipids that play essential roles in cell growth, survival, and death [95, 96]. It is well established that many cancer treatments often result in the generation of ceramide, which has been implicated in mediating the cell death response [97]; conversely a common survival strategy employed by cancer cells is the generation of the pro-survival lipid S1P formed by phosphorylating sphingosine, the product of ceramide hydrolysis [98]. As the sphingolipid metabolites mentioned above can elicit both pro-survival and pro-apoptotic effects within the cell in response to DNA damage depending on which metabolite is formed, the regulation of the enzymes that produce these bioactive lipids is of great importance to cell fate and is the focus of this review. Here, we provide background about DNA damage response (DDR) and sphingolipid metabolism and discuss the currently known points of connection between the two, along with the therapeutic potential of targeting certain key sphingolipid metabolizing enzymes.

2.2 Overview of Sphingolipid Enzymes and Metabolism

As major constituents of cellular membranes, sphingolipids (SLs) were once thought to play merely structural roles within the cell, but are now well characterized as being bioactive signaling molecules that are important mediators of numerous biological processes including cell growth and survival as well as cellular senescence and death [99]. Ceramide (Cer), is considered the "hub" of SL metabolism and can be generated via three different pathways. *De novo* synthesis of Cer begins with condensation of serine and palmitoyl-CoA catalyzed by the enzyme serine palmitoyl transferase, forming 3-keto-dihydorsphingosine. Following subsequent reduction and acylation reactions, dihydroceramide is produced and undergoes a final desaturation reaction catalyzed by dihydroceramide desaturase to form Cer. Cer can also be generated as a result of the catabolism of more complex SLs such as sphingomyelin (SM), through the action of a family of enzymes termed the sphingomyelinases (Smase). This group of

enzymes catalyzes the hydrolysis of the phosphocholine headgroup of sphingomyelin to form Cer and free phosphocholine. Lastly, Cer can be generated via the salvage pathway where a family of enzymes known as the ceramide synthases (CerS) catalyze the N-acylation of fatty acids of differing chains lengths at the C2 position of the 18-carbon amino alcohol sphingosine (Sph) resulting in the formation of Cer. Once generated Cer can undergo further catabolism to produce Sph by a group of enzymes, the ceramidases (Cdases). Following the generation of Sph, phosphorylation of this molecule by the sphingosine kinases (SKs) can occur to produce sphingosine-1-phosphate (S1P) [99]. An illustration outlining this set of reactions with inducers and biological outcome is outlined in **Scheme 3**. The sphingolipid metabolic network is a complex and interconnected set of reactions that generates abundant bioactive molecules therefore the regulation of the enzymes in this complex signaling pathway must be tightly regulated.

2.3. The Generation of Ceramide

There are two major sources of ceramide generation: sphingomyelin hydrolysis by sphingomyelinases, and *de novo* ceramide synthesis by ceramide synthases. The following section addresses the families of enzymes responsible for these ceramide-generating processes, and how they relate to the cellular DNA damage response.

Sphingomyelinases

The sphingomyelinases (Smases) are a family of phosphodiesterases that catalyze the hydrolysis of sphingomyelin to ceramide and phosphorylcholine. The Smases are classified into three groups dependent on their optimum pH for activity: neutral sphingomyelinases (nSMases), acid sphingomyelinases (ASMases) and alkaline sphingomyelinases (alk-Smases). Each Smase occupies a distinct niche in terms of cellular localization and physiological function.

Neutral sphingomyelinase

Neutral Smases are so-called because they exhibit a neutral optimum pH. There are currently four identified human nSMases: nSMase 1, nSMase 2, nSMase3, and MA-nSMase (mitochondrial associated-nSMase), encoded by genes *SMPD2-5* respectively. nSMase2 is by far

the best characterized of the nSMases. nSMase2 is localized to the inner leaflet of the plasma membrane, which is thought to be the major site for sphingomyelin hydrolysis [100-102]. nSMase2 is also localized to a lesser extent to the Golgi, and recycling between the two sites has been shown to be important for the regulation of its enzymatic activity [101]. nSMase2 activity and localization are dependent on binding of Mg^{2+} ions and the anionic phospholipid phosphatidylserine (PS) [103, 104]. nSMase2 has been implicated with a wide variety of biological functions and pathologies, including bone mineralization and skeletal development, lung disease, tumorigenesis, and the inflammatory response [105-109]. Of particular interest in this discussion is the role of nSMase2 activation in driving apoptosis as part of the DDR; this will be addressed in detail in the following section.

2.3.1.2. Acid sphingomyelinase

ASMase, encoded by gene *SMPD1*, is characterized by its activity at an acidic optimum pH [110]. It is a soluble, highly disulfide-bonded structure, which is either localized to the lysosome or secreted [111]. ASMase was identified to be lacking in patients suffering from Niemann-Pick's disease (NPD) [112], a lysosomal storage disease in which sphingomyelin accumulates in the lysosome. Of particular interest with respect to the DDR, cells from NPD patients are resistant to apoptosis induced by ionizing radiation [113]. Hence the study of cells and tissues derived from NPD patients has greatly assisted in our current understanding of the roles and functions of ASMase in the DDR. Endothelial secretion of ASMase and increased ASMase activity plays a role in the early stages of atherosclerosis, diabetes, and chronic heart failure [114-116]. ASMase activity has also been linked to depression, dementia, and cancer, amongst other [117, 118]

2.3.1.3. Alkaline sphingomyelinase

Alk-Smases are the least-studied of all Smases. They are almost exclusively expressed in intestinal mucosa and liver tissue [119] and appear to function in the digestion of dietary sphingomyelin [120] . Alk-Smases are structurally unrelated to other Smases; in fact, they are classified as part of the family of nucleotide pyrophosphate/phosphodiesterases (NPPs) [121]

2.3.2. Ceramide Synthases

Ceramide synthases (CerS) catalyze the *de novo* synthesis of ceramide through the condensation of a sphingoid base and a fatty acyl-coA [122]. There are six human CerS proteins, CerS1-6, which differ in their defined utilization of acyl-chain lengths, such that each CerS preferentially generates a specific subset of ceramide chain-lengths [123, 124]. CerS are small, multi-pass transmembrane proteins located in the ER membrane [125, 126]. CerS6 has been predicted to possess five transmembrane domains, with a luminal N-terminus and cytosolic C-terminus [123]. The other CerS proteins are predicted to display similar topology due to their homology. CerS proteins have repeatedly been proven to play a significant role in the induction of apoptosis through the DDR (described in detail later in this review).

(A)0.....□罘□□ **Ceramide in the DDR**

Ceramide was first linked to the cellular apoptotic mechanism in the early 1990s, when several studies identified ceramide elevation and sphingomyelinase activation as key mediators in the apoptotic response to TNFα, Fas and ionizing radiation [127-130]. It is becoming increasingly clear that the mechanism of this ceramide-mediated apoptotic response is, at least in part, due to the ability of ceramide to trigger or hijack the cellular DNA damage response. In a similar fashion, ceramide is also able to induce cell cycle arrest through DDR elements. The following discussion presents our current understanding of the network surrounding ceramide as a secondary messenger, mediating the DDR to result in apoptosis or cell cycle arrest.

2.4.1. Sphingomyelin catabolism versus ceramide synthesis

Initially there was debate as to the source of ceramide elevation in the DDR: Smase activity or CerS activity. Membrane preparations devoid of nuclei exhibit ceramide elevation in response to ionizing radiation, via a rapid activation of nSMases [128]. nSMases were also implicated in ceramide elevation in leukemia cell lines in response to the chemotherapeutic drug daunorubicin [131]. In this study, two sphingomyelin hydrolysis cycles were observed, causing an increase in ceramide production. These cycles were accompanied by nSMase activation and were unaffected by treatment with CerS inhibitor fumonisin (FB1). ASMase has also been implicated in the ceramide-mediated apoptotic mechanism. Lymphoblasts from patients suffering from Nieman-Pick's disease (NPD) do not experience an elevation in ceramide production in

response to irradiation, and are subsequently unable to undergo apoptosis [132]. This effect is surmounted by retroviral insertion of human ASMase cDNA, indicating that ASMase is responsible for ceramide accumulation leading to apoptosis.

Bose *et al.*, [133] first proposed the alternative CerS-mediated mechanism for induction of apoptosis. Treatment of human and mouse leukemia cell lines with daunorubicin causes ceramide elevation due to activation of ceramide synthesis by ceramide synthases. Pre-incubation of cells with FB1 ablated this ceramide elevation and the apoptotic response, confirming the role of CerS in this mechanism. CerS was also reported to be activated in response to irradiation of endothelial cell lines, generating ceramide and inducing apoptosis [134].

These differences in observations were reconciled when ceramide generation was shown to be biphasic in nature in human lymphoblasts; ASMase activity causes a peak in ceramide within minutes following irradiation, whereas CerS activity increases ceramide levels several hours later [113]. The initial peak in ceramide is modest and transient, occurring with a corresponding decrease in sphingomyelin and an observed increase in ASMase activity. The later ceramide elevation is a more substantial increase occurring 8-24 hours post-irradiation. It is accompanied by an increase in CerS activity and is inhibited by pre-treatment with FB1. Interestingly, the second phase of ceramide elevation was observed to be dependent on the first, since it is absent in irradiated NPD lymphoblasts despite a normal increase in CerS activity. This implies that some product of sphingomyelin hydrolysis by ASMase is required for the second phase of ceramide generation. This split mode of ceramide generation appears to be characteristic of ceramide signaling in the DDR, and further study is needed to elucidate and thoroughly understand the differential activities of Smases and CerS and their downstream effects in the DDR.

Whilst overall CerS inhibition is known to protect cells from apoptosis, there are evidently some specific effects mediated by individual CerS proteins in the DDR. Overexpression of different CerS proteins in HEK-293 cells rendered them susceptible to different chemotherapeutic agents: CerS1 overexpression sensitizes cells to cisplatin, carboplatin, doxorubicin and vincristine; CerS5 overexpression sensitizes cells only to

doxorubicin and vincristine; whereas overexpression of CerS4 sensitizes cells to none of the above [135]. Whilst the general role of CerS in apoptosis makes them of interest as targets for chemotherapeutics or radiation sensitization, the observed differential signaling of different CerS proteins offers promise for more specific therapeutic targeting. However, there is currently little understanding about the differential actions of CerS proteins, and this is one area that requires further work before therapeutic intervention can be pursued.

2.4.2. Ceramide and p53

Dbaibo *et al.*, [136] probed the involvement of p53 in ceramide-mediated induction of apoptosis, based on similarities in biological functions of p53 and ceramide. Actinomycin D and irradiation were used to induce apoptosis in Molt4 lymphocyte leukemia cells. Ceramide accumulation was observed to be p53-dependent, since p53 upregulation precedes ceramide elevation, and E6-mediated inhibition of p53 prevents accumulation of ceramide.

P53 is characteristically activated by ATM in the DNA damage response. A-T (ataxia-telangiectasia) cells possessing mutant ATM do not undergo apoptosis in response to irradiation, consistent with evidence that ceramide accumulation is p53-dependent. The first ASMase-dependent phase of ceramide elevation is observed as normal in A-T cells, whereas the second phase is absent and CerS activity is reduced [113]. These results indicate that the ASMase-mediated ceramide peak is ATM-independent, whereas CerS activation for the second phase is mediated by ATM and possibly, by extrapolation, p53.

Topoisomerase II inhibitor etoposide causes apoptosis in human glioma cells in a p53-dependent manner. Activation of p53 and subsequent apoptosis were shown to be accompanied by an elevation in ceramide and activation of nSMase2, but not ASMase [137]. This is consistent with previous reports of DNA damaging agents, such as daunorubicin, causing ceramide-mediated apoptosis through activation of nSMase2 [131]. However, it is now interesting that evidence is building for a model in which CerS and nSMase2 activation in the DDR are mediated by p53 and ATM, whereas activation of ASMase is not. There is also evidence that nSMase3 serves a distinct purpose in the DDR compared to other Smases. DNA

damaging agent Adriamycin has been shown to down-regulate expression of nSMase3 in human colon cancer cells, and it appears that this down-regulation is mediated by activated p53 [138].

2.4.3. Ceramide, caspase 3 and PARP

The role of caspase-3 and PARP in ceramide-mediated apoptosis is controversial and complex. Ceramide has been identified as a necessary mediator required for caspase-3 activation in response to irradiation. Inhibition of caspase-3 does not affect ceramide levels, indicating that ceramide elevation is upstream from caspase-3 activation in the DDR. Cleavage of PARP and activation of capsase-3 is entirely absent in NPD lymphoblasts or wild-type lymphoblasts pre-treated with FB1, indicating their requirement for ceramide generation[113]. Ceramide elevation was also observed to precede capsase-3 activation and PARP cleavage in a human lung adenocarcinoma cell line [139].

Human leukemia cells treated with the inducer of apoptosis sodium nitroprusside (SNP) demonstrate nSMase2 activation, ceramide generation, and downstream apoptosis. Caspase inhibition is seen to block nSMase2 activation, preventing apoptosis [140]. Furthermore, purified, recombinant caspase-3 was observed to increase activity of nSMase2 in a cell-free system. Studies focusing on late-stage CerS-mediated ceramide accumulation in UV-induced apoptosis also indicate that there is a pool of ceramide downstream from caspase activation [141]. In this study, caspase inhibition was seen to block UV-induced apoptosis. Although total cellular ceramide levels were unaffected by caspase inhibition, medium long-chain ceramide species were seen to be reduced. Whilst this observation implicates medium long chain ceramide with a role in UV-induced apoptosis downstream from caspase activation, it also more broadly implicates specific chain-length ceramide species with particular roles within the DDR. Taken altogether, the literature indicates a possible feed-forward network between caspase-3 and ceramide (possibly distinguishing between different chain lengths at different levels of the DDR), driving towards apoptosis in the DDR.

There is also evidence of a caspase-independent ceramide-mediated apoptotic mechanism in the DDR. Fas-resistant Hodgkin's disease-derived cells showed no activation of caspase-3 or cleavage of PARP in response to increased ceramide. Inhibition of caspase-1 or caspase-3, or

treatment with a pan-caspase inhibitor did not prevent ceramide-induced apoptosis, indicating an alternative mechanism in this instance [142].

2.4.4. Ceramide and cell cycle arrest

The role of ceramide in the cell cycle arrest pathways of the DDR is less well characterized and in need of further study for a thorough grasp on its complexities. It is well-known that DNA damage results in cell cycle arrest through a number of complex mechanisms [143]. Evidence is gradually emerging that poses ceramide as a key mediator in this DDR pathway. Ceramide elevation results in cell cycle arrest at the G0/G1 phase. This effect is abrogated in the absence of retinoblastoma protein (Rb) in MOLT4 cells, indicating that Rb acts as a mediator in ceramide-induced cell cycle arrest [144, 145]. Ceramide accumulation has also been shown to cause cell cycle arrest at the G2 phase, through induction of p21 [146]. ATM and p53 are established as mediators of cell cycle arrest in the DDR [147]. Since ceramide elevation has been shown to be a consequence of ATM and p53 activation (see previous section), it may be that ceramide acts a downstream effector for ATM/p53, at least in some instances.

NPD lymphoblasts experience normal induction of p53 and p21 – changes in which are important for induction of cell cycle arrest. Hence, irradiation-induced cell cycle arrest is not dependent on ASMase activity [113], making it likely that this response is mediated either by CerS or nSMase2. Specific studies are needed to establish explicitly the dependence of DDR-induced cell cycle arrest on CerS and nSMase2 activity.

The mechanism of ceramide-induced cell cycle arrest is distinct from the apoptotic pathway, although both occupy branches of the DDR. Whereas ceramide-mediated apoptosis can be blocked by regulator of cell death bcl-2 [139], cell cycle arrest resulting from ceramide-induced Rb activation is not bcl-2 dependent [146, 148]. Overall, multiple modes of action within the DNA damage response have been identified for ceramide, sometimes with interdependent cross talk between them. The future of ceramide research in DDR will undoubtedly elucidate the complex network therein, particularly with respect to specificities in target and pathway switching.

(A)0.....□罘□□ **The Catabolism of Ceramide**

The conversion of Cer to Sph serves as an important step in sphingolipid metabolism. Cer can be acted upon by a group of enzymes called Ceramidases (Cdases) whose action cleaves the fatty acid from Cer to produce Sph, an 18-carbon amino alcohol. Importantly once produced Sph then serves as a substrate to produce the pro-survival sphingolipid S1P; therefore the catabolism of Cer can alter the balance of pro-death to pro-survival sphingolipids.

2.5.1 Ceramidases

Ceramidases (Cdases) comprise a heterogeneous family of enzymes that function to catalyze the deacylation of ceramide, thereby releasing a free fatty acid of differing chain length depending on the ceramide species to form the 18-carbon amino alcohol sphingosine. Cdases are currently classified into three categories (acid, neutral and alkaline) based on their optimal pH and primary structure. To date, five human Cdases encoded by five distinct genes have been cloned, including acid ceramidase (AC), alkaline ceramidase (for which there are three alkaline ceramidase (ACER1), alkaline ceramidase 2 (ACER2), and alkaline ceramidase 3 (ACER3)), and neutral ceramidase (NC). Below we will discuss acid and neutral ceramidase, how they are regulated in response to DNA damage, and the role they play in the DDR through mediating ceramides and sphingosine.

2.5.1.1. Acid Ceramidase

Acid ceramidase (AC), a member of the N-terminal nucleophile (Ntn) hydrolase superfamily, is a lysosomal enzyme encoded by the *ASAH1* gene. During maturation, AC undergoes cysteine-dependent auto-proteolysis of a 50kDa polypeptide forming the mature heterodimeric enzyme that consists of two subunits, α (13kDa) and β (40kDa). This maturation process is accelerated at acidic pH, presumably to prevent premature maturation before entering the lysosomal compartment [149, 150]. In addition to a preference for acidic pH (~5), AC also shows increased activity towards medium and long chain ceramides (C12 and C14) over short and very long chain ceramides, and also prefers unsaturated over saturated ceramides as substrates [151].

The physiological importance of AC is highlighted by the role it plays in the lysosomal storage disorder Farber's disease, which is characterized by a mutation in the AC gene leading to

a deficiency in its activity and subsequent accumulation of lysosomal ceramide [152]. This disease thus provides a powerful tool to investigate AC and consequently many researchers have used different cell types from patients with Farber's Disease in order to elucidate the role AC plays in a number of biological processes, including the DDR. For example, both lymphocytes and fibroblasts from Farber's Disease patients were shown to be equally as sensitive to a number of stress stimuli and DNA damaging agents, demonstrating similar caspase activation compared to normal control cells. [153] [154].

In contrast, numerous studies have provided strong evidence that manipulations of AC, both genetically and pharmacologically, can have significant effects on cell fate in response to DNA damage. Several studies have demonstrated that AC is upregulated in approximately 60% of primary prostate cancer tissues [155, 156]. In order to investigate the biological consequence of this overexpression, Saad *et. al*. generated human prostate cancer cells stably overexpressing AC and found that these cells were resistant to cell death induced by doxorubicin, cisplatin, etoposide, gemcitabine or C6-ceramide. Conversely, these AC-overexpressing cells could be sensitized to these DNA damaging agents following knock down of AC using siRNA [157]. In addition, Hara *et. al*. reported that AC protein expression in human U-87 glioblastoma cells was increased in a p53-dependent manner in response to γ-radiation and that inhibition of AC activity resulted in significant accumulation of ceramide and increased apoptosis in response to γ-radiation [158] . Similarly, an elegant study by Cheng *et. al* demonstrated in prostate cancer cells ceramide production in response to radiation therapy, resulted in c-Jun/activator protein 1 mediated upregulation of AC at the mRNA level with subsequent increases in protein and enzyme activity level. This study identified a novel feedback system in cancer cells, where DNA damage-induced ceramide accumulation leads to induction of AC ultimately to reverse the proapoptotic effects of this ceramide accumulation. They subsequently demonstrated that interference with AC induction and activity resulted in significant ceramide accumulation and radiosensitization of cancer cells [159]. These observations, along with several other studies reviewed more extensively by Mao *et. al*. [160], suggest that the regulation of AC by DNA damaging agents can greatly impact cell fate.

2.5.1.2. Neutral Ceramidase

Neutral ceramidase (NC), encoded by the *ASAH2* gene, is synthesized as a type II integral membrane protein via the secretory pathway. The N-terminal cleavage of NC produces a soluble protein that can peripherally associate with the outer leaflet of the plasma membrane. NC also contains mucin box domains, allowing for a high level of O-glycosylation that is necessary for its association with the plasma membrane [161]. NC is most active at neutral pH, as its name would suggest, and prefers long chain ceramides to medium chain as substrates [162].

NC is expressed in diverse cellular locations. In particular the enzyme has been shown at very high levels in the intestinal epithelium and consequently its role in the digestion of dietary sphingolipids has been intensely studied. *In vivo* studies in the *ASAH2-/-* mice revealed that these mice were deficient in the ability to degrade dietary ceramides, although no other obvious abnormalities or major alterations in total ceramide levels in tissues were observed. As ceramide is a constituent in the diet of animals including humans, the enzymatic activity of NC in the intestines represents a homeostatic mechanism for maintaining cellular integrity and physiological function by preventing the inadvertent initiation of apoptosis by dietary ceramides [163, 164].

Although a role of NC in intestinal tissues and digestion, is emerging, how this enzyme is regulated by the DDR is still under investigation. To this end, Wu *et. al*. demonstrated that treatment of polyoma middle T transformed murine endothelial cells with the chemotherapeutic agent Gemcitabine (GMZ) resulted in a selective reduction in NC protein level and enzyme activity, concomitant with increased levels of very long chain ceramides. The authors went on to show that GMZ treatment resulted in cell cycle arrest at the G0/G1 phase accompanied by dephosphorylation of the retinoblastoma protein (Rb) and that these effects of GMZ on cell cycle arrest and ceramide accumulation could be recapitulated by siRNA knockdown of NC [165]. Another study by Huwiler *et. al*. established a role for NC in apoptosis of rat renal mesangial cells in response to nitric oxide (NO). In this study the authors demonstrate that chronic exposure of renal mesangial cells to compounds releasing NO resulted in a decrease in ceramidase activity concomitant with increased sphingomyelinase activity, and significant increases in ceramide [166]. This group went on to demonstrate that NO induces NC

degradation through the ubiquitin/proteasome complex, and that this proteasomal degradation is inhibited by direct phosphorylation of NC by protein kinase C (PKC) [167, 168].

Many more studies are needed in order to fully elucidate the role of NC in the DDR, as is the case with the alkaline ceramidases as there are currently no studies published on this topic. As the activity of these enzymes is responsible for the catabolism of ceramide, a key mediator of cell death, understanding how these enzymes are regulated in response to DNA damage is of great importance and could have significant implications in the identification of novel therapeutic targets.

2.6. The Generation and breakdown of Sphingosine 1-Phosphate

The generation of S1P has many consequences for the cell. First, S1P is considered a pro-survival lipid that can increase cell proliferation, angiogenesis and inflammation among other things. Second, the breakdown of S1P by the action of the enzyme S1P lyase constitutes the only exit point of sphingolipid metabolism within the cell.

2.6.1. Sphingosine 1-Phosphate and the DDR

S1P is a potent bioactive lipid that plays roles in cell proliferation, angiogenesis and inflammation in addition to other functions [99] [169] [170]. S1P provokes these responses in cells by either acting directly on intracellular targets or through activation of a family of S1P-specific G-protein coupled receptors, S1P receptors 1-5 [171]. There are several enzymes responsible for the synthesis and breakdown of S1P and many studies have shown that in response to DNA damage these enzymes are differentially regulated in order to control S1P levels. The regulation of these enzymes by the DDR will be discussed in detail below.

2.6.2. Sphingosine Kinases

The Sphingosine kinases, consisting of Sphingosine kinase 1 (SK1) and 2 (SK2) are a group of lipid kinases that utilize ATP to catalyze the phosphorylation of the C-1 hydroxy group of free sphingosine, producing the bioactive lipid product Sphingosine 1-Phosphate (S1P). The action of these two enzymes constitutes the only means for the production of S1P in the cell and therefore SK's hold a crucial position in sphingolipid metabolism: regulating the balance of pro-

survival and pro-apoptotic signaling lipids [172, 173]. Subsequently, alterations in these enzymes' activity in response to different stimuli, specifically in the context of DNA damage, could have major implications on cell fate.

2.6.2.1. Sphingosine Kinase 1

SK1, the best characterized of the two SK isoforms, is predominantly a cytosolic enzyme that is known to translocate to the plasma membrane in response to activation of protein kinase C (PKC) and/or phospholipase D (PLD) or upon phosphorylation by ERK, move into the nucleus and even get secreted from endothelial cells [174-178]. Many studies have shown that overexpression of SK1 occurs in many cancers and this overexpression correlates with advancement of disease progression, resistance to chemotherapeutic drugs and an overall poor prognosis [179-182].

Over the past decade, the regulation of SK1 in response to DNA damage has been intensely studied, and the mechanisms of its regulation downstream of the DDR are now being elucidated. Work by Taha *et. al.* established a connection between the tumor suppressor p53 and SK1, whereby treatment of Molt-4 leukemia cells with a number of chemotherapeutics, including actinomycin D (act D), doxorubicin, etoposide, and γ-radiation resulted in a reduction in SK1 protein levels while mRNA levels remain unchanged, and that this reduction of SK1 protein was concomitant with p53 accumulation. This work also established that p53 was required for SK1 degradation through the use of a Molt-4 cell system expressing either the retroviral empty vector L*X*SN or the vector into which the E6 gene of human papilloma virus was inserted [183]. The E6 protein has been shown to target p53 to ubiquitination and subsequent proteasomal degradation [136, 184]. Treatment of the vector control cells with act D resulted in a significant decrease in SK1 protein level and an approximately 50% decrease in enzymatic activity; in contrast, cells overexpressing E6 failed to show loss of SK1 protein or activity in response to act D. To define further the mechanism behind p53-mediated SK1 degradation in response to act D a number of protease inhibitors were employed. Inhibition of caspases 3, 6, 7, and 9 only partially reversed Act D-induced SK1 loss, whilst inhibition of

cathepsin B, a lysosomal protease, produced a significant reversal of SK1 decline by Act D [183].

Similarly, work by Heffernan-Stroud *et. al.* demonstrated that ultraviolet radiation treatment of mouse embryonic fibroblasts (MEFs) wild type for p53 resulted in significant decreases in SK1 protein and enzymatic activity, and that this decrease was abrogated in MEFs null for p53. Moreover they showed that p53-mediated SK1 degradation could be rescued by pretreating wild type MEFs with a caspase -2 inhibitor, suggesting that p53, through its activation of caspase-2, negatively regulates SK1 in response to genotoxic stress [185]. To further define SK1 as key downstream target of p53 tumor suppressor activity, in vivo studies using p53 null mice were performed. These mice spontaneously develop thymic lymphoma and showed elevated SK1 levels and activity as well as increased S1P levels and decreased ceramide levels compared to wild type mice. Interestingly, deletion of SK1 in p53 null mice completely abrogated the formation of thymic lymphomas and increased the life span of these mice by approximately 30%. The double knockout mice also displayed significant increases in ceramide and sphingosine concomitant with reduction in S1P levels [185].

These studies provide strong evidence that SK1 is a key downstream target of p53 in response to DNA damage and the resulting loss of SK1 may be essential for p53-mediated initiation of apoptosis or cell senescence [183, 185]. As p53 is most commonly mutated, not completely lost in human cancers, with more than 50% of all human cancers harboring a mutation in p53 [47, 186-188], it will be of great interest to investigate the regulation of SK1 in response to DNA damage in the presence of mutant p53. To this end, our lab has begun to investigate how SK1 is regulated in response to DNA damage in mutant p53 breast cancer cells. These studies have revealed that MDA-MB-231 mutant p53 breast cancer cells do not activate Caspase 2 and SK1 proteolysis does not occur in response to doxorubicin treatment. Interestingly, we found that inhibition of the cell cycle protein, Checkpoint Kinase 1 (CHK1) a known inhibitor of Caspase 2 activation [94, 189], results in loss of SK1 protein that bypasses p53 (unpublished). This work could have important clinical application as CHK1 inhibitors are currently in clinical trial [87].

It is worth noting at this point that p53 mediates ceramide levels through activation/expression of Smases and CerS, as described previously in this review. In addition, both *in vitro* and *in vivo* studies have demonstrated that loss of SK1 leads to decreases in cell and tissue S1P levels and increases in ceramide levels, therefore loss of SK1 downstream of the DDR is another mechanism to regulate ceramide levels in addition to regulation of CerS and Smase [185]. Given the universally-acknowledged importance of p53 as a tumor suppressor protein, it would be interesting to pursue and dissect the mechanisms by which p53 apparently connects the DDR and sphingolipid pathways at multiple points**.**

2.6.2.2. Sphingosine Kinase 2

Although they are members of the same lipid kinase family, SK2 differs from SK1 in many respects including sub-cellular localization, substrate specificity and biological function. Unlike SK1, SK2 is found predominantly in the nucleus or perinuclear region of the cell and displays broader substrate specificity with the ability to phosphorylate sphingosine as well as phytosphingosine and dihydrosphingosine [190, 191]. Most surprisingly, SK2 and SK1 seem to elicit opposing roles within the cell; while SK1 activity is well established to enhance survival and prevent apoptosis in response to DNA damage [179-182], SK2 has been shown to augment the apoptotic response and even induce apoptosis through its overexpression [192, 193].

To this effect, Sankala *et. al.* demonstrated that endogenous SK2 is important for p53-independent induction of p21 expression in response to doxorubicin in MCF7 human breast cancer cells. The authors showed that down-regulation of SK2 with siRNA resulted in decreased basal and doxorubicin-induced p21 expression as well as decreased G_2/M cell cycle arrest in p53-inactivated MCF7 cells [192]. Also of interest, increased SK2 localization to the endoplasmic reticulum in response to serum starvation was shown to promote apoptosis concomitant with increased cytosolic free calcium and transfer of calcium to the mitochondria in NIH 3T3 fibroblasts [193].

These studies are just beginning to unravel the function of SK2 in mediating cell fate in response to stress and DNA damage and therefore more studies are needed to fully clarify the role of SK2 in the DDR.

2.6.3. Sphingosine 1-Phosphate Phosphatases and Lyase

A cell has several modes of regulating S1P levels via the action of a number of enzymes. First S1P can be dephosphorylated at the cell surface by a family of broad specificity lipid phosphate phosphatases [194] or more specifically at the ER by a family of S1P specific phosphatases, SPP1 and SPP2 [195-197]. The action of both of these families of phosphatases on S1P generates its substrate sphingosine that can then serve as the backbone to produce complex sphingolipids, ceramides or phosphorylated to reform S1P. Secondly, S1P can be irreversibly broken down into hexadecenal and phosphoethanolamine by S1P lyase (S1PL) at the ER and therefore this enzyme serves as the terminal enzyme of sphingolipid catabolism [198].

2.6.3.1. Sphingosine 1-Phosphate Phosphatases

As mentioned above, SPP1 and SPP2 are S1P and ER specific phosphatases that have been shown to play a role in regulating the reintroduction of sphingoid bases into ceramide species at the ER [199, 200]; more specifically overexpression of SPP1 has been shown to result in an increase in ceramide accumulation suggesting that dephosphorylation of S1P is a rate limiting step in the salvage pathway [195, 196, 200]. Interestingly, Johnson *et al.* found that siRNA knockdown of SPP1 protects MCF7 breast cancer cells from daunorubicin-induced DNA damage and cell death [201]. Also of interest, Oskouian *et al.* found by quantitative real-time PCR that both SPP1 and SPP2 were significantly down-regulated in human colorectal cancer tissue samples compared to normal adjacent tissue [202].

Although these studies do not elucidate how the enzymatic activity of SPPases are regulated in response to DNA damage, one could imagine (as these enzymes can greatly effect the levels of S1P and ceramide within the cell) that they are tightly regulated and more studies are needed to reveal the mechanism of this regulation.

2.6.3.2. Sphingosine 1-Phosphate Lyase

SPL holds a pivotal position in sphingolipid metabolism, as it is the terminal enzyme. Due to the location of SPL at the ER membrane, with its catalytic site facing the cytosolic surface of the ER, it has access to cytosolically produced S1P and all sphingoid phosphate bases must reach the ER for their final degradation by SPL [198].

An interesting study by Oskouian and colleagues, found that increased SPL expression and activity in response to the topoisomerase II inhibitor etoposide or by overexpression of the enzyme promotes apoptosis, as shown by increased caspase-3 activity, annexin-V binding, poly-ADP-ribose (PARP) cleavage and nuclear condensation in several human cell lines. The authors then went on to determine that SPL promotes apoptosis in response to DNA damage through a pathway involving p53 and the protease Caspase 2, as chemical inhibition of p53 transcription activity and caspase 2 activity by pifithrin- α and Z-VDVAD-FMK respectively resulted in abrogation of SPL-mediated apoptosis [202]. This study begins to characterize SPL as a mediator in the physiological response to DNA damage.

2.7. Conclusion

To date, there have been identified a number of points at which sphingolipid metabolizing enzymes affect and are affected by the DNA damage response pathway (summarized in **Table 1**). These findings position sphingolipids with a potentially prominent role in the overall mechanism by which cells elicit the appropriate response to DNA damaging agents. Further study within this field will undoubtedly shed more light on the complexities of connections between sphingolipid metabolism and the DNA damage response, thus opening up new avenues for therapeutic manipulation and clinical intervention.

Chapter 3

Role for the CHK1-Suppressed Pathway in Regulating Inflammatory Responses in p53-Defecient Cells

Abstract

The DNA damage response (DDR) is a complex and interconnected signaling network that dictates whether a cell repairs itself and survives or is damaged beyond repair and eliminated; therefore the proteins in this network must be tightly regulated in order to ensure genomic integrity. Conversely, mutational or epigenetic inactivation of DDR components leads to genomic instability, a hallmark of cancer. Indeed there is a high frequency of DDR defects in human cancers of which mutations in the DDR effector and tumor suppressor protein p53 are the best characterized and occur in greater than 50% of all human cancers. Interestingly, a novel DDR pathway has emerged termed the CHK1-Suppressed (CS) pathway that is activated by inhibition or loss of the cell cycle kinase CHK1, leading to an apoptotic response to DNA damage in the presence of mutant p53 that is mediated by the protease Caspase 2. Although the functions of the CS-pathway have been probed through pharmacological inhibition and siRNA knockdown it is unclear whether and how CHK1 inhibition can be regulated endogenously. Our data characterize the first endogenous activation of the CS –pathway; whereby upon DNA damage wild type p53 acts an endogenous regulator of CHK1 levels that modulates Caspase 2 activation and ultimately controls cell fate. Moreover, my data demonstrate that CHK1 levels persist in response to DNA damage in mutant p53 cancer cells, leading to CHK1-mediated activation of the pro-survival transcription factor NF-κB and induction of a pro-inflammatory response that is abrogated by loss or inhibition of CHK1. These data constitute a novel role for CHK1 in response to DNA damage outside of the cell cycle in regulating inflammation. Moreover these data have important clinical applications as many CHK1 inhibitors are in clinical trials and my data provide evidence that targeting CHK1 in mutant p53-mediated cancers may abrogate NF-κB signaling that is associated with increased cellular survival and chemoresistance.

3.1. Introduction

P53 in its wild type form plays a role in preserving genomic integrity upon cellular stress through regulating cell cycle progression, DNA damage repair, and apoptosis [47]. Given the high frequency of p53 alterations in human cancers and the ability of these cells to evade apoptosis that can lead to therapeutic resistance, elucidating p53-independent DNA damage response (DDR) pathways that could overcome this resistance has been an intense area of research [94, 203-205]. Recently a novel apoptotic pathway has emerged termed the "CHK1-Suppressed" (CS) pathway [94, 189]. CHK1 is a serine/threonine kinase and an effector of the DDR that, once activated, acts to halt progression through the cell cycle by phosphorylating downstream targets [206]. Importantly, during the CS-pathway, loss or inhibition of CHK1 in the context of mutant p53 circumvents p53 status to promote a Caspase 2 apoptotic response to DNA damage [94, 189].

Caspase 2 is a poorly defined but evolutionarily conserved member of the caspase family. It is activated by proximity-induced oligomerization via recruitment to a high molecular weight platform termed the PIDDosome. The PIDDosome is comprised of three proteins, PIDD (p53-induced death domain protein) and RAIDD (RIP associated Ich-1/CED homologous protein with death domain) that interact through Death Domains (DD) existing in both proteins and Caspase 2 which is recruited to RAIDD via the caspase recruitment domain (CARD) present in both. Once assembled, Caspase 2 then undergoes trans-cleavage producing the fully active enzyme [70]. Interestingly, in addition to activating Caspase 2, PIDD can also activate NF-κB in response to DNA damage forming a separate PIDDosome complex that lacks RAIDD and Caspase 2 but contains RIPK1 and NEMO (NF-κB essential modulator)/IKKγ [207]. Unlike Caspase 2, NF-κB is a transcription factor whose activity is known to induce pro-survival genes in addition to a number of chemokines and cytokines [208]; therefore, PIDD can elicit either pro-survival or pro-death signals according to its protein interactions [209].

The DDR is a complex and interconnected signaling network that dictates whether a cell repairs itself and survives or is damaged beyond repair and eliminated; therefore the proteins in this network must be tightly regulated. Consequently, the relationship between CHK1 and p53,

both important proteins in the DDR, is complex. CHK1 can phosphorylate p53, which is important for p53 stabilization in response to DNA damage [210] while, on the other hand, p53 has been shown to induce CHK1 down regulation although the functional significance has not been determined [211, 212]. Elevated CHK1 levels have been shown in numerous cancers including p53 mutant cancers [74]. Moreover, high CHK1 expression positively correlates with tumor grade and disease recurrence and has been associated with therapeutic resistance [74, 75, 213, 214]. The presence of two different PIDDosome complexes whose assembly may be differentially regulated by CHK1 levels and potentially p53 only adds to the complexity and importance of deciphering this signaling pathway as CHK1 has been identified as an inhibitor of Caspase 2 PIDDosome formation, but its effect on NF-κB activation is unknown and could be of great clinical significance. Given the importance of these pathways on cell fate and the intricacies and interconnectivity of the signaling network, this study aims to investigate the role p53 plays in the CS-pathway and identify the effects of perturbations of this pathway on Caspase 2 and NF-κB signaling that may ultimately decide cell fate and response to chemotherapy.

3.2. Material and Methods

3.2.1. Materials

Lipofectamine® RNAiMAX, Annexin-V and Propidium Iodide were purchased from Life Technologies (Grand Island, NY). X-tremeGENE 9 DNA Transfection Reagent was purchased from Roche Diagnostics (Indianapolis, IN). iTAQ and SYBR® Green master mix master mix was purchased from Bio-Rad (Hercules, CA). CHK1/2 inhibitor AZD7762 purchased from Selleckchem (Houston, TX). pcDNA3.1-WTp53 plasmids kindly provided by Dr. Ute Moll (Stony Brook University). pcDNA3.1-R280Kp53 generated by Janet Allopenna (Stony Brook University).

3.2.2. Cell Culture

MCF7 cells were purchased from ATCC and cultured in RPMI 1640 medium with 10% fetal bovine serum (FBS) both from Life Technologies (Grand Island, NY). MDA-MB-231 and HCT116 p53+/+ and HCT116 p53-/- were purchased from ATCC and cultured in Dulbecco's modified Eagle's medium (DMEM) with 10% FBS both both from Life Technologies (Grand

Island, NY). Humanized mutant p53 knock-in (HUPKI) mouse embryonic fibroblasts (MEFs) harboring either the R248Q or G245S hotspot mutations and wild type MEFs were a kind gift from Dr. Ute Moll (Stony Brook University) and cultured in DMEM with 10% FBS.

3.2.3. RNA isolation, quantitative RT-PCR and RT² Profiler™ PCR Array

RNA extraction and cDNA synthesis were performed using PureLink® RNA Mini Kit and SuperScript III First-Strand Synthesis kit (Life technologies) respectively and according to the manufacturer's. The cDNA was then diluted (1:15) in RNAse-free water, and 5 µl was used in a total reaction volume of 20 µl. Each 20-µl real-time PCR contained a ratio of 10:1:4 (iTaq: Taqman probe (20X): nuclease-free water). PCR was carried out using the Applied Biosystems 7500 Real-Time PCR System (Applied Biosystems, Foster City, CA, USA). The following Taqman probes (life technologies) were used: human *BMP4* (ID: Hs03676628_s1), human *CHK1* (ID: Hs00967506_m1), human *IL6* (ID: Hs00985639_m1), human *IL8* (ID: Hs00174103_m1), human *CXCL1* (ID: Hs00236937_m1), *CXCL10* (ID: Hs01124251_g1), *TGF-B* (ID: Hs00820148_g1), *VEFGA* (ID: Hs00900055_m1) and human *β-actin* (ID: Hs99999903_m1) that was used as a housekeeping gene. Cycle threshold (Ct) values were obtained for each gene of interest and *β-actin*. ΔCt values were calculated and the relative gene expression normalized to control samples was calculated from ΔΔ Ct values. RT² Profiler™ PCR human Cytokines & Chemokines array from Qiagen (Valencia, CA) was performed according to the manufacturer's. Data was then analyzed using the Excel-based data analysis template provided by Qiagen. Data analysis is based on the $\Delta\Delta C_T$ method with normalization of the raw data to either housekeeping genes.

3.2.4. Western Blot Analysis

Cultured or transfected cells were washed with ice cold PBS and then directly lysed in cold RIPA buffer containing 1 mM sodium orthovanadate, 2 mM PMSF, and protease inhibitor cocktail (Santa Cruz Biotechnology). Cellular lysates were then clarified by centrifugation at 14,000 rpm for 10 min at 4^{o}C; protein concentration was quantitated by BCA Protein Assay kit from Thermo Scientific (Suwanee, GA). Equal amounts of protein (25 µg) were boiled in Laemmli buffer (Boston Bio Product), and separated on SDS-PAGE (4-15%, Tris-HCl) using the Bio-Rad Criterion system. Separated proteins were then transferred onto nitrocellulose

membranes (Bio-rad) and blocked with 5% non-fat milk in PBS-0.1% Tween-20 (PBS-T) for at 1 hour at RT. Primary antibodies diluted 1:1000 or 1:20000 for β-actin were then added to membranes and incubated at 4 °C overnight. Membranes were washed 3 times with PBS-T then incubated with diluted 1:5000 HRP-conjugated secondary antibodies for 1 hour at room temperature. Membranes were then incubated with Pierce ECL Western Blotting Substrate (Pierce) and exposed to X-ray films that were then processed and scanned. Anti-total CHK1, anti-Phospho(296)-CHK1, anti-Phospho(317)-CHK1, anti-Phospho(345)-CHK1, anti-p53, anti-Caspase 2, anti-Phospho-ATM, anti-IKB-alpha, anti-β-actin, anti-GAPDH and anti-p21 were from Cell Signaling Technology (Danvers, MA). RIPA lysis buffer system, HRP-labeled secondary antibodies, anti-PIDD, anti-Arf6 and anti-PARP were from Santa Cruz Biotechnology (Santa Cruz, CA).

3.2.5. Cell Cycle Analysis

3.2.6. Bimolecular Fluorescence Complementation

As described previously [215, 216]. The plasmids pBIFC-C2-CARD VC and pBIFC-C2-CARD VN were kindly provided by Dr. Douglas Green (St. Jude's Children Hospital). pDsRed-Mito purchased from Clonetech (Mountain View, CA).

3.2.7. Measurement of Cytokine Levels in Media

The ELISA kit for human BMP4 and IL6 were obtained from R&D Systems (Minneapolis, MN). Measurement of secreted cytokine in DMEM was done according to the manufacturer's protocol. Secreted protein levels were normalized to the total amount of cellular protein determined by BCA assay.

3.2.8. Luciferase Assay

Transcriptional activity of NF-κB was measured using an NF-κB consensus sequence upstream of the luciferase reporter gene (Stratagene). Briefly, cells were plated in 60-mm dishes and co-transfected with NF-κB luciferase (1.5 μg) and constitutively expressing galactosidase (0.5 μg) (Invitrogen) using Xtremegene 9 (Roche Applied Science) according to the manufacturer's protocol. After 8 hours of transfection, media was replaced for 1 h prior to

incubation with inhibitors and stimulation with doxorubicin for 24 hours. For siRNA experiments, cells were treated with AllStar or CHK1 siRNA for 48 h prior to transfection with reporter constructs. Following stimulation, luciferase activity was assessed using the Luciferase reporter kit (Stratagene) according to the manufacturer's protocol. Galactosidase activity was assayed using the High Sensitive B-galactosidase kit (Stratagene) according to the manufacturer's protocol. Measured luciferase activity (NF-κB-dependent) was normalized to measured galactosidase activity (constitutive).

3.2.9. Microvesicle visualization and isolation

Live cell imaging analysis was performed on a Leica Laser-scanning confocal microscopy. Briefly, MDA-MB-231 cells were grown on poly-D-lysine-coated 35-mm confocal dishes (MatTek Corporation). The following day, meida was changed and the cells were treated with 0.8uM Doxorubicin for 24hours. Thirty minutes prior to imaging, Annexin-V and Propidium Iodide were added to the media to label the membrane and nucleic acids of the microvesicles, respectively.

3.2.10. Statistical Analysis

The data are represented as the means ± S.E. Unpaired Student's *t* test and two-way ANOVA with Bonferroni post-test statistical analyses were performed using Prism/GraphPad software.

3.3. Results

3.3.1. Wild type p53 is an endogenous regulator of the CS-Pathway.

Although the functions of the CS-pathway have been probed through pharmacological inhibition and siRNA knockdown [94, 189], it is unclear whether and how CHK1 inhibition can be regulated endogenously. Therefore we set out to determine whether wild type p53 plays a role in the CS-pathway through regulation of CHK1. To this end, levels of p53 and CHK1 were assessed as well as Caspase 2 processing in a time and dose dependent manner in response to doxorubicin in MCF7 breast cancer cells that are wild type for p53. As shown in Figure 1A, doxorubicin dose-dependently resulted in p53 accumulation, and this was accompanied by

CHK1 down regulation at the protein **(Figure 1A)** and message level **(Figure 1B).** This was also accompanied by Caspase 2 processing. Next to determine the kinetics of p53 accumulation, CHK1 down regulation, and Caspase 2 activation, a time course assay was performed using 0.8uM doxorubicin, a dose in which CHK1 levels were approximately 80% reduced at the protein level and there was a significant reduction in pro-Caspase 2 (Figure 1A). Consistent with the dose response, p53 accumulation was concomitant with a significant down regulation of CHK1 followed by Caspase 2 processing **(Figure 1C).** Caspase 2 activation was also observed in approximately 60% of total cells at 24 hours, as measured by Bimolecular Fluorescence Complementation (BIFC) **(Figure 1D).** Representative BIFC confocal images are shown in **Figure 1E**.

Next, to determine whether the observed CHK1 down regulation was p53-mediated siRNA was used to deplete p53 in order to access the effects on CHK1 levels and Caspase 2 processing 24 hours after doxorubicin treatment. Indeed p53 knockdown not only rescued CHK1 down regulation but also restored levels of pro Caspase 2 **(Figure 1F).** To corroborate these data, the p53 isogeneic colon cancer cell lines HCT-116 either wild type (+/+) or null (-/-) for p53 were investigated. The HCT-116 p53+/+ cells showed down regulation of CHK1 and Caspase 2 processing upon doxorubicin treatment that was abrogated in the HCT-116 p53-/- cells, similar to p53 knockdown in MCF7 cells **(Figure 1G).**

Collectively, these data provide evidence that p53 is a regulator of the CS-pathway and Caspase 2 activation at the level of CHK1.

3.3.2. The CS-Pathway can be activated in wild type p53 cells

Next to investigate whether abrogation of CHK1 signaling results in Caspase 2 activation in wild type (WT) p53 cells, two different methods were employed: depletion of CHK1 by siRNA (Figure 2A) and inhibition of CHK1/2 activity through the use of the ATP competitive inhibitor AZD-7762 (Figure S1A) in combination with 0.4uM doxorubicin, a low dose where CHK1 levels remain detectable and Caspase 2 processing is minimal **(Figure 1A).** The results showed that in the absence of CHK1 there was an approximately 50% reduction in pro-Caspase 2 upon doxorubicin treatment at 0.4uM concentration compared to doxorubicin alone **(Figure**

2A). Similarly under the same conditions, inhibition of CHK1 activity resulted in a decrease in pro-Caspase 2 **(Figure S1A)** as well as a 2-fold increase in the number of Venus-positive cells with CHK1 inhibition in combination with 0.4uM doxorubicin compared to doxorubicin alone as measured by BIFC microscopy **(Figure S1B).** Also of note, CHK1 knockdown resulted in the abrogation of doxorubicin-induced G2/M arrest and a significant increase in the amount of apoptotic cells **(Figures 2B and C)**, suggesting that apoptosis can be achieved at a lower dose of doxorubicin in combination with inhibition/loss of CHK1 in WT p53 cells.

Altogether these data suggest that the CS-pathway can be activated in wild type p53 cells at low dos of doxorubicin to initiate cell death as opposed to cell cycle arrest.

3.3.3. P53 deficiency triggers deregulation of the CHK1-Caspase 2 pathway

It was recently demonstrated that targeting CHK1 is therapeutically beneficial in p53 deficient cells as well as in triple negative breast cancers (TNBC), which harbor alterations in p53 at a frequency of approximately 40% of cases [75, 92, 217]. Given the clinical relevance of targeting CHK1 in p53-mediated cancers and my data that demonstrate that wild type p53 regulates CHK1 and the CS pathway, we set out to investigate whether p53 deficiency promotes deregulation of the CHK1-Caspase 2 pathway.

Therefore, it became important to investigate whether the CHK1-Caspase 2 pathway is deregulated in the TNBC cell line MDA-MB-231 that also harbors a missense mutation R280K in p53. In contrast to MCF7 cells, doxorubicin treatment did not result in down regulation of CHK1 **(Figure 3A).** Next to determine whether Caspase 2 was activated in MDA-MB-231 cells in response to doxorubicin BIFC microscopy was utilized. MDA-MB-231 cells showed no significant increase in Caspase 2 dimerization after doxorubicin treatment from vehicle treated cells **(Figure 3B).** Representative images are shown in **Figure 3C**. Similarly, a doxorubicin dose response was also performed. Down regulation of CHK1 was not observed at any dose tested at the protein **(Figure 3D)** or message **(Figure 3E)** level nor was there a decrease in pro-Caspase 2 **(Figure 3D).**

Moreover, to determine whether deregulation of the CHK1-Caspase 2 pathway occurred in other cell lines with p53 deficiency, humanized mutant p53 knock-in (HUPKI) mouse

embryonic fibroblasts (MEFs) harboring the G245S hotspot mutation were treated with doxorubicin. Similar to MCF7 cells, WT MEFs showed significant down regulation of CHK1 and processing of pro- Caspase 2 in response to doxorubicin that was abrogated in G245S MEFS **(Figure S2A).**

Collectively these data establish that p53 deficiency results in sustained cellular CHK1 levels in response to genotoxic stress which acts to inhibit Caspase 2 activation whereas p53 sufficiency can launch the CS-caspase2 pathway at least upon induction of the DDR.

3.3.4. CHK1 levels regulate NF-κB signaling in p53 deficient cells in response to doxorubicin

As mentioned previously, two distinct PIDDosome signaling complexes have been identified that exert opposing effects within the cell; one resulting in Caspase 2 activation and a second that activates prosurvival NF-κB signaling. In light of the results from Figure 2, demonstrating that p53 deficient cells display high levels of CHK1, which acts to inhibit Caspase 2 activation, we set out to determine whether NF-κB activity is induced in response to doxorubicin via the alternate PIDDosome. To this end, experiments were performed to determine whether doxorubicin induced degradation of IKB-α, an inhibitor of NF-κB translocation to the nucleus and subsequently NF-κB activity in MDA-MB-231 cells. Indeed, upon doxorubicin treatment of MDA-MB-231 cells, IKB-α became almost undetectable, reduced at the protein level by approximately 95%, while in MCF7 cells there was no significant reduction in IKB-α levels **(Figure 4A)**. Interestingly, PIDD auto-processing also differed between these two cells lines. PIDD-C, the fragment associated with NF-κB activation was the predominant fragment in MDA-MB-231 cells upon doxorubicin treatment, while the fragment associated with Caspase 2 activation, PIDD-CC, was the most abundant fragment in MCF7 cells after treatment with doxorubicin **(Figure 4A)**. Given the prosurvival signaling associated with NF-κB activity it was important to determine whether CHK1 knockdown could abrogate IKB-α degradation and therefore inhibit NF-κB activity. As shown in **Figure 4B**, loss of CHK1 abolished IKB-α degradation and induced Caspase 2 processing in MDA-MB-231 cells. To corroborate these data in a functional manner, NF-κB promoter activity was measured. As shown in **Figure 4C** an approximate 1.8-fold increase in NF-κB promoter activity was observed upon doxorubicin

treatment that was brought back to baseline upon CHK1 knockdown in MDA-MB-231 cells. Similar results were also observed in the HUPKI G245S MEFs using the CHK1/2 inhibitor AZD7762. **(Figure S3A)**. In accordance with the data from **Figure 4A**, no induction in NF-κB promoter activity was observed in MCF7 upon doxorubicin treatment **(Figure S3B)**. Therefore, these results suggest that loss or inhibition of CHK1 could abrogate doxorubicin-induced NF-κB signaling in mutant p53 cells.

To determine the biological significance of doxorubicin-induced NF-κB signaling and the effect of CHK1 knockdown, levels of chemokines and cytokines of which many are known targets of NF-κB were evaluated by utilizing a quantitative PCR array. Of the 84 genes examined, 81% of the genes were down regulated with 20% of these genes showing significant down-regulation greater than 2-fold upon doxorubicin treatment of MDA-MB-231 cells in combination with CHK1 knockdown compared to doxorubicin alone **(Table 2)**. Moreover, real time PCR analysis using independent primers of several genes found to be significantly down regulated in the PCR array confirmed the array results. Loss of CHK1 significantly reduced the doxorubicin-mediated induction of the chemokines CXCL1, CXCL10, IL8 and the cytokines IL-6 and BMP4 (a member of the TGF-B family) at the mRNA level **(Figure 4D)**. **Figure 4E** shows significant knock down of CHK1 at the message level. In order to confirm the changes in mRNA after doxorubicin treatment was also reflected in secreted protein levels, an ELISA for both BMP4 and IL6 was performed. Significant increases in secreted BMP4 protein was observed at 36 hours after doxorubicin, increasing over time to an approximately 4-fold increase at 48 hours **(Figure 4F)**. Similarly, a 3-fold increase in secreted IL6 protein was observed at 24 hours post-doxorubicin treatment **(Figure S3C)**. Next, to confirm CHK1 knockdown resulted in a reduction in the amount of secreted BMP4 protein, a subsequent ELISA was performed. Indeed, CHK1 knockdown in combination with doxorubicin treatment resulted in a significant reduction in the amount of secreted BMP4 compared to doxorubicin treatment alone at 36 hours **(Figure 4G)**.

Taken together these results, define a novel role for CHK1 outside of its role in the cell cycle in regulating the inflammatory response of p53-deficient cells to the chemotherapeutic doxorubicin.

3.3.5. Doxorubicin induces the shedding of tumor-derived microvesicles containing inflammatory mediators

Communication between cells mainly involves the secretion of soluble proteins, such as BMP4 and IL6 from Figure 3, that interact and elicit signaling responses through binding of receptors on neighboring cells [218] but over the past decade, another form of cellular communication via the release of membrane microvesicles has emerged [219, 220]. Research has shown that tumor-derived microvesicles (TMVs) are shed from very invasive and aggressive cancer cells such as MDA-MB-231 cells and these membrane-bound vesicles contain genetic information that can be transferred to recipient cells and can therefore greatly effect the tumor microenvironment [221, 222]. Interestingly during confocal experiments a number vesicles were observed that increased in number upon doxorubicin treatment; therefore it became important to determine whether MDA-MB-231 cells shed TMVs and whether these TMVs contain inflammatory mediators in response to doxorubicin.

To this end confocal microscopy was used to investigate whether MDA-MB-231 shed TMVs in response to doxorubicin treatment. Annexin-V was used to detect TMVs since the membranes of these vesicles have been established to contain phosphatidylserine, and propidium iodide was used to label nucleic acids within the TMVs. As shown in **Figure 5A**, approximately 20% of vehicle treated cells were observed to shed TMVs while doxorubicin induced the shedding of microvesicles in approximately 80% of the total number of cells counted. **Figure 5B** shows a confocal image of a cell treated with doxorubicin and the significant amount of shed TMVs containing nucleic acids. A time-lapse video showing recruitment of TMVs to surrounding cells is shown in **Figure S4A**. Next to examine the mRNA cargo inside these vesicles, differential centrifugation was used to isolate TMVs found within the 50,000xg pellet followed by RNA extraction and real-time PCR. Interestingly, the mRNA of a number of chemokines and cytokines IL6 **(Figure 5C)**, BMP4 **(Figure 5D)** and VEGF **(Figure 5E)** were found to be significantly elevated in the TMVs from the doxorubicin treated cells compared to vehicle. To ensure the population of microvesicles isolated was pure, a marker of tumor microvesicles, Arf6 was utilized. Western blot analysis showed the presence of Arf6 exclusively

in the 50,000xg pellet and enriched in the doxorubicin sample while it was absent in the 100,000xg pellet that should contain exosomes (Figure S4B).

All together these data establish that TMV shedding in MDA-MB-231 cells is significantly increased in response to doxorubicin. Also, the TMVs similar to the cells contain elevated levels of chemokines and cytokines that can not only affect the tumor microenvironment, but also travel long distances to affect cells in distant sites, such as sites of metastasis.

3.3.6. Loss of CHK1 alters the cargo of TMVs

Next the role of CHK1 in regulating TMVs and/or their cargo was investigated. Initial studies showed that CHK1 knockdown did not affect the number of microvesicles secreted (data not shown). Next, real time PCR was performed on the 50,000xg pellet, and the results showed that loss of CHK1 significantly reduced the doxorubicin-mediated induction of the chemokines and cytokines IL6 **(Figure 6A)**, VEGF **(Figure 6B)** and BMP4 **(Figure 6C)** in the isolated TMVs compared to doxorubicin alone.

All in all these data establish that CHK1 can modulate the cargo of TMVs by regulating the levels of inflammatory mediators within the cell.

3.4. Discussion

In conclusion, my data provide new insight into why wild type p53 has evolved to down regulate CHK1 and also insight into the deleterious effects on this regulatory network when p53 is altered. This work identified the first physiological example of the CS-pathway and established that WT p53 acts as an endogenous inhibitor of CHK1 upon DNA damage to activate the CS-pathway. In p53-deficient cells, we demonstrate a novel role for CHK1 in regulating NF-κB activity and the production inflammatory chemokines and cytokines within the cell and also within TMVs in response to genotoxic stress. The significance of these findings is underscored by the fact that CHK1 has already been identified as an important pharmacological target. Importantly thus far two possible mechanisms have been proposed to explain CHK1

inhibitor sensitivity: increased oncogenic replicative stress and reduced DNA repair capabilities, both of which are associated with CHK1's role in the cell cycle. My work identifies a potential novel mechanism for CHK1 inhibitor sensitivity, through regulation of the NF-κB pathway.

P53 mediates effects through the activation of many genes that regulate cell cycle checkpoints, DNA damage and repair and apoptosis [223], although transcriptional independent roles of p53 are emerging [224]. Interestingly, several reports have demonstrated p53-mediated down-regulation of the cell cycle protein CHK1 [211, 212]. Although these studies only speculate as to why p53 has evolved to down regulate CHK1, Lezina and collegues correlate disruption of this regulatory pathway with poor prognosis and decreased survival of breast cancer patients [212]. This study identifies a novel role of p53-mediated down regulation of CHK1 in activating the CS-pathway leading to Caspase 2 activation.

As p53 is mutated or deleted in over half of all human cancers [225], we set out to determine whether alterations of p53 promote deregulation of the CHK1-Caspase 2 pathway. We demonstrate that p53-deficiency promotes sustained CHK1 levels in the presence of genotoxic stress. In accordance, with previous studies [94, 189] we show that high CHK1 levels inhibit the CS-pathway and Caspase 2 activation but in addition we also establish a novel function for CHK1 in regulating NF-κB activity and the production of inflammatory mediators in p53-deficient cells in response to doxorubicin. The role of CHK1 in regulating cell cycle progression is well established [226, 227] and the development of specific pharmacological inhibitors of CHK1 is an intense area of research as CHK1 inhibition has been shown to promote death via "mitotic catastrophe" specifically in p53-deficient cells [75, 92]. The data reveal a novel role of CHK1 outside of its cell cycle responsibilities, providing evidence that CHK1 is a mediator of pro-survival NF-κB signaling and ultimately the production of inflammatory mediators such as IL6, VEGF and BMP4 that can augment tumor progression and that have been associated with angiogenesis and metastasis in breast cancer cells. Of note several recent studies have shown that p53-deficiency promotes NF-κB signaling [228, 229]. Specifically, it was demonstrated that mutant p53 via gain-of-function activity prolongs NF-κB activation and promotes chronic inflammation and inflammation-associated colorectal cancer *in vivo* [228]. Moreover, Dalmases *et al.* established that p53 deficiency is necessary for doxorubicin induced

transcriptional activation of NF-κB target genes associated with invasion in human breast cancer and this was correlated with reduced disease free-survival of breast cancer patients [229]. In light of these data, the authors hypothesize that targeting NF-κB in p53-deficient cancers that respond to chemotherapeutics by activating NF-κB could be therapeutically beneficial. My work in unraveling the mechanism that drives p53-deficient cells to activate NF-κB in response to doxorubicin, provide evidence that inhibiting CHK1 in these cancers maybe a better alternative, as targeting transcription factors has proven challenging [230].

Interestingly, we also found that doxorubicin treatment of MDA-MB-231 cells resulted in a significant increase in the amount of shed TMVs and the enrichment of a number of chemokines and cytokines inside these vesicles. TMVs are carriers of molecular information that act as signaling platforms, diffusing into the extracellular space to target cells in the microenvironment, modulate the interactions of tumor cells and also prime the formation of the metastatic niche [219, 222]. The packaging of chemokines and cytokines inside TMVs provides another means of cell-to-cell communication outside of conical secretory pathways that can greatly influence the tumor microenvironment. We found that although loss of CHK1 does not affect the amount of vesicles shed, it does modulate the cargo within the vesicles, significantly reducing the levels of a number of chemokines and cytokines compared to doxorubicin treatment alone.

TMVs have recently gained attention as potential biomarkers as tumor cells release these vesicles into body fluids such as urine, blood and saliva where they can then be isolated and analyzed [219, 231]. Interestingly, the data 47phingolipi that TMVs become enriched with chemokines and cytokines in response to doxorubicin in p53-deficient cells, mirroring what occurs inside the cell. This is important because as mentioned previously, several studies have shown poor therapeutic outcome in cancers that activate NF-κB in response to chemotherapeutics [229, 232]. These data provide evidence that isolating TMVs from body fluids may provide a rapid, noninvasive and economical way to monitor therapeutic efficacy specifically in cancers where repeated biopsies are not feasible and allow for early modulation of therapeutic regime.

In conclusion, the results establish a novel benefit of CHK1 inhibition, outside of promoting "mitotic catastropohe," in the inhibition of NF-κB signaling in response to genetoxic stress in p53 deficient cells; thus providing more evidence in support of discovering new more specific CHK1 inhibitors. Although this work begins to establish CHK1 as a critical downstream target of p53 tumor suppressor activity and to unravel the multiple signaling contexts outside of the cell cycle that are effected by CHK1 inhibition further studies are needed to fully elucidate this signaling network and are essential for successful therapeutic development of CHK1 inhibitors.

Chapter 4

Caspase 2 is Required for Sphingosine Kinase 1 Proteolysis in Response to Doxorubicin in Breast Cancer Cells: Implications to the CHK1-Suppressed Pathway

Abstract

Sphingosine Kinase 1 (SK1) is a lipid kinase whose activity produces the potent bioactive lipid sphingosine 1-phosphate. Sphingosine 1-phosphate is a pro-survival lipid associated with proliferation, angiogenesis and invasion; subsequently SK1 overexpression has been observed in numerous cancers. Recent studies have demonstrated SK1 proteolysis downstream of the tumor suppressor p53 in response to several DNA damaging agents. Moreover, loss of SK1 in p53 knockout mice resulted in complete protection from thymic lymphoma providing evidence that regulation of SK1 constitutes a major tumor suppresser function of p53. Given this profound phenotype, this study aims to investigate the mechanism by which wild type p53 regulates proteolysis of SK1 by doxorubicin in breast cancer cells. We find that p53-mediated activation of Caspase 2 was required for SK1 proteolysis and that Caspase 2 activity significantly alters the levels of endogenous sphingolipids. As p53 is mutated in 50% of all cancers, we extended the studies to investigate whether SK1 is deregulated in the context of triple negative breast cancer cells (TNBC) harboring a mutation in p53. Indeed Caspase 2 was not activated in these cells and SK1 was not degraded. Moreover, Caspase 2 activation was recently shown to be downstream of the CHK1-Suppressed pathway in mutant p53 cells, whereby inhibition of the cell cycle kinase CHK1 leads to Caspase 2 activation and apoptosis. Indeed knock-down and inhibition of CHK1 led to loss of SK1 in p53 mutant TNBC cells, providing evidence that SK1 maybe the first identified effector of the CHK1-Suppressed pathway.

4.1. Introduction

Bioactive sphingolipids are recognized as important signaling molecules that play significant roles in a diverse array of biological processes from cell death and senescence to cell survival and proliferation [99, 233]. Sphingolipid metabolism is a multifaceted and interconnected network consisting of many enzymes that are responsible for coordinating the production of bioactive lipids that at times may elicit very opposing effects within the cell; therefore the activity of the enzymes in this network must be tightly regulated.

Sphingosine Kinase 1 (SK1) is an important sphingolipid enzyme that is involved in maintaining the balance between the pro-survival lipid and product of its kinase activity, sphingosine 1-phosphate (S1P), and the upstream pro-apoptotic sphingolipid metabolites, ceramide and sphingosine; therefore alterations in SK1 activity could have critical impact on cell fate. In line with this, previous work from our laboratory showed that SK1 mRNA and protein levels are significantly increased in numerous types of human cancers [179, 234]. Subsequent complimentary work from several other labs has demonstrated that deregulation of the SK1/S1P pathway plays a role in carcinogenesis and promoting cancer cell viability as well as chemotherapeutic resistance [235-239]. In addition there is an emerging body of literature implicating SK1 as a critical downstream target of the tumor suppressor p53 in response to DNA damage. Previous work from our laboratory showed that actinomycin D (Act-D) induces SK1 degradation in Molt-4 T-Cell leukemia cells, and this degradation is rescued in Molt-4 cells overexpressing the papilloma virus E6 protein, which targets p53 to degradation, suggesting SK1 proteolysis is p53-mediated. This work also showed that pretreatment of Molt-4 cells with the pan-caspase inhibitor Z-VAD rescued SK1 degradation in response to Act-D suggesting that SK1 proteolysis is Caspase mediated [183]. Building on this work, Heffernan-Stroud *et al.* showed that UVC-induced SK1 proteolysis in WT mouse embryonic fibroblast (MEFs) is abrogated in p53 null MEFs (p53-/-) [185]. This led to the hypothesis that SK1 could be deregulated (i.e does not get proteolyzed) in p53 null tissues. Indeed in that study it was also demonstrated that SK1 was overexpressed and more active in the thymus of p53 null mice. Moreover, deletion of SK1 in p53 null mice completely abrogated thymic lymphomas in the double knockout mice and prolonged life span by approximately 30% compared to p53-/- mice with SK1 [185].

The above data provide strong evidence, identifying SK1 as an important downstream target of the tumor promoting activity in null p53 mice, although many questions still remain as to the exact mechanism of SK1 proteolysis in cancer cells in response to DNA damage, and whether this pathway is perturbed in mutant p53 cells. As a corollary, what are the biologic implications to loss of SK1 in mutant p53 cancers?

Although there are hints in the literature that SK1 proteolysis in response to DNA damage maybe caspase-mediated [183, 185], these studies utilized caspase inhibitors that lack the specificity to monitor the activity of a specific caspase as the common peptide sequences used have been demonstrated to inhibit many members of the Caspase family [240]. Moreover, p53 activity is well documented to be involved in the activation of a number of caspases [241, 242]; nevertheless, a strong connection between p53 and the poorly studied Caspase 2 is emerging via its activation platform, the PIDDosome [70]. The PIDDosome consists of three proteins, PIDD (p53-induced death domain protein) that interacts with RAIDD (RIP associated Ich-1/CED homologous protein with death domain) via their Death Domains (DD) and Caspase 2 which is recruited to RAIDD via the caspase recruitment domain (CARD) present in both proteins. Once assembled, full-length Caspase 2 can then undergo auto-proteolytic cleavage producing the fully active enzyme [70].

To date only sixteen substrates of Caspase 2 have been identified [243], whose physiological functions range from vesicular trafficking and translation initiation to cell cycle regulation and apoptosis. In addition Caspase 2-/- mice are viable, fertile and show now overt phenotype further confounding efforts to define a physiological function for Caspase 2 [244, 245]**.** Interestingly, a novel Caspase 2 dependent apoptotic pathway termed the CHK1-Suppressed pathway was recently identified such that loss or inhibition of the cell cycle checkpoint kinase CHK1 in the presence of mutant p53 promotes a Caspase 2-mediated apoptotic response to DNA damage. However, critical downstream targets and components of this pathway are yet to be identified [94, 189].

In light of the above data, we hypothesized that Caspase 2 may mediate p53-dependent SK1 proteolysis in response to DNA damage. To test this hypothesis we evaluated whether SK1 proteolysis is downstream of Caspase 2 activation using a variety of methods in WT p53 human

breast cancer cells and also whether Caspase 2 is required for SK1 proteolysis using both biochemical and genetic models. Given that p53 mutations occur in 50% of all human cancers [246-248] and in a high proportion of Triple Negative Breast Cancers (TNBC) cells [217] we next wanted to extend these studies to investigate whether Caspase 2 activation and SK1 proteolysis is deregulated in these situations and if so, whether SK1 proteolysis can be restored by activation of the CHK1-Suppressed pathway in mutant p53 TNBC cells.

4.2. Experimental Procedure

4.2.1. Chemicals and Reagents

Lipofectamine® RNAiMAX and Annexin-V and Propidium Iodide were purchased from Life Technologies (Grand Island, NY). X-tremeGENE 9 DNA Transfection Reagent was purchased from Roche Diagnostics (Indianapolis, IN). iTAQ and SYBR® Green master mix master mix was purchased from Bio-Rad (Hercules, CA). CHK1/2 inhibitor AZD7762 purchased from Selleckchem (Houston, TX). Doxorubicin hydrochloride and cyclohexamide purchased from Sigma Aldrich (St. Louis, MO). D-*erythro*-sphingosine (C17 base) purchased from Avanti Polar Lipids (Alabaster, AL). Thiazoyl Blue Tetrazolium Bromide –MTT purchased from Amresco (Solon, OH). Ski-II (4-[4-(4-chloro-phenyl)-thiazol-2-ylamino]-phenol was purchased from Cayman Chemical (Ann Arbor, MI).

4.2.2. Cell Culture and siRNA

MCF7 and MDA-MB-231 cells were purchased from ATCC and cultured in RPMI 1640 medium and Dulbecco's modified Eagle's medium (DMEM), respectively with 10% fetal bovine serum (FBS) both from Life Technologies (Grand Island, NY). WT and Cas2-/- MEFs were a kind gift from Dr. Douglas Green (St. Jude's Children Hospital) and cultured in Dulbecco's modified Eagle's medium (DMEM) with 10% fetal bovine serum (FBS) both from Life Technologies (Grand Island, NY). Before all doxorubicin treatments, the media was changed on cells to fresh new media. Gene silencing was then carried out using siRNA directed against human SK1 (target sequence 5′-AAGGGCAAGGCCTTGCAGCTC-3) and all-star siRNA as a

negative control purchased from Qiagen. The siRNA directed against CHK1 and p53 were validated predesigned sequences from Invitrogen. Transfections were carried out using Lipofectamine® RNAiMAX from Life Technologies (according to the manufacturer's protocol). For siRNA experiments, cells were seeded into 60-mm plates at ~75,000 cells/dish and treated with 20 nM siRNA for 48 h prior to stimulation.

4.2.3. RNA isolation and quantitative RT-PCR

RNA extraction and cDNA synthesis were carried out using PureLink® RNA Mini Kit (Life technologies) and Quanta qScript cDNA SuperMix (Quanta Biosciences) respectively and according to the manufacturer's. The cDNA was then diluted (1:15) in RNAse-free water, and 5 µl was used in a total reaction volume of 20 µl. For each 20-µl real-time PCR, a ratio of 10:1:4 (iTaq: Taqman probe (20X): nuclease-free water) was used. PCR was performed using the Applied Biosystems 7500 Real-Time PCR System (Applied Biosystems, Foster City, CA, USA). The following Taqman probes (life technologies) were used: mouse SK1 (Mm00448841_g1), mouse SK2 (Mm00445021_m1). Cycle threshold (Ct) values were obtained for each gene of interest and *β-actin*. ΔCt values were calculated and the relative gene expression normalized to control samples was calculated from ΔΔ Ct values.

4.2.4. Western Blot Analysis

Cultured or transfected cells were washed with ice cold PBS and then directly lysed in cold RIPA buffer containing 1 mM sodium orthovanadate, 2 mM PMSF, and protease inhibitor cocktail (Santa Cruz Biotechnology). Cellular lysates were then clarified by centrifugation at 14,000 rpm for 10 min at 4^{o}C; protein concentration was quantitated by BCA Protein Assay kit from Thermo Scientific (Suwanee, GA). Equal amounts of protein (25 µg) were boiled in Laemmli buffer (Boston Bio Product), and separated on SDS-PAGE (4-15%, Tris-HCl) using the Bio-Rad Criterion system. Separated proteins were then transferred onto nitrocellulose membranes (Bio-rad) and blocked with 5% non-fat milk in PBS-0.1% Tween-20 (PBS-T) for at 1 hour at RT. Primary antibodies diluted 1:1000 or 1:20000 for β-actin and GADPH were then

added to membranes and incubated at 4 °C overnight. Membranes were washed 3 times with PBS-T then incubated with diluted 1:5000 HRP-conjugated secondary antibodies for 1 hour at room temperature. Membranes were then washed for 1 hour, incubated with Pierce ECL Western Blotting Substrate (Pierce) and exposed to X-ray films that were then processed and scanned. Anti-SK1, anti-total CHK1, anti-Phospho (296)-CHK1, anti-p53, anti-Caspase 2 and anti-GAPDH were from Cell Signaling Technology (Danvers, MA). RIPA lysis buffer system, HRP-labeled secondary antibodies and anti-PARP were from Santa Cruz Biotechnology (Santa Cruz, CA). Anti-CERT was from Bethyl Laboratories (Montgomery, TX). Anti-Caspase 2 (clone 11B4) was from Millipore (Billerica, MA).

4.2.5. Sphingolipidomic Analysis

Following the indicated treatment, cells were directly lysed with 2mL of 2:3 ratio of 70% isopropanol/ethyl acetate, followed by gentle scraping of the cell from the culture plate. Lysate was then transferred to 15 ml falcon tubes. Upon addition of internal standards to the tubes, samples were then briefly centrifuged at 2000 × g and the upper phase was transferred to a new glass tube. An additional round of extraction was performed on the remaining volume. After combining the two extracts, sphingolipids and inorganic phosphates were measured by the Lipidomics Core Facility at the Stony Brook University of New York using HPLC/MS determination of sphingolipid mass levels as described previously [249].

4.2.6. C17-Sph labeling

Cells were plated at ~150,000 cells/60-mm dish. Fifteen minutes prior to the end of treatment time cells were incubated with 1 μM C17 sphingosine for the remaining fifteen minutes. The cells were then washed with PBS and 2mL of cell extraction mixture (2:3 70% isopropanol/ethyl acetate) was then directly added to the cells. The cells were then gently scraped and extracts were sent for analysis at the Lipidomics Core Facility of Stony Brook University Medical Center as described above and previously [249].

4.2.7. Bimolecular Fluorescence Complementation

As described previously [215, 216]. Briefly, ~75,000 cells were grown on poly-D-lysine-coated 35-mm confocal dishes (MatTek Corporation) overnight. The following day cells were transiently transfected with C2-CARD VN (500ng) and C2-CARD VC (500ng) along with pshooter.dsRed-mito (250ng) as a reporter for transfection. Twenty-four hours after transfection, cells were treated with doxorubicin for 24h and then the percentage of pshooter.ds.Red-mito-positive (red) cells that were Venus positive (green) was determined from a minimum of 100 cells per plate. Live cell imaging was conducted using a Leica TCS SP8 scanning-laser confocal microscope in a chamber at 37 °C and 5% CO_2. The plasmids pBIFC-C2-CARD VC and pBIFC-C2-CARD VN were kindly provided by Dr. Douglas Green (St. Jude's Children Hospital). pDsRed-Mito purchased from Clonetech (Mountain View, CA).

4.2.8. Flow Cytometric Analysis of Apoptosis

Apoptotic cells were detected by Annexin-V/Propidium Iodide (PI) staining using Alexa Fluor® 488 Annexin V and PI detection kit (Life Technologies, Grand Island, NY) according to the manufacturer's protocol. Briefly, after the indicated treatment cells were trypsinized, collected by brief centrifugation and washed with ice-cold PBS. Cells were then re-suspended in buffer containing Alexa Fluor® 488 Annexin-V and PI (at concentrations indicated in manufacture's protocol) for 15 min at room temperature and in the darkness. After incubation cells were immediately analyzed using a Becton Dickinson FACSCalibur. Ten thousand events were acquired on the FACSCalibur (Becton Dickinson Biosciences, San Jose, CA, USA) and followed by analysis with CellQuest (Becton Dickinson) software.

4.2.9. MTT Assay

Cells were plated at ~150,000 cells/well in a 6-well plate. After indicated treatment, media was replaced with 1mL of fresh media with 1mL of 12mM MTT (Amresco) solution and incubated at 37 °C in the dark for thirty minutes. The media/MTT mixture was then replaced with 2mL of DMSO and incubated with gently rocking for ten minutes. Following incubation,

200uL from each well in triplicate was then assayed in 96-well plate using a spectrophotometer at 570nm.

4.2.10. Caspase Activity Assay

Caspase 3 activity was measured using BioVision (Milpitas, CA) Caspase-Family Fluorometric Substrate Set according to the manufacturer's protocol. Briefly, ~150,000 cells/well were plated in a 6-well plate. The following day cells were treated accordingly in addition to control cells. Cells were lysed with 50uL of cell lysis buffer and protein concentration determined by BCA Protein Assay kit from Thermo Scientific (Suwanee, GA). In a 96-well plate, a total of 50ug of cell lysate in a volume of 50uL was added to 50uL of 2X reaction buffer containing 10mM DTT and 5uL of the AFC-conjugated Caspase 3 substrate, AC-DEVD-AFC. Samples were incubated at 37 °C in the dark for one hour and then read by a fluorometer equipped with a 400-nm excitation filter and 505-nm emission filter.

4.2.11. Statistical Analysis

The data are represented as the means ± S.E. Unpaired Student's *t* test and two-way ANOVA with Bonferroni post-test statistical analyses were performed using Prism/GraphPad software.

4.3. Results

4.3.1. P53-mediated SK1 proteolysis is downstream of Caspase 2 activation

Doxorubicin is an anthracycline frequently used in the treatment of breast cancer. It is a well-known inducer of p53 [250], has been shown to initiate p53-dependent SK1 proteolysis [183], and to induce apoptosis in a number of cell lines via Caspase activation [246, 250]. Several studies have demonstrated Caspase 2 activation upon doxorubicin treatment in a number of cell systems including leukemia cells, mouse embryonic fibroblasts (MEFs) and mouse oocytes. These studies also showed that loss of Caspase 2 in these cells results in significantly

reduced sensitivity to doxorubicin compared to control cells [244, 251]; albeit effects in breast cancer cells have not been studied. We therefore first set out to determine whether doxorubicin activates Caspase 2 in wild type p53 MCF7 breast cancer cells and also whether SK1 proteolysis is downstream of Caspase 2 activation.

A dose response of doxorubicin revealed that with increasing dose from 0.2uM to 1uM, p53 accumulation was followed by a significant reduction in pro-Caspase 2 that was concomitant with loss of SK1 at the protein level **(Figure 7A).** These data are consistent with previous studies showing that loss of SK1 by genotoxic stress is a post-translational event [183, 185]. Similarly, a time course using 0.8uM doxorubicin showed substantial accumulation of p53 at eighteen hours, corresponding with significant processing of full-length Caspase 2 followed by almost complete loss of SK1 protein by twenty-four hours **(Figure 7B).** To further validate activation of Caspase 2, 0.8uM doxorubicin was used at twenty-four hours to monitor cleavage of full-length Caspase 2 into its active fragments by western blot as well as dimerization of Caspase 2 as measured by Bimolecular Fluorescence Complementation (BIFC) [216]. As shown in **Figure 7C**, there was significant accumulation of the cleaved form of Caspase 2 concurrent with an approximate 80% reduction in SK1 at the protein level, as quantified in **Figure 7D**. In accordance with the western blot data, Caspase 2 activation was observed in approximately 60% of transfected cells counted at 24 hours after doxorubicin treatment as measured by BIFC **(Figure 7E).** Representative images from the BIFC experiment are shown in **Figure 7F**. Taken together, these results show activation of caspase 2 in response to doxorubicin in a time frame corresponding to the loss of SK1.

4.3.2. Doxorubicin significantly alters sphingolipid metabolism

Next to investigate whether doxorubicin-induced SK1 proteolysis results in a decrease in SK activity, the incorporation of C_{17}-Sphingosine into C_{17}-S1P was measured. As shown in **Figure 8A**, upon doxorubicin treatment there was approximately a 50% reduction in the incorporation of C_{17}-Sphingosine into C_{17}-S1P, demonstrating attenuation of ongoing SK activity. In agreement with this reduction in SK activity, a significant increase in SK's endogenous substrate sphingosine was observed **(Figure 8B)** as well as a 1.5-fold increase in

total ceramide **(Figure 8C).** Moreover, although SK activity was significantly decreased **(Figure 8A)** we observed an increase in endogenous S1P at 0.8uM upon doxorubicin treatment. To further investigate S1P levels upon doxorubicin treatment, we performed a dose response from 0.6uM to 1uM. Interestingly although S1P levels are increased at 0.8uM doxorubicin they are decreased from 0.6uM doxorubicin, a dose where SK1 is not proteolyzed and S1P levels decreased further at a higher dose of 1uM doxorubicin **(Figure 8D)**. S1P levels are maintained in the cell via the action of a number of enzymes, SK1 and SK2, which are responsible for its production and also a S1P lyase and phosphatases which are responsible for its breakdown; therefore these results can be explained for instance through action of SK2 or delayed breakdown of S1P by the lyase or phosphatase. These results demonstrate a biochemical and functional role for the effects of doxorubicin on SK1 activity and the levels of key bioactive sphingolipids.

4.3.3. Caspase 2 activation and SK1 proteolysis are p53-mediated

To consolidate that Caspase 2 activation and subsequent SK1 proteolysis are p53-mediated, we depleted p53 in MCF7 cells by siRNA. Indeed, loss of p53 abrogated both processing of full-length Caspase 2 and proteolysis of SK1 **(Figure 9)**.

These data indicate for the first time and using a variety of different methods that the chemotherapeutic doxorubicin as an inducer of Caspase 2 activation in MCF7 breast cancer cells. These data also provide strong evidence that SK1 proteolysis is accompanied by Caspase 2 activation in response to doxorubicin in a time and dose dependent manner both of which are abrogated in the absence of p53.

4.3.4. Caspase 2 is required for SK1 proteolysis in response to DNA damage

Next in order to build on the findings of a mechanistic connection between genotoxic stress, p53, Caspase 2 activation, and SK1 proteolysis, we set out to investigate whether Caspase 2 is required for SK1 degradation. To this end we employed two methods, a siRNA approach in MCF7 cells and a genetic model using mouse embryonic fibroblasts (MEFs) expressing wild type Caspase 2 (WT) or with Caspase 2 knocked out (Cas2-/-). As shown in **Figure 10A**

depletion of Caspase 2 by siRNA significantly abrogated doxorubicin-induced SK1 proteolysis compared to All-Star siRNA transfected cells. Next, to ensure the effect on SK1 proteolysis we observed with Caspase 2 knockdown was not due to off-target effects of Caspase 2 siRNA we investigated SK1 proteolysis in WT and Cas2-/- MEFs. In accordance with the Caspase 2 siRNA data, doxorubicin treatment resulted in a significant reduction in SK1 protein that was reversed by genetic deletion of Caspase 2 **(Figure 10B and C).** Analysis of SK1 mRNA levels showed no significant changes in WT or Cas2-/- MEFs after doxorubicin **(Figure S5A)** while there was a slight reduction in SK2 mRNA levels in both the WT and Cas2-/- MEFs **(Figure S5B)**, providing further evidence that the reduction in SK1 protein is a post-translational event. To further investigate the regulation of SK1 in WT and Cas2-/- MEFs, we analyzed protein stability of SK1 in the MEFs using cyclohexamide. Interestingly, in the WT MEFS within twelve hours after treatment with cyclohexamide, SK1 protein was reduced by approximately 30% compared to vehicle treated MEFs, whereas there was no significant change in SK1 levels in the Cas2-/- MEFs **(Figure S5C)**. Only after thirty hours of cyclohexamide treatment was a reduction of SK1 protein level of approximately 40% observed in the Cas2-/- MEFs compared to vehicle treated MEFs **(Figure S5C)**, indicating that SK1 protein is likely somewhat more stable in the Cas2-/- MEFs compared to WT MEFs.

Accordingly, we sought to investigate the effects loss of Caspase 2 has on sphingolipid metabolism. To accomplish this, we first measured SK activity in WT and Cas2-/- MEFs. Consistent with the observations at the protein level, the significant reduction in SK activity observed in the WT MEFs after doxorubicin treatment, as measured by the reduction in the incorporation of C17-Sphingosine into C17-S1P, was not observed in the Cas2-/- MEFs **(Figure 10D).** A similar reduction in SK activity in WT MEFs that was abrogated in Cas2-/- MEFs was also observed after UV-irradiation **(Figure S5D).** Of note, the levels of S1P, the endogenous product of SK activity, were significantly reduced after doxorubicin treatment in WT MEFs **(Figure 10E)** concomitant with a significant increase in pro-apoptotic total long chain ceramide species [252] (Figure 4F). Both the decrease in S1P and increase in long chain ceramide species were abrogated in the Cas2-/- MEFs **(Figure 10E and 10F).**

Collectively these data provide strong evidence that Caspase 2 is required for SK1 proteolysis and that lose of Caspase 2 significantly affects endogenous sphingolipid levels in

response to genotoxic stress. Importantly, these data support a novel and important role for Caspase 2 in regulating sphingolipid metabolism in response to cellular stress.

4.3.5. SK1 is deregulated in p53 mutant TNBC cells

Next in order to investigate whether p53 mutations affect SK1 proteolysis and endogenous sphingolipid levels in response to genotoxic stress, we utilized the TNBC cell line, MDA-MB-231 that harbors a missense mutation, R280K, in the DNA-binding motif of p53. Interestingly, in contrast to MCF7 cells, doxorubicin treatment did not result in Caspase 2 activation as measured by cleavage of the pro-form of Caspase 2 **(Figure 11A and D)** and by BIFC, with less than 20% of the total number of transfected cells counted positive for activated Caspase 2 **(Figure 11B and C)**. In accordance with Caspase 2-mediated proteolysis of SK1 as described in Figure 4, no significant reduction in SK1 protein level was observed in response to doxorubicin at any dose tested in MDA-MB-231 cells **(Figure 11A and D)**; conversely an increase in SK1 protein level was observed with increasing doses of doxorubicin **(Figure 11D)**. Interestingly, the ceramide transport protein CERT was recently characterized as a Caspase 2 substrate in response to tumor necrosis factor α [253]. Given that CERT is involved in sphingolipid homeostasis, we hypothesized it would also be deregulated in this system. Indeed, in MCF7 cells when Caspase 2 is activated, cleavage of CERT was observed; importantly Caspase 2 processing and cleavage of CERT were not detectable in UV-irradiated MDA-MB-231 **(Figure S6)**.

We next wanted to investigate the levels of endogenous sphingolipids after genotoxic stress in MDA-MB-231 cells. There was no significant change in the substrate or product of SK activity, sphingosine and S1P, respectively **(Figure 11E and F)**. Furthermore, there was no significant increase in pro-apoptotic ceramide after doxorubicin treatment **(Figure 11G)**. Taken together, these results demonstrate that Caspase 2 activation is not achieved in mutant p53 cells, and likewise, SK1 is not reduced, further cementing the relationship between p53, caspase 2, and SK1. We also extend these findings to a previously identified Caspase 2 substrate and sphingolipid protein CERT.

4.3.6. Loss of SK1 sensitizes mutant p53 TNBC cells to doxorubicin

We next sought to determine the functional consequence of deregulation of SK1. We hypothesized that SK1 deregulation in mutant p53 TNBC cells may contribute to enhanced survival in response to doxorubicin. To test this hypothesis, SK1 was depleted by siRNA to evaluate whether loss of SK1 in combination with doxorubicin could sensitize MDA-MB-231 cells to DNA damage. Indeed, knockdown of SK1 in combination with doxorubicin resulted in significant PARP and Caspase 3 cleavage **(Figure 12A)** and an approximately 2-fold increase in Caspase 3 activity **(Figure 12B)** compared to doxorubicin alone. On the other hand, knockdown of SK1 in MCF7 breast cancer cells had no effect on the doxorubicin response **(Figure S7).** This is expected as SK1 protein levels are already significantly reduced in response to genotoxic stress in MCF7 cells therefore knock down provided no further sensitization.

All together these data identify deregulation of SK1 proteolysis in the context of mutant p53 TNBC cells as a possible mechanism of resistance to DNA damage in response to doxorubicin and consequently loss of SK1 sensitized these cells to doxorubicin.

4.3.7. SK1 is downstream of the CHK1 Suppressed-pathway in mutant p53 TNBC cells in response to doxorubicin

As mentioned previously, there is an emerging apoptotic pathway, the CHK1-Suppressed pathway that identifies loss or inhibition of CHK1 as being essential for Caspase 2 activation in mutant p53 cells [94, 189]; therefore we reasoned that activation of the CHK1-Suppressed pathway in MDA-MB-231 cells would result in Caspase 2 activation and subsequent SK1 proteolysis in response to doxorubicin. Indeed inhibition of CHK1, with the CHK1/2 inhibitor AZD7762, led to a reduction in full-length Caspase 2 concomitant with a significant loss of SK1 at the protein level **(Figure 13A and 13B)**. As AZD7762 is also known to inhibit other kinases in addition to CHK1 including CHK2, we next depleted CHK1 by siRNA to evaluate the specific role of CHK1. As shown in **Figure 13C**, knockdown of CHK1 in combination with doxorubicin resulted in a decrease in SK1 protein, in accordance with the data obtained with CHK1 inhibition.

Next, the functional effects of CHK1 loss and activation of the CHK1-Suppressed pathway on endogenous sphingolipid levels were evaluated in combination with doxorubicin treatment. As demonstrated in Figure 13D there was a significant increase in SK1's substrate sphingosine in response to loss of CHK1 and doxorubicin compared to doxorubicin alone. Moreover there was a decrease in SK1's product and pro-survival sphingolipid, S1P, upon CHK1 loss **(Figure 13E)**; although this decrease was not statistically significant, even small changes in this potent bioactive lipid can significantly affect cell fate. Also of note, under the same conditions no significant increase in the upstream metabolite ceramide was detected **(Figure S8)**. Taken together, these results demonstrate a role for CHK1 upstream of caspase2 leading to loss of SK1 and significant changes in bioactive sphingolipids.

4.3.8. SK1 as an effector of the CHK1-suppressed Pathway of Apoptosis

Currently there are numerous CHK1 inhibitors in clinical trial as a combination therapy to treat cancers such as breast and ovarian [87, 254]. Intriguingly several studies and reports have indicated CHK1 inhibition as being very effective as a combination therapy to treat TNBC cells [75, 92]. As we identified SK1 as being a target of the CHK1-Suppressed pathway, we wanted to investigate whether loss of SK1 in MDA-MB-231 TNBC cells could have similar effects in promoting apoptosis. Remarkably, doxorubicin combined with loss of SK1 resulted in roughly 60% of cells undergoing apoptosis as measured by Annexin-V staining **(Figure 14A)**. This compares with only approximately 30% apoptotic cells when CHK1 was depleted **(Figure 14B)**.

In light of these results indicating that SK1 may be an effector of the Caspase 2 apoptotic response, we next wanted to determine if inhibition of SK1 with the non-lipid SK inhibitor Ski-II could also sensitize Cas2-/- MEFs to doxorubicin. Indeed, WT MEFs were very sensitive to doxorubicin, and as expected inhibition of SK had no additive effects when combined with doxorubicin. In contrast, Cas2-/- MEFs displayed less sensitivity to doxorubicin than WT MEFs but when combined with SK1 inhibition the Cas2-/- MEFs become as sensitive as WT **(Figure 14C)**.

Altogether, these data indicate SK1 as a novel downstream target of the CHK1-Suppressed pathway and provide evidence that loss of SK1 may be a crucial step in the CHK1-Suppressed pathway and Caspase 2-mediated apoptosis. The data also provide evidence that loss of SK1 can specifically sensitize p53 mutant TNBCs to a greater extent than CHK1 loss in addition to cells deficient in Caspase 2 to the cytotoxic effects of doxorubicin.

4.4. Discussion

The aim of this study was to elucidate the mechanism of p53-mediated SK1 proteolysis. Consolidating previous studies using non-specific Caspase inhibitors that hint at a role of this family of proteases in SK1 proteolysis, we demonstrate that Caspase 2 is required for SK1 degradation in human breast cancer cells and that loss of Caspase 2 significantly affects sphingolipid metabolism in response to DNA damage. Interestingly, in unraveling the mechanism of SK1 proteolysis in WT p53 cells we then could identify perturbations of this pathway in mutant TNBC cells where persistent SK1 levels and deregulation of sphingolipid metabolites in response to DNA damage were observed. We found a defect in Caspase 2 activation in mutant p53 cells that could be overcome by CHK1 inhibition and activation of the CHK1-Suppressed pathway leading to SK1 proteolysis.

As much research is currently focused on unraveling the role Caspase 2 plays within the cell, this study adds to an emerging literature implicating Caspase 2 activity with the regulation of both lipid and sphingolipid metabolism [253, 255, 256]. As stated above, the data indicate that Caspase 2 activity is required for SK1 proteolysis. This is important as SK1 holds a crucial position in sphingolipid metabolism, acting to maintain homeostasis between pro-apoptotic sphingolipids such as ceramide and pro-survival sphingolipid S1P; therefore deregulation of SK1 could greatly effect cell survival. In line with this, we show that inhibition of SK1 can sensitize Cas2-/- MEFs to similar levels as WT MEFs to doxorubicin. Interestingly, a recent study revealed that the microRNA mir-708 directly down-regulates Caspase 2 and this down-regulation is necessary to induce carcinogenicity of bladder cancer [257]. Moreover, SK1 levels are documented as increased in bladder cancer, and elevated SK1 levels are associated with poor prognosis in bladder cancer [258]. As more studies begin to elucidate the role of Caspase 2 in

cancer, it will be interesting to investigate how levels of sphingolipid proteins that are regulated by Caspase 2 such as SK1 and CERT and subsequent sphingolipid levels are altered in these cancers and whether these alterations play an important role in tumorigenesis or response to therapy.

Although the current results indicate that Caspase 2 is required for SK1 proteolysis after DNA damage, we could not find evidence that SK1 is a direct substrate of Caspase 2. One plausible explanation for this comes from research describing the Caspase-2-PIDDosome as an important factor in maintaining p53 levels and regulating p53 dynamics after DNA damage [259]. Oliver *et al.* eloquently demonstrated that DNA damage and PIDD-induced activation of Caspase-2 result in Mdm2 cleavage, bolstering p53 stability and activity in a positive feedback loop and alternatively loss of Caspase 2 results in decreased p53 levels [259]. We know from our research [183, 185] that SK1 proteolysis is dependent on p53; therefore one could imagine that a threshold of p53 needs to be achieved in order to initiate SK1 proteolysis. Our data in fact show decreased levels of p53 with both Caspase 2 knockdown and in the Cas2-/- MEFs compared to control cells, providing evidence that this decreased level of p53 could hypothetically be insufficient to drive SK1 proteolysis.

Finally in this report we identify SK1 as a novel target of the CHK1-Suppressed pathway. To our knowledge this is the first potential effector of the CHK1- Suppressed pathway to be identified. CHK1 plays significant roles in maintaining cellular homeostasis and is indispensible for normal development as CHK1 knockout mouse are embryonic lethal; therefore repeated or high dose use of CHK1 inhibitors could have undesired side-effects in patients [40, 41]. As the CHK1-Suppressed pathway is an emerging apoptotic pathway whose activation by CHK1 inhibitors can sensitize p53 mutant cells, it is of great clinical significance to identify targets that are effectors of this pathway that could also be potential targets for therapeutic intervention. In this study we provide evidence that targeting SK1 offers an exciting potential therapeutic avenue for patients with altered p53 status, which has proven a challenging obstacle in cancer therapy for many years.

Chapter 5

Discussion and Future Directions

5.1. Introduction

The work presented in this dissertation makes significant progress in advancing the understanding of the CS-pathway and its regulation of sphingolipid metabolism in response to DNA damage **(Scheme 4).** We provide evidence of the first endogenous example of the CS-pathway and also identify SK1 as a novel potential downstream effector of the CS-pathway. Although much progress has been made, many questions and interesting possibilities remain to be elucidated and are outlined below.

5.2. Determine the biological consequences of CHK1 regulation of NF-κB signaling upon doxorubicin treatment in mutant p53 breast cancer cells

Activation of NF-κB by chemotherapeutics has been observed in many human cancers including breast cancer and is associated with resistance to chemotherapy and enhanced survival [229, 260]. Interestingly it was recently shown that p53 deficiency is necessary for doxorubicin-induced NF-κB activation that limits doxorubicin cytotoxicity, leads to induction of a number of genes associated with invasion, metastasis and chemoresistance and is linked to an aggressive clinical behavior [229]. Thus far the exact mechanism of NF-κB activation by doxorubicin in mutant p53 cancer cells has not been elucidated and therefore inhibition of the NF-κB pathway has been proposed although the development of drugs that target NF-κB has proven difficult and are associated with severe side effects [261]. As targeting NF-κB directly has proven insurmountable, identifying key druggable upstream regulators and/or downstream effectors is of great importance. For instance, it was recently shown that inhibiting the downstream effector of the NF-κB pathway GADD45β/MKK7 could selectively kill multiple myeloma cancer cells by interfering with NF-κB pro-survival functions [262].

Importantly, my data provide evidence that CHK1 is an upstream regulator of NF-κB activity in response to doxorubicin in mutant p53 cancer cells and subsequently targeting CHK1 in these cells abrogates NF-κB signaling and could therefore be therapeutically beneficial as a combination therapy. This is an exciting possibility as there are many CHK1 inhibitors already in clinical trials. Although these studies begin to investigate the potential of this *in vitro* further studies are needed and are outlined below.

5.2.1. Investigate the effect of CHK1 inhibition on invasion in response to doxorubicin

It was recently shown that doxorubicin induces NF-κB-mediated expression of metastasis-associated genes in p53-defeicient breast tumors. Along these same lines, the data demonstrated doxorubicin-induced expression of a number of genes associated with metastasis including BMP4 and IL6 that were dependent on NF-κB activity and that could be inhibited by loss or inhibition of CHK1. Therefore we hypothesized that doxorubicin would induce the invasiveness of the mutant p53 breast cancer cells, MDA-MB-231 via increased NF-κB signaling that could be inhibited by CHK1 inhibition.

In order to test this hypothesis we plan to use a trans-well matrigel cell invasion assay, using invasion as a read-out of metastatic behavior. Briefly, MDA-MB-231 cells either treated with doxorubicin alone or in combination with CHK1 inhibitor in addition to proper controls will be assessed for their ability to invade through matrigel. This is an intriguing scenario as there are many studies documenting the effects of CHK1 inhibition in combination with many chemotherapeutics on cell killing but no studies on the combination of drugs on cell invasion.

5.2.2. Determine the role of CHK1 inhibition on NF-κB signaling *in vivo*

The data presented in Chapter 3, identify a novel role for CHK1 outside of its cell cycle responsibilities in regulating NF-κB signaling and subsequently the production of chemokines and cytokines in response to doxorubicin treatment. To build on the *in vitro* results, we are currently performing xenograft studies in nude mice. In these studies, six to eight week old female nude mice will be injected subcutaneously through 25-gauge needle into the right flank with 5.10^6 MDA-MB-231 resuspended in 50 μL of DMEM containing 10% FBS and 50 μL of Matrigel. Once the tumor reaches 150 mm^3 (about 4 weeks later) mice will be randomized into four groups, vehicle control, CHK1 inhibitor control, doxorubicin only and doxorubicin with CHK1 inhibitor. The control groups will receive PBS containing the same percentage of DMSO (with or without CHK1 inhibitor) as inhibitor and doxorubicin treated mice. All the solutions will be given intraperitoneally every week for one or two weeks. Body weight will be measured before injection. 72h after doxorubicin or control treatment, mice will be euthanized using isoflurane inhalation and cervical dislocation and then tumor removed. RNA and protein will be

extracted from the tumor for analysis. Real-time PCR will be used to investigate the mRNA levels of chemokine and cytokines among the four groups. Similarly, western blot analysis will be conducted to determine NF-κB activation in addition to the levels of other proteins such as SK1. Next in order to evaluate the levels of circulating chemokines and cytokines at the protein level, ELISA will be performed on the plasma.

The goal is to confirm that the signaling observed *in vitro* also occurs in an animal model, providing more evidence in support of the use of CHK1 inhibitors in combination with doxorubicin to abrogate NF-κB signaling in p53-defeicient tumors.

5.3. Investigate doxorubicin-induced TMVs: mechanism of induction and biology

TMVs are extra-cellular vesicles that are ubiquitously shed from tumors cells, although it has been demonstrated that the amount of vesicles shed is increased with cell invasiveness and disease progression [221]. TMVs contain genetic cargo such as proteins, oncogenes, mRNAs and microRNAs that can transferred to recipient cells to modulate the recipient cell's activity and the overall tumor micro-environment [263-265]. These data establish that doxorubicin induces the shedding of TMVs from MDA-MB-231 cells that contain a number of chemokines and cytokines. Moreover, it was demonstrated that loss of CHK1 could modulate the cargo within the TMVs in response to doxorubicin. In light of these results, the following experiments are proposed in order to gain mechanistic insight into how doxorubicin induces TMV shedding and the biological consequence of TMVs on recipient cells.

5.3.1. Investigate the mechanism of doxorubicin-induced TMV shedding

An exact mechanism defining how TMVs are shed from cancer cells has yet to be defined although research over the past several years has made significant progress elucidating the proteins and processes that are involved in TMV release. For instance it is now known that TMV shedding appears to occur at areas of the plasma membrane that are enriched in certain lipids such as cholesterol which may promote shape changes in the plasma membrane that are conducive to membrane curvature, allowing for TMV formation [266]. It was also recently discovered that "shedding" is facilitated by actin-myosin-based contraction via ARF6-mediated

ERK activation [267]. Interestingly several reports have also demonstrated that both increased intracellular and extracellular calcium induces TMV shedding [268-270].

My data demonstrate that doxorubicin induces the shedding of TMVs from MDA-MB-231 cells. Interestingly, although MCF7 cells do shed a small number of TMVs basally, this is not increased by doxorubicin treatment. To begin to investigate the mechanism behind doxorubicin-induced TMV shedding we first chose to look at changes in intracellular calcium levels upon doxorubicin treatment between these two cell lines. Preliminary data using a commercially available kit to measure intracellular calcium (Fluo-8 No Wash Calcium Assay Kit (ab112129)) show that calcium levels are increased in MDA-MB-231 cells and decreased in MCF7 cells after 24 hours of doxorubicin treatment **(Figure 15).** These data corroborate what is known in the literature that increased intracellular calcium levels are associated with increased TMV shedding. Next in order to establish that the observed increase in calcium levels in MDA-MB-231 cells is required for induction of TMV shedding in response to doxorubicin treatment, the intracellular calcium chelator, BAPTA will be utilized in combination with doxorubicin followed by confocal live cell imaging to monitor TMV shedding. Also TMVs will be isolated and subjected to Nanoparticle Tracking Anaylsis (NTA). NTA utilizes the properties of both light scattering and Brownian motion to obtain particle size and concentration. This analysis will provide a quantitative measurement of how many TMVs are shed in response to different treatments.

5.3.2. Determine TMV-mediated biologies on recipient cells

Tumor progression involves the ability of cancer cells to communicate with each other and with neighboring normal cells in their microenvironment. It is now well-established that TMVs can serve as a form of cell-to-cell communication via the horizontal transfer of genetic material to recipient cell, providing a "path of less resistance" for tumor progression and metastasis [271-273]. In light of this we aim to determine what effect doxorubicin-induced vesicles from MDA-MB-231 have on recipient cells and also the consequence of manipulating the cargo within the vesicles via CHK1 inhibition in this system.

5.3.2.1. Co-Culture Experiments

As many proteins that are associated with invasion and metastasis were observed inside doxorubicin-induced TMVs we hypothesized that TMVs isolated from doxorubicin treated MDA-MB-231 cells would induce invasion when co-cultured with the less invasive MCF7 breast cancer cells compared to TMVs isolated from vehicle treated cells. Indeed preliminary reults show that MCF7 cells co-cultured with TMVs from doxorubicin treated MDA-MB-231 cells for 48 hours are more invasive than cells co-cultured with TMVs from vehicle treated MDA-MB-231 cells **(Figure 16)**. Next in order to investigate whether CHK1 inhibition which alters the cargo within the TMVs can abrogate the invasive phenotype observed in Figure 16, the same co-culture experiment will be performed as above with the addition of TMVs isolated from MDA-MB-231 cells treated with CHK1 inhibitor alone and CHK1 inhibitor plus doxorubicin. If the proteins such as IL6 and BMP4 that are present in doxorubicin-induced TMVs are mediating the observed invasion of recipient cells, we would expect this to be abrogated in MCF7 cells co-cultured with CHK1 inhibitor plus doxorubicin treated TMVs.

5.3.3. Investigate the role of SK1 in doxorubicin-induced TMVs

Interestingly, in investigating the cargo of TMVs we found that SK1 is present exclusively in TMVs and not in exosomes; moreover we found that SK1 was enriched in TMVs from doxorubicin treated MDA-MB-231 cells compared to TMVs from vehicle treated cells **(Figure 17)**. To build on this observation and establish a role for SK1 in TMVs the following experiments are proposed:

5.3.3.1. Live cell imaging to monitor SK1 inside TMVs

For these studies we first overexpressed GFP-tagged SK1 in MDA-MB-231 cells to monitor SK1 presence in TMVs in live cells. As shown in **Figure 18** GFP-tagged SK1 can be imaged inside TMVs shed from MDA-MB-231 in response to doxorubicin. To build on these studies we plan to once again overexpress GFP-SK1 followed by doxorubicin treatment, isolate these vesicles and label the vesicles with PKH26, a yellow-orange fluorescent dye with long aliphatic tails that stably incorporates into lipid regions of membranes. The labeled TMVs will then be co-cultured with MCF7 cells plated in confocal dishes for live cell imaging. These experiments will allow for visualization of the uptake of TMVs containing SK1.

5.3.3.2. Lipidomic analysis of TMVs

In light of the observation that SK1 is packaged within TMVs, we next sought to determine the sphingolipid profile in TMVs, i.e. is S1P or ceramide inside these vesicles? Briefly TMVs will be isolated from either vehicle or doxorubicin treated MDA-MB-231 followed by lipidomic analysis. These results could have several important implications: 1) S1P within TMVs could provide increased survival, angiogenesis, proliferation of recipient cells. 2) Packaging of ceramide in TMVs could provide a means to eliminate pro-apoptotic ceramide from the cell.

5.4. Establish the mechanism of SK1 proteolysis

Although we establish that caspase 2 is required for loss of SK1, we could not prove SK1 is a direct target of caspase 2. This leads to a couple of interesting possibilities: 1) Caspase 2 is activating another protease that is then directly cleaving SK1. 2) Caspase 2 is upstream of mitochondrial outer membrane permeabilization (MOMP), leading to the release of a number of proteases that could then lead to SK1 proteolysis. 3) SK1 is bound to a protein that can be cleaved by caspase 2, allowing for SK1 proteolysis by another protease.

5.4.1. Determine whether SK1 proteolysis is downstream of MOMP

Although caspase 2 is characterized as an initiator caspase, thus far there is no evidence to suggest it directly cleaves and activates any other members of the caspase family. Interestingly, caspase 2 has been shown to be upstream of MOMP via the cleavage of BID, a member of the Bcl-2 family of proteins. Cleavage of BID by caspase 2 produces an active fragment of BID which promotes the oligomerization of the proteins BAX and BAK that then insert themselves into the mitochondrial outer membrane, a critical step for MOMP. MOMP is characterized by the release of apoptogenic factors and proteins that are normally sequestered in the mitochondrial intermembrane space into the cytosol, constituting a “point of no return” in the initiation of cell death [274]. Among the proteins released is cytochrome c, which serves as a co-factor for APAf-1. APAf-1 can then promote the formation of the apoptosome, leading to activation of the initiator caspases, caspase 9 and subsequently the executioner caspase 3 [275,

276]. Given these data the following experiments are proposed to investigate whether SK1 is downstream of the BID-BAK/BAX-MOMP pathway.

5.4.1.1. siRNA knockdown of BID

We first propose to deplete BID using siRNA and evaluate the effect on SK1 proteolysis after doxorubicin treatment. If caspase 2 activation of BID (via cleavage) is required for SK1 proteolysis, knockdown of BID should abrogate SK1 proteolysis. A pitfall of this approach is that BAK could compensate for the loss of BID to initiate MOMP.

5.4.1.2. siRNA knockdown of Caspase 9

As activation of caspase 9 occurs downstream of MOMP we propose to investigate first whether caspase 9 is required SK1 proteolysis. Caspase inhibitors are notoriously non-specific therefore we propose to knock down caspase 9 by siRNA and evaluate SK1 proteolysis in response to doxorubicin.

5.4.2. SK1 Binding partners as potential substrates

In this approach we will immunoprecipitate SK1 in MCF7 cells with magnetic beads, that are in turn cross-linked with SK1 antibody and submit for analysis by mass spectrometry. These results will allow us to identify SK1 binding partners. We will then try to identify any binding partners that are known substrates of caspase 2.

5.5. Conclusion

In conclusion this work provides new insight into how the CS-pathway is regulated and identifies a potential critical downstream target, SK1. The therapeutic potential of targeting CHK1 in mutant p53 cancers in combination with DNA damaging agents has shown by many groups [75, 79, 80, 84-87] and is an intense and exciting area of research. The data outlined in this dissertation demonstrating that CHK1 inhibition abrogates DNA damage-induced NF-κB signaling, a major contributor to chemotherapeutic resistance, provides additional evidence in support of CHK1 as a promising therapeutic target. Although, the data thus far is promising,

many questions and obstacles remain before CHK1 inhibitors are used in the clinic. The need for more specific CHK1 inhibitors that display fewer off-target effects is crucial. Also studies investigating the effects of CHK1 inhibitors on normal cells are needed. Are patients now more susceptible to secondary tumors because of aberrant cell cycle checkpoints? These obstacles highlight the need to identify other druggable targets within this pathway that also sensitize cells to chemotherapeutics. We identify SK1 as an exciting potential therapeutic target in mutant p53 cancers downstream of CHK1. As new more specific SK1 inhibitors become available it will be very exciting to investigate these inhibitors as a combination therapy in mutant p53 cancers both *in vitro* and *in vivo*.

Figures

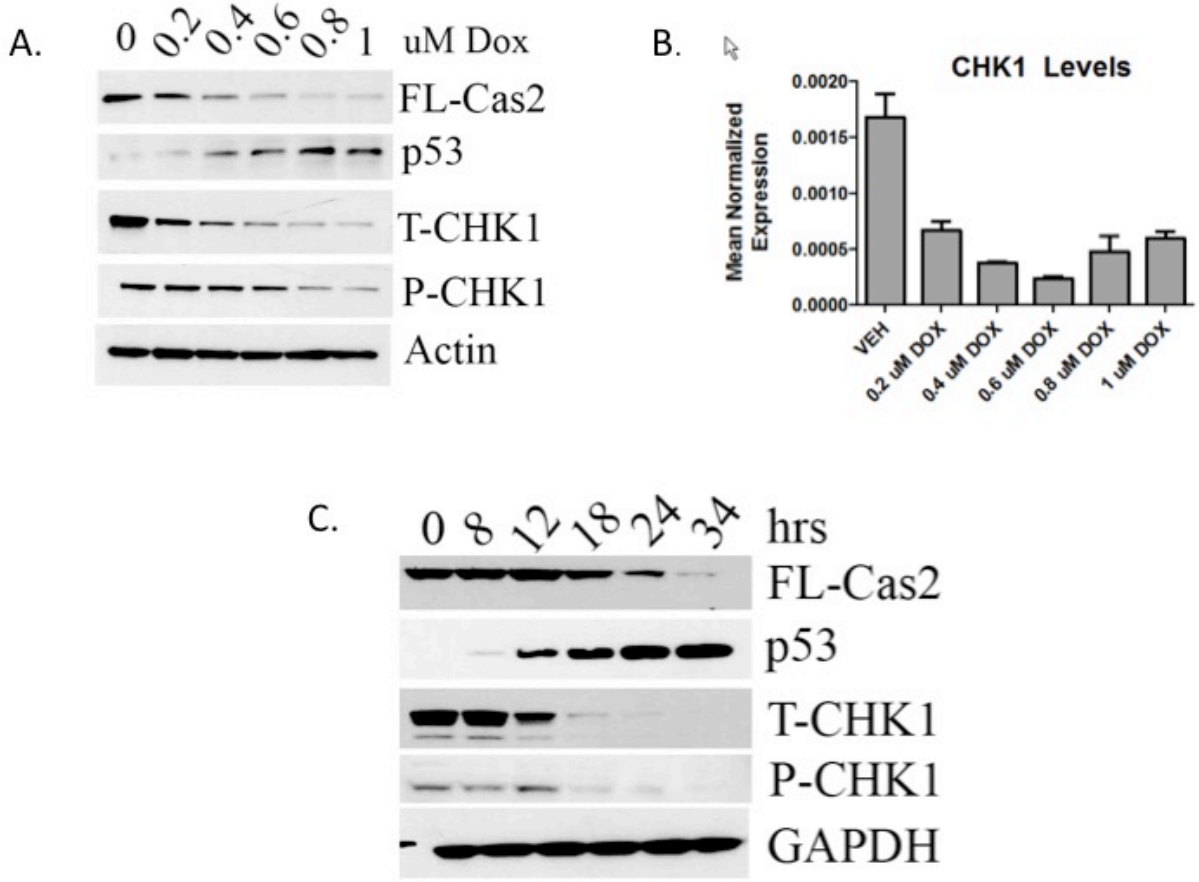

Figure 1: Wild type p53 is an endogenous regulator of the CS-Pathway

MCF7 cells were treated with the indicated dose of doxorubicin for 24h. Cells were then (A) harvested in RIPA buffer and total cell lysate was analyzed by western blot for the proteins indicated or (B) harvested in RLT buffer, prepared for quantitative reverse transcriptase-PCR, with enzyme expression normalized to b-actin expression for each reaction in triplicate. Data are presented as mean ± SEM of 3 independent experiments. (C) MCF7 cells were treated with 0.8uM doxorubicin for the indicated times, harvested and total cell lysate was analyzed by western blot for the proteins indicated.

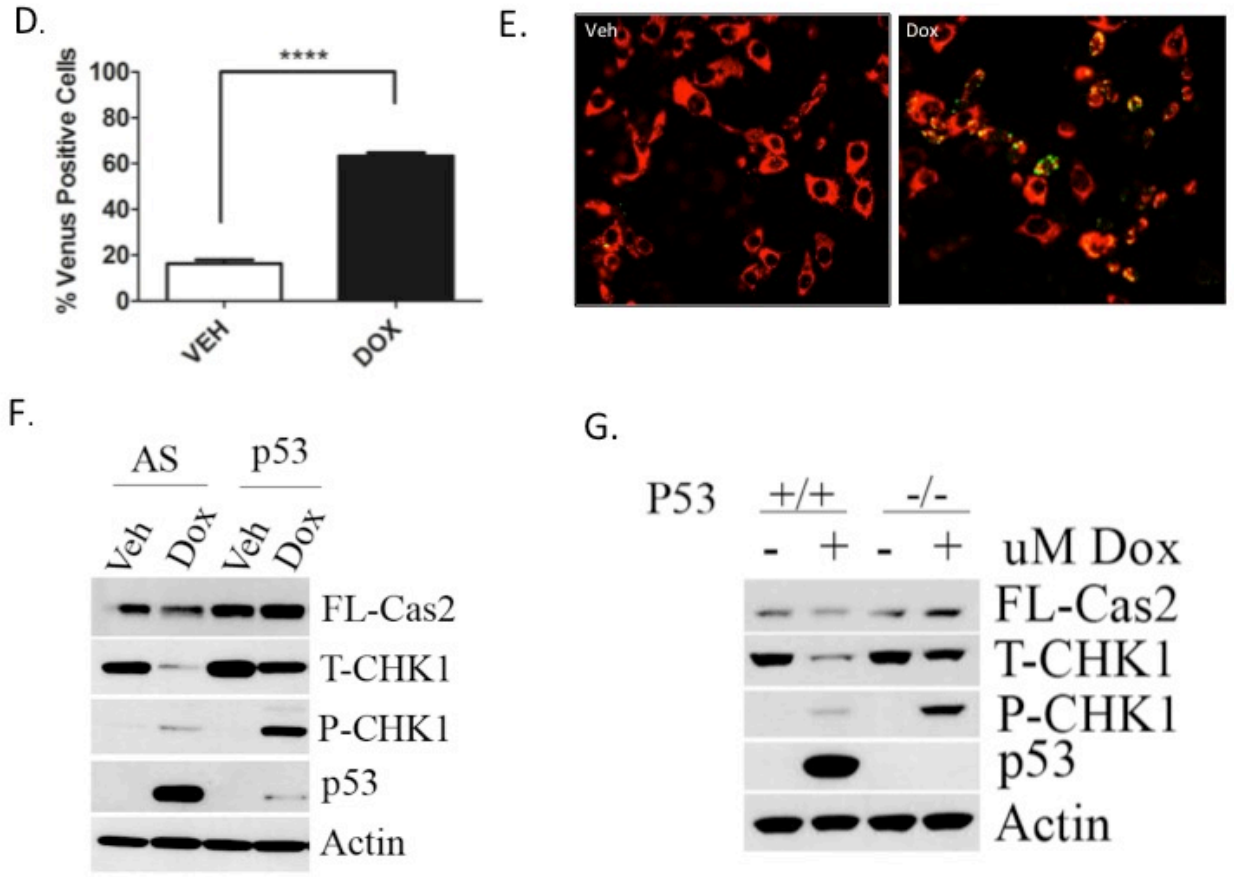

Figure 1 (Continued): Wild type p53 is an endogenous regulator of the CS-Pathway

(D) MCF7 cells were transiently transfected with C2-CARD VN (500ng) and C2-CARD VC (500ng) along with pshooter.dsRed-mito (250ng) as a reporter for transfection. Twenty-four hours after transfection, cells were treated with 0.8uM doxorubicin for 24h and then the percentage of pshooter.ds.Red-mito-positive (red) cells that were Venus positive (green) was determined from a minimum of 100 cells per plate. Data are presented as mean ± SEM of 3 independent experiments. (E) Representative confocal images of cells from (D) are shown. (F) MCF7 were transfected with p53 siRNA (20nM). Forty-eight hours after transfection, cells were treated with 0.8uM doxorubicin for 24 hours, harvested and total cell lysate was analyzed by western blot for the proteins indicated. (G) HCT-116 cells either wild type or null for p53 were treated with 0.8uM doxorubicin for 24 hours, harvested in RIPA buffer and total cell lysate was analyzed by western blot for the proteins indicated.

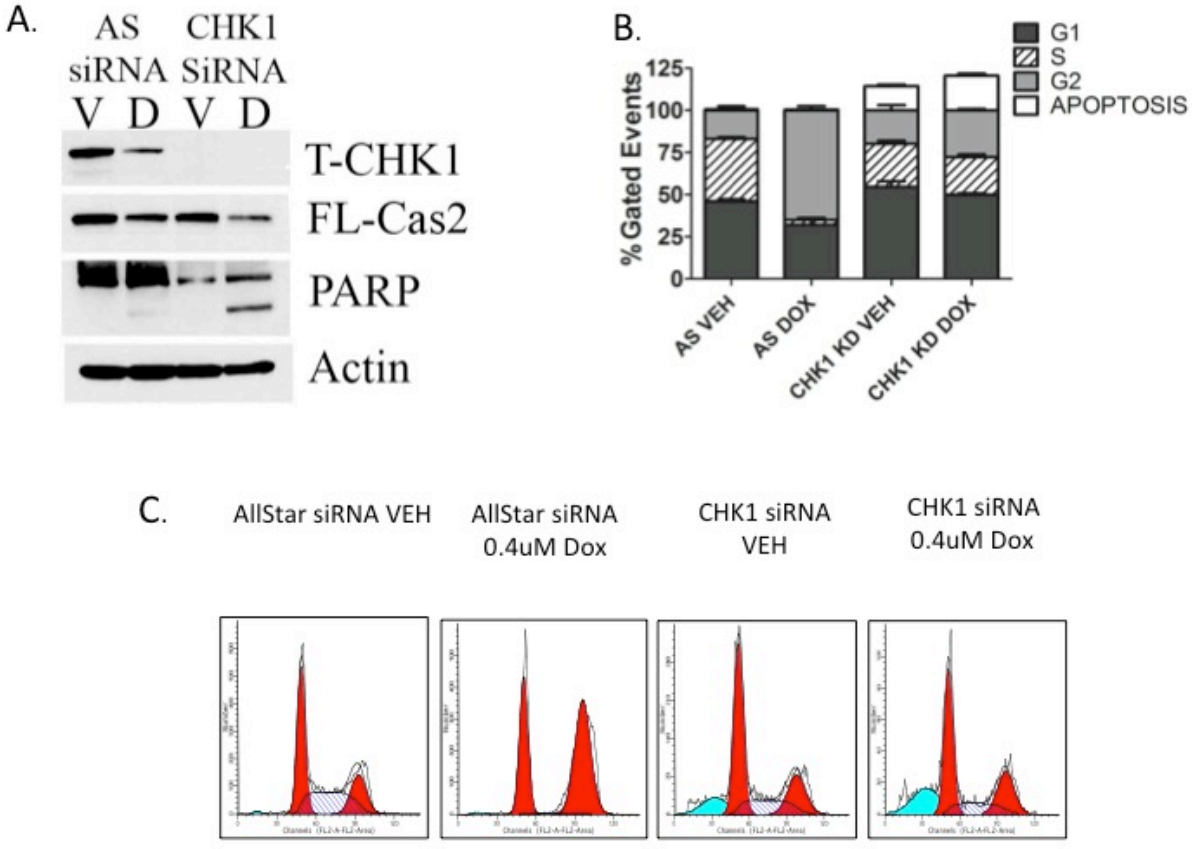

Figure 2: The CS-Pathway can be activated in wild type p53 cells

MCF7 were transfected with CHK1 siRNA (20nM). Forty-eight hours after transfection, cells were treated with 0.4uM doxorubicin for 24 hours and either harvested in RIPA and total cell lysate analyzed by western blot for the proteins indicated (A) or harvested, fixed and labeled with propidium iodide for cell cycle analysis (B). Data are presented as mean ± SEM of 3 independent experiments. (C) Images of cell cycle analyzed by ModFit LT software.

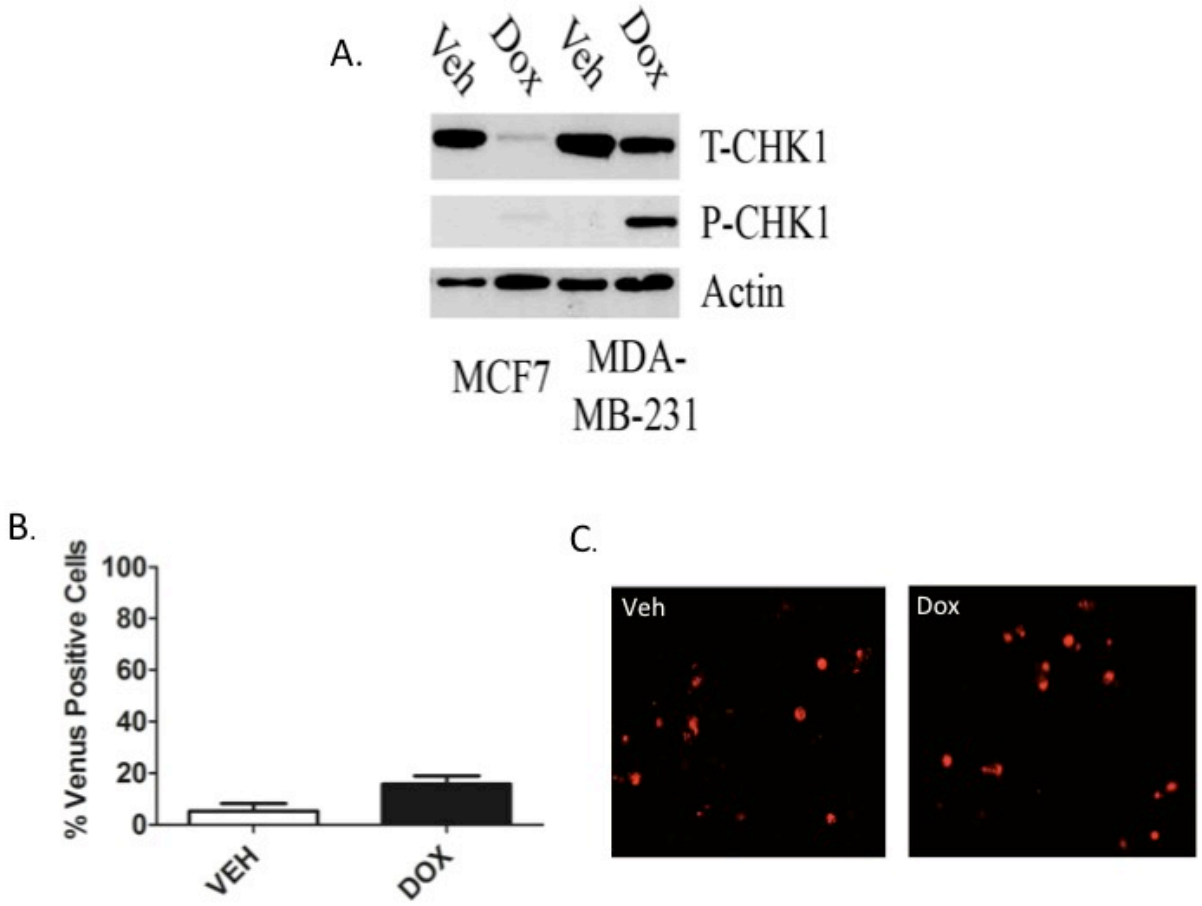

Figure 3*:* P53 deficiency triggers deregulation of the CHK1-Caspase 2 pathway

(A) MCF7 and MDA-MB-231 cells were treated 0.8uM doxorubicin for 24 hours, harvested and total cell lysate was analyzed by western blot for the proteins indicated. (B) MDA-MB-231 cells were transiently transfected with C2-CARD VN (500ng) and C2-CARD VC (500ng) along with pshooter.dsRed-mito (250ng) as a reporter for transfection. Twenty-four hours after transfection, cells were treated with 0.8uM doxorubicin for 24 hours and then the percentage of pshooter.ds.Red-mito-positive (red) cells that were Venus positive (green) was determined from a minimum of 100 cells per plate with representative confocal images of cells from (B) shown (C). Data are presented as mean ± SEM of 3 independent experiments.

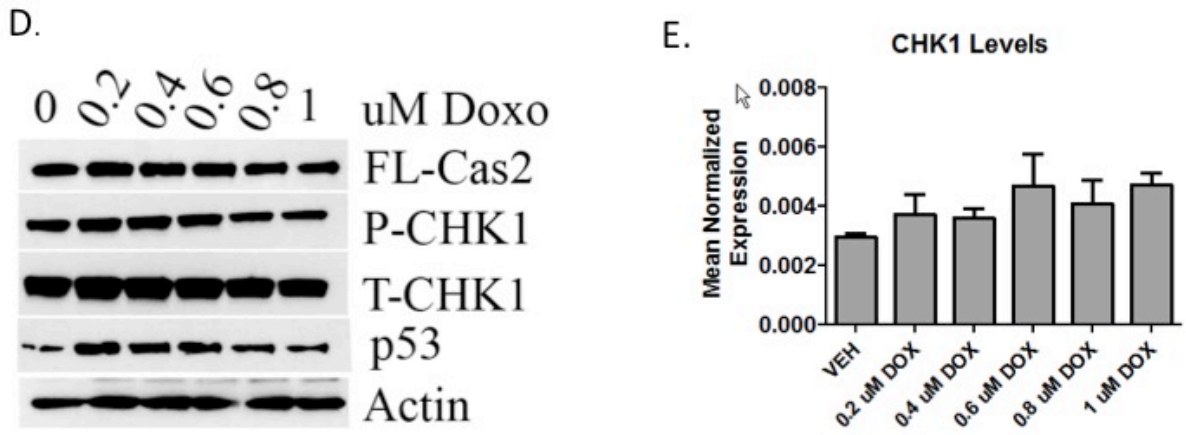

Figure 3 (continued): P53 deficiency triggers deregulation of the CHK1-Caspase 2 pathway

MDA-MB-231 cells were treated with the indicated dose of doxorubicin for 24 hours. Cells were then harvested in RIPA buffer and total cell lysate was analyzed by western blot for the proteins indicated (D) or harvested in RLT buffer, prepared for quantitative reverse transcriptase-PCR, with enzyme expression normalized to b-actin expression for each reaction in triplicate (E). Data are presented as mean ± SEM of 3 independent experiments.

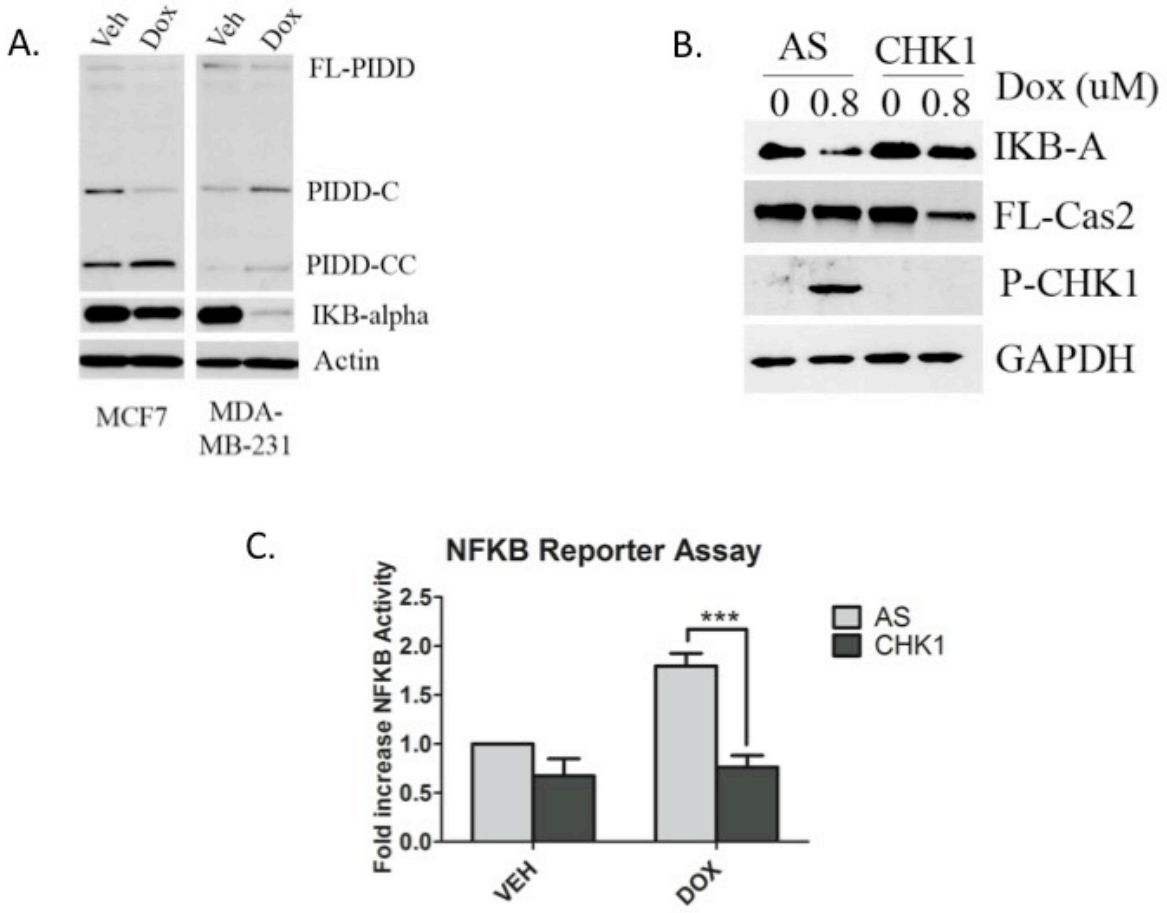

Figure 4: CHK1 levels regulate NFKB signaling in p53 deficient cells

(A) MCF7 and MDA-MB-231 cells were treated 0.8uM doxorubicin for 24 hours, harvested and total cell lysate was analyzed by western blot for the proteins indicated. (B) MDA-MB-231 cells were transfected with CHK1 siRNA (20nM). Forty-eight hours after transfection, cells were treated with 0.8uM doxorubicin for 24 hours, harvested and total cell lysate was analyzed by western blot for the proteins indicated. (C) MDA-MB-231 cells were co-transfected with 1ug of NFKB promoter-luciferase construct and V5 luciferase construct for 18 hours followed by treatment with 0.8uM doxorubicin for 24 hours. Luciferase and galactosidase activities were extracted and assayed as described in "Material and Methods" and measured luciferase activity was normalized to measured galactosidase activity. Data are presented as mean ± SEM of 3 independent experiments.

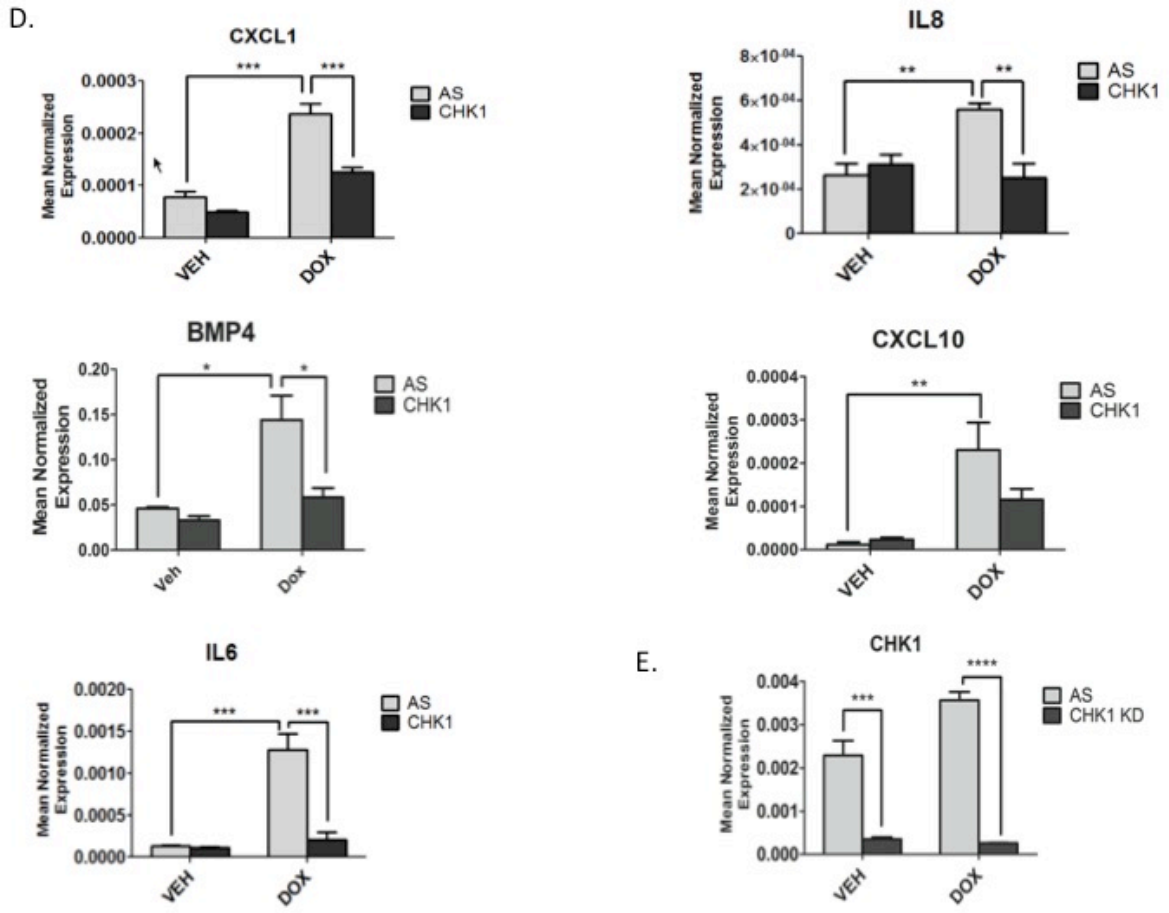

Figure 4 (continued): CHK1 levels regulate NFKB signaling in p53 deficient cells

(D and E) MDA-MB-231 cells were transfected with CHK1 siRNA (20nM). Forty-eight hours after transfection, cells were treated with 0.8uM doxorubicin for 24 hours, harvested in RLT buffer and prepared for quantitative reverse transcriptase-PCR, with enzyme expression normalized to b-actin expression for each reaction in triplicate. Data are presented as mean ± SEM of 3 independent experiments.

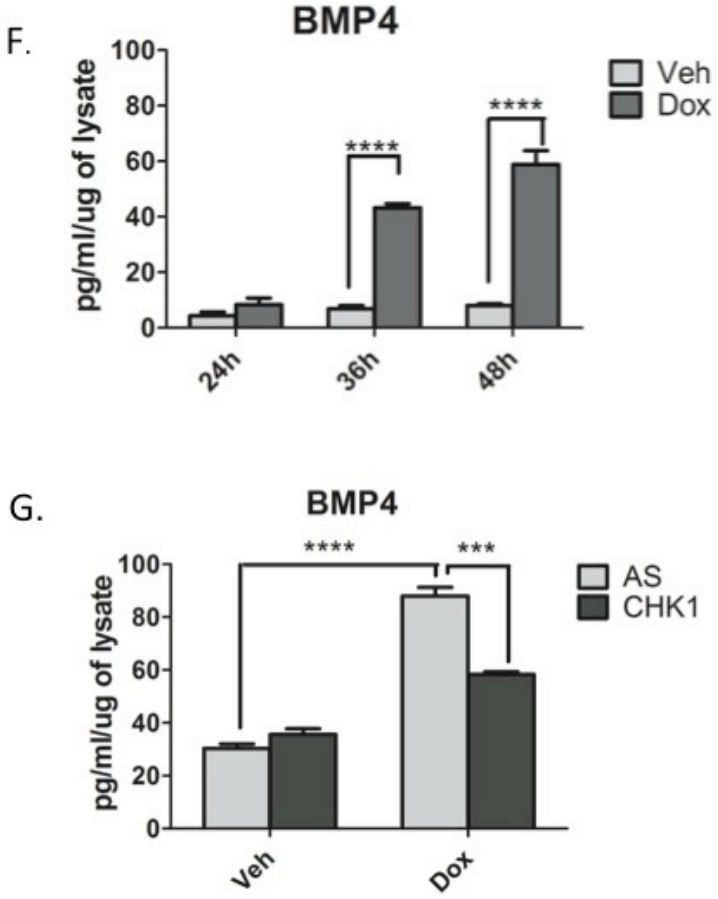

Figure 4 (continued): CHK1 levels regulate NFKB signaling in p53 deficient cells

(F) MDA-MB-231 cells were treated with 0.8uM doxorubicin for the indicated times, media was then collected and ELISA was performed to assess levels of protein in the media. (G) The media from (D) was then used for ELISA. Data are presented as mean ± SEM of 3 independent experiments.

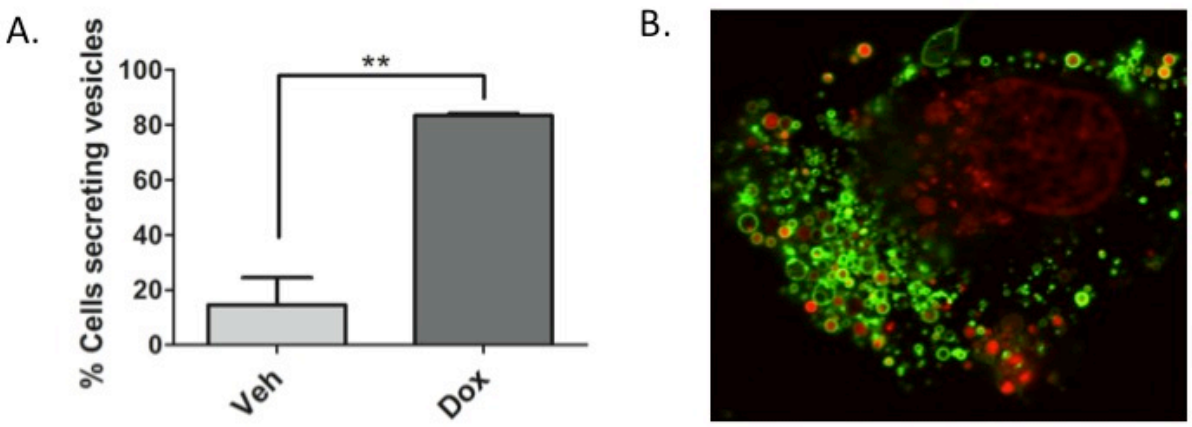

Figure 5: Doxorubicin induces the shedding of tumor-derived microvesicles containing inflammatory in MDA-MB-231 cells

(A) MDA-MB-231 cells were treated 0.8uM doxorubicin for 68 hours. After 68 hours cells were stained with DRAQ5 to label all cells followed by labeling with Annexin-V and Propidium to specifically label TMVs and live cell imaging was performed. The number of cells secreting TMVs out of the total number of cells in the field was counted and quantified, blindly. Data are presented as mean ± SEM of 3 independent experiments. (B) MDA-MB-231 cells were treated 0.8uM doxorubicin for 68 hours. After 68 hours Annexin-V and Propidium were added to the media to label TMVs. Live cell imaging was then performed on the samples (B) is a representative image.

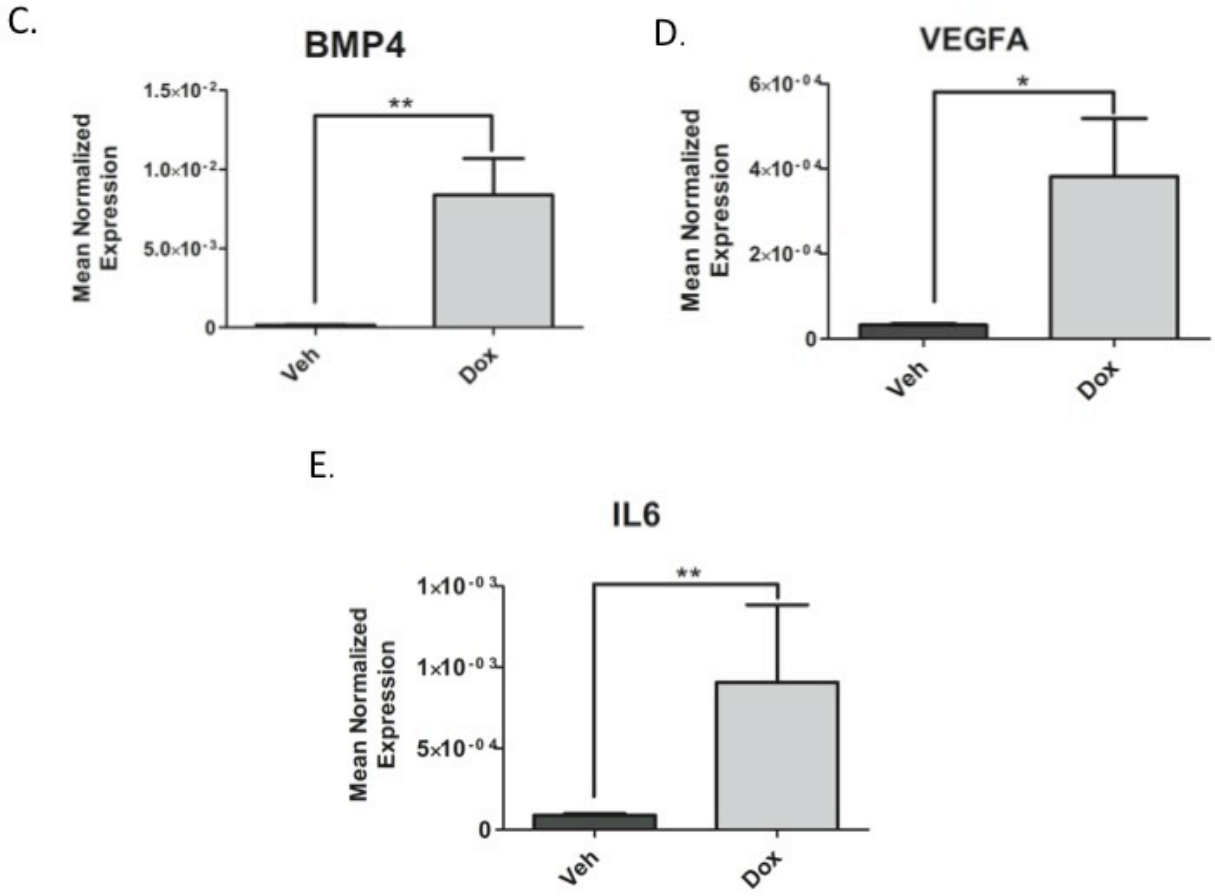

Figure 5 (continued): Doxorubicin induces the shedding of tumor-derived microvesicles containing inflammatory in MDA-MB-231 cells

(C-E) MDA-MB-231 cells were treated with 0.8uM doxorubicin for 68 hours. Cells were harvested in RIPA buffer. The media was collected and subjected to differential centrifugation (outlined in "material and methods"). RNA was then extracted from the 50,000xG pellet and the cells and prepared for quantitative reverse transcriptase-PCR, with enzyme expression normalized to b-actin expression for each reaction in triplicate. Data are presented as mean ± SEM of 3 independent experiments.

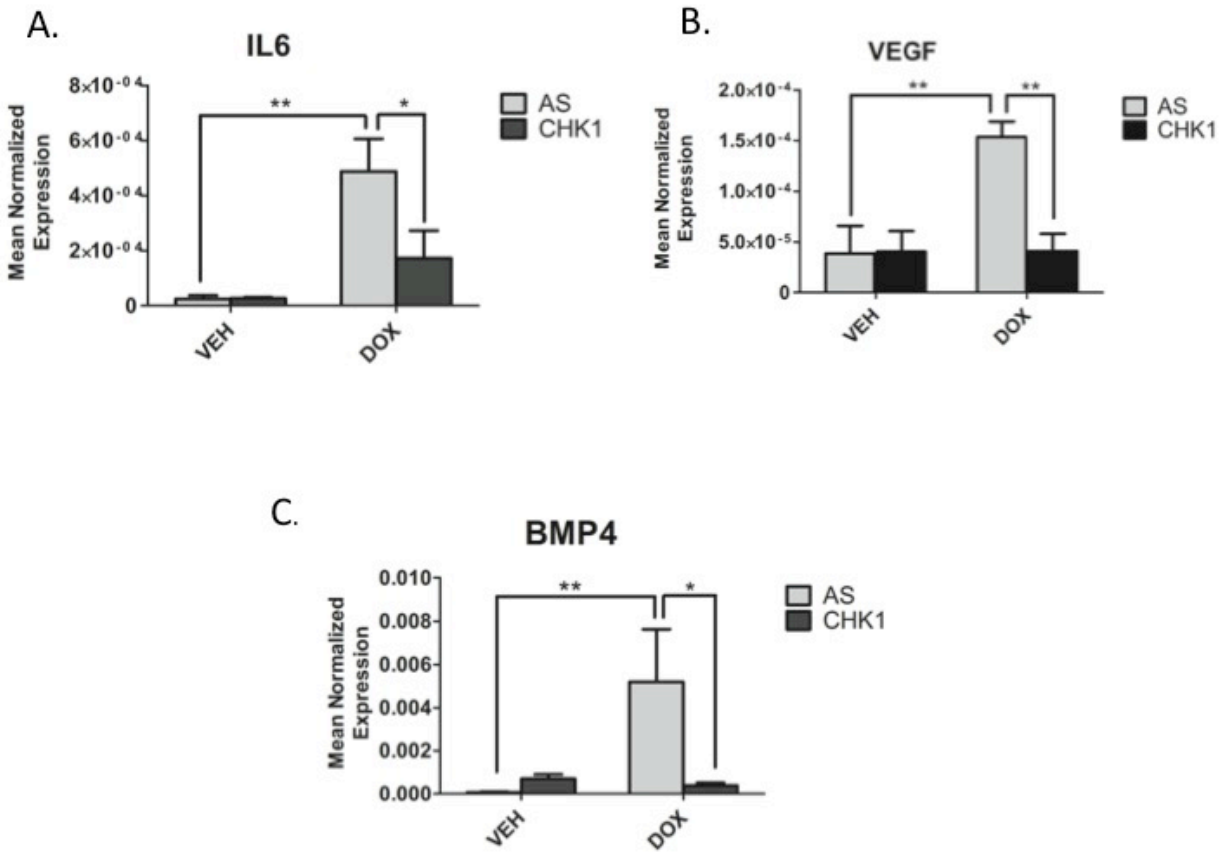

Figure 6: Loss of CHK1 alters the cargo of TMVs

(A-C) MDA-MB-231 cells were transfected with CHK1 siRNA (20nM). Eighteen hours after transfection, cells were treated with 0.8uM doxorubicin for 68 hours. Cells were harvested in RIPA buffer. The media was collected and subjected to differential centrifugation (outlined in "material and methods"). RNA was then extracted from the 50,000xG pellet and the cells and prepared for quantitative reverse transcriptase-PCR, with enzyme expression normalized to b-actin expression for each reaction in triplicate. Data are presented as mean ± SEM of 3 independent experiments.

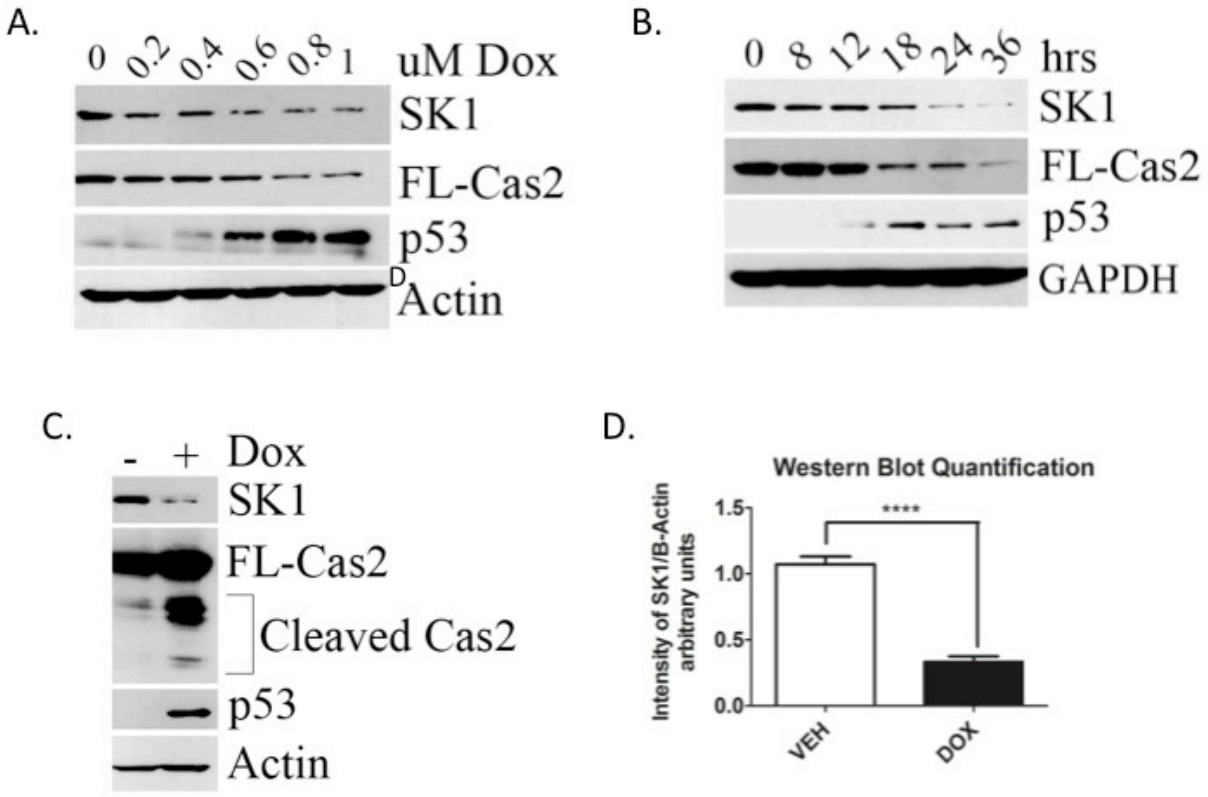

Figure 7: SK1 proteolysis is downstream of Caspase 2 upon doxorubicin treatment in MCF7 breast cancer cells.

(A) MCF7 cells were treated with the indicated dose of doxorubicin for 24h. Cells were then harvested in RIPA buffer and total cell lysate was analyzed by western blot for the proteins indicated. (B) MCF7 cells were treated with 0.8uM doxorubicin for the indicated times, harvested, and total cell lysate analyzed by western blot for the proteins indicated. (C) MCF7 cells were treated with 0.8uM doxorubicin for 24h, harvested in RIPA buffer, and total cell lysate was analyzed by western blot for the proteins indicated. (D) ImageJ was used to quantify SK1 protein levels normalized to actin from (C) and all replicates (n=6 ****$p<0.005$ by Student's T-test).

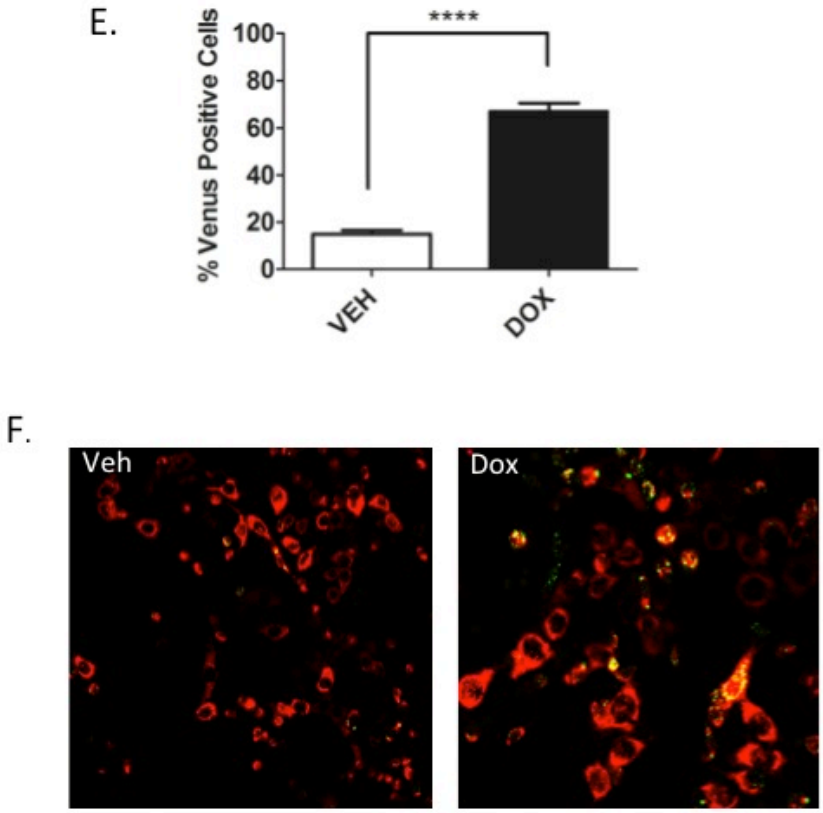

Figure 7 (continued): SK1 proteolysis is downstream of Caspase 2 upon doxorubicin treatment in MCF7 breast cancer cells.

E) MCF7 cells were transiently transfected with C2-CARD VN (500ng) and C2-CARD VC (500ng) along with pshooter.dsRed-mito (250ng) as a reporter for transfection. Twenty-four hours after transfection, cells were treated with 0.8uM doxorubicin for 24h and then the percentage of pshooter.ds.Red-mito-positive (red) cells that were Venus positive (green) was determined from a minimum of 100 cells per plate. Data are presented as mean ± SEM of 3 independent experiments (n=3 ****$p<0.001$ by Student's T-test). Representative confocal images of cells from (F) are shown.

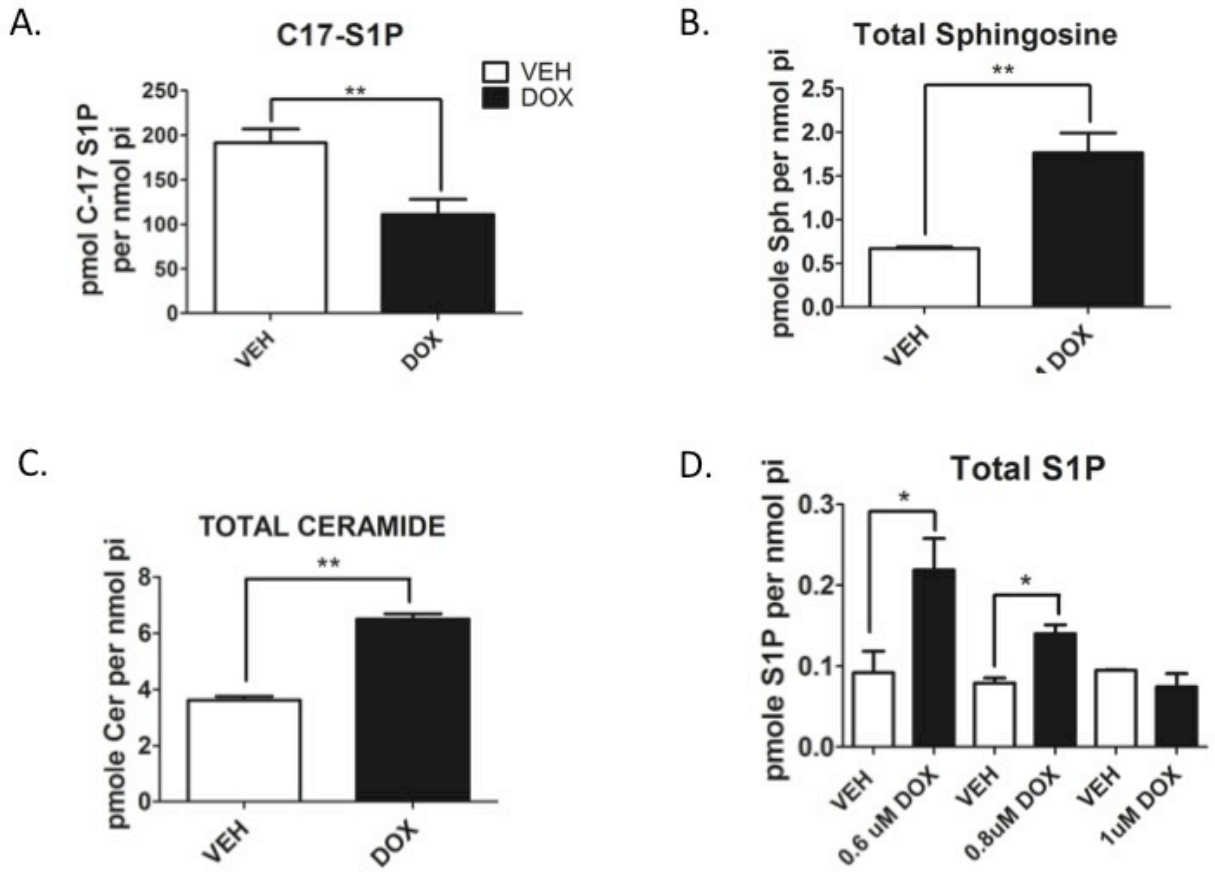

Figure 8: Effects of doxorubicin on SK activity and endogenous sphingolipids

(A) MCF7 cells were treated with 0.8uM doxorubicin for 24h and then incubated with C_{17}-sphingosine for 15 minutes. Following incubation, cells were harvested for 89phingolipidomic analysis by liquid chromatography mass spectrometry (LC/MS) and the C_{17}-containing S1P was normalized to the amount of lipid phosphate for each sample (n=3 **p<0.01 by Student's T-test). MCF7 cells were treated with 0.8uM doxorubicin for 24 hours and then harvested for 89phingolipidomic analysis as in (A) to measure sphingosine (B) and total ceramides (C) (n=3 **p<0.01 by Student's T-test). (D) MCF7 cells were treated with the indicated dose of doxorubicin for 24 hours, harvested as in (A) to measure S1P (n=3 *p<0.05 by Student's T-test).

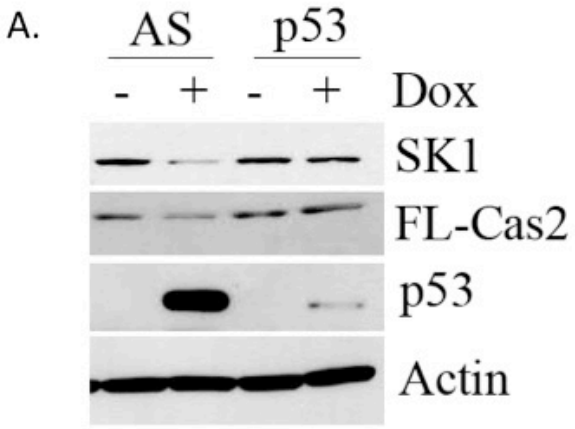

Figure 9: P53-mediated SK1 proteolysis and activation of Caspase 2

MCF7 cells were transfected with p53 siRNA (20nM). Forty-eight hours after transfection, cells were treated with 0.8uM doxorubicin for 24 hours, harvested and total cell lysate was analyzed by western blot for the proteins indicated.

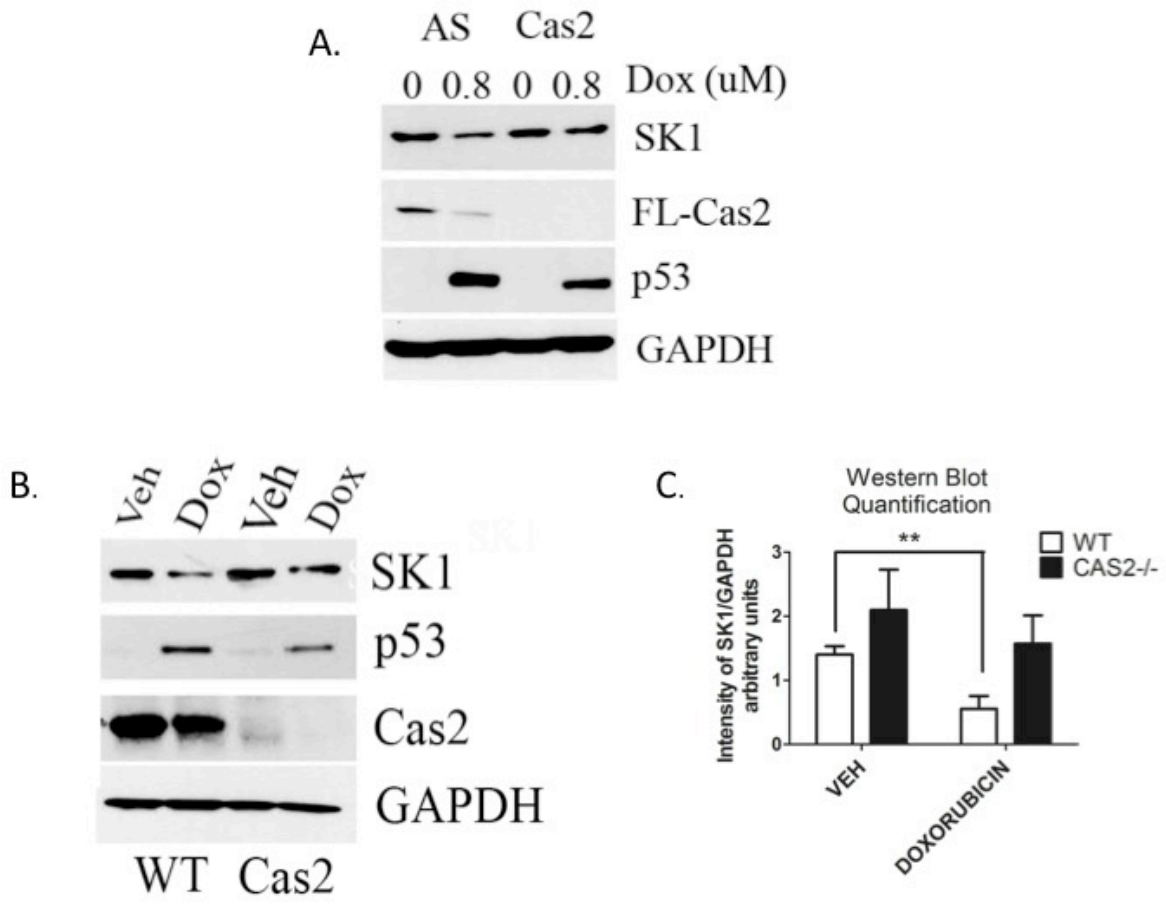

Figure 10: Caspase 2 is required for SK1 proteolysis in response to DNA damage

(A) MCF7 cells were transfected with Caspase 2 siRNA (20nM) or control siRNA (AS). Forty-eight hours after transfection, cells were treated with 0.8uM doxorubicin or vehicle for 24 hours, harvested, and total cell lysate then analyzed by western blot for the proteins indicated. (B) Mouse embryonic fibroblasts (MEFs) expressing wild type Caspase 2 or with Caspase 2 knocked out were treated with 0.2uM doxorubicin for 24h, harvested, and total cell lysate analyzed by western blot for the proteins indicated. (C) ImageJ was used to quantify SK1 protein levels normalized to GAPDH from (B) and all replicates (n=4 **$p<0.01$ by Two-Way ANOVA).

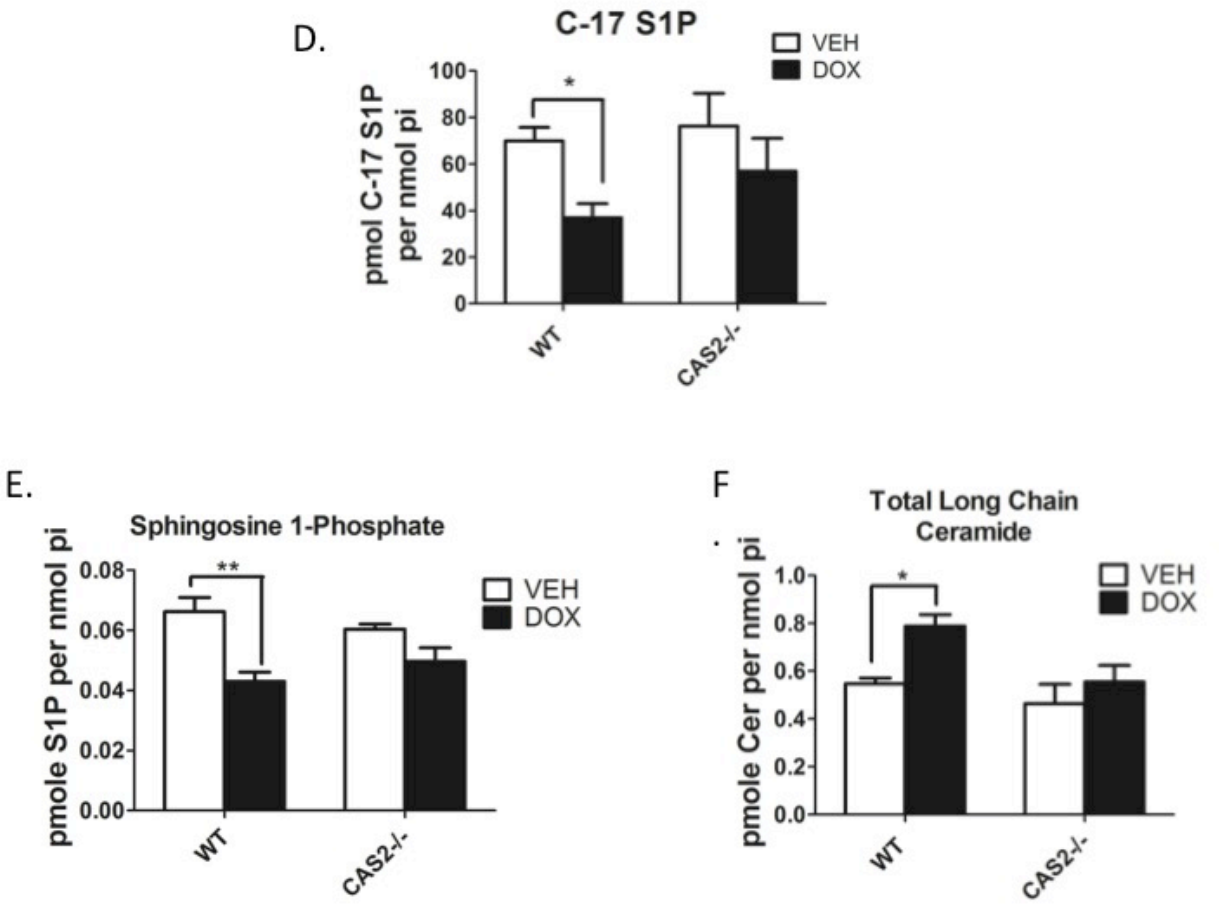

Figure 10 (continued): Caspase 2 is required for SK1 proteolysis in response to DNA damage

(D) MEFS were treated with 0.2uM doxorubicin for 24h and then incubated with C_{17}-labeled sphingosine for 15 minutes. Following incubation, MEFS were harvested for 92phingolipidomic analysis by liquid chromatography mass spectrometry (LC/MS) and the C_{17}-containing S1P was normalized to the amount of lipid phosphate for each sample (n=3 *p<0.05 by Two-Way ANOVA). MEFs were treated with 0.2uM doxorubicin and then harvested for 92phingolipidomic analysis as in (D) to measure S1P (n=3 ** p<0.01 by Two-way ANOVA) (E) and ceramide (n=3 * p<0.05 by Two-way ANOVA) (F).

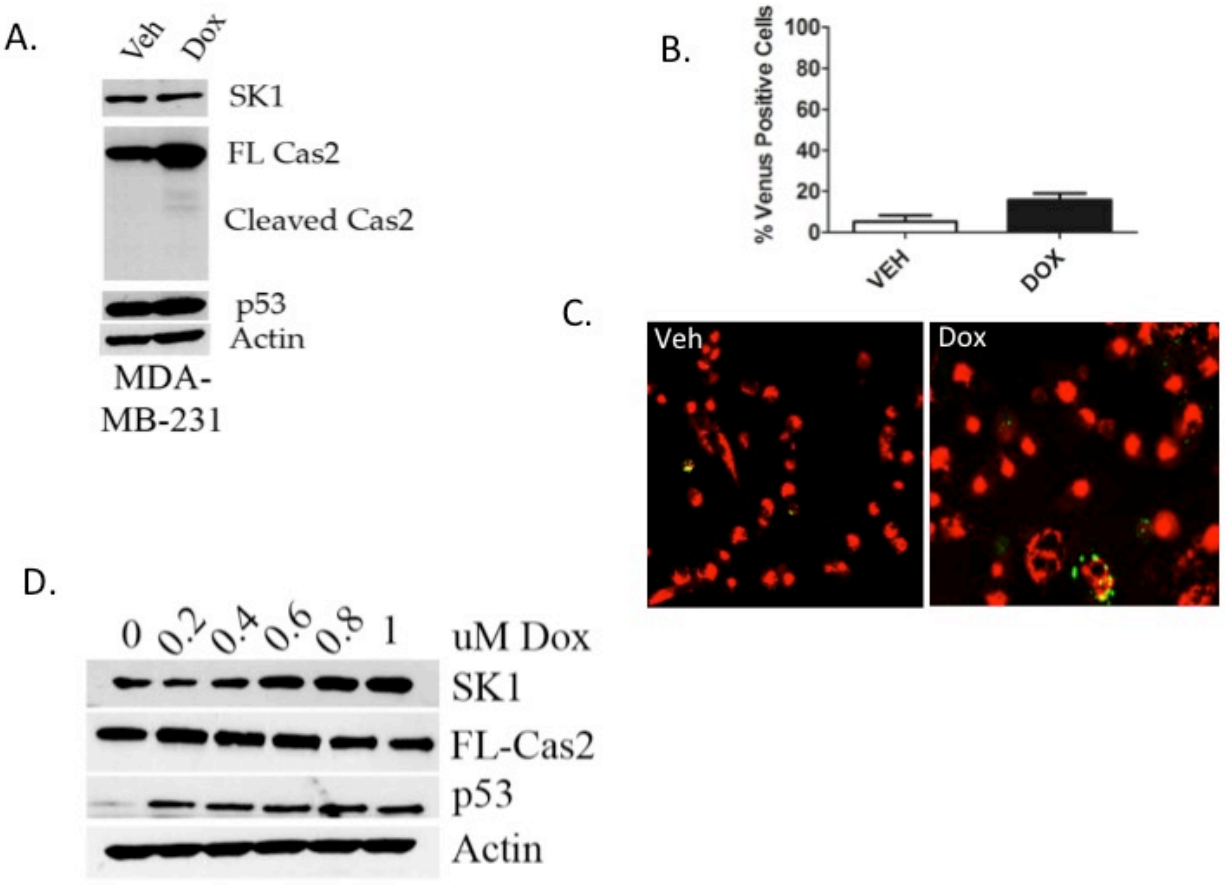

Figure 11: SK1 is deregulated in p53 mutant TNBC cells in response to doxorubicin

(A) MDA-MB-231 cells were treated with 0.8uM doxorubicin for 24h, harvested in RIPA buffer, and total cell lysate analyzed by western blot for the proteins indicated. (B) MDA-MB-231 cells were transiently transfected with C2-CARD VN (500ng) and C2-CARD VC (500ng) along with pshooter.dsRed-mito (250ng) as a reporter for transfection. Twenty-four hours after transfection, cells were treated with 0.8uM doxorubicin for 24h, and then the percentage of pshooter.ds.Red-mito-positive (red) cells that were Venus positive (green) was determined from a minimum of 100 cells per plate. Data are presented as mean ± SEM of 3 independent experiments. Representative confocal images of cells from (C) are shown. (D) MDA-MB-231 cells were treated with

the indicated dose of doxorubicin for 24h. Cells were then harvested in RIPA buffer and total cell lysate was analyzed by western blot for the proteins indicated.

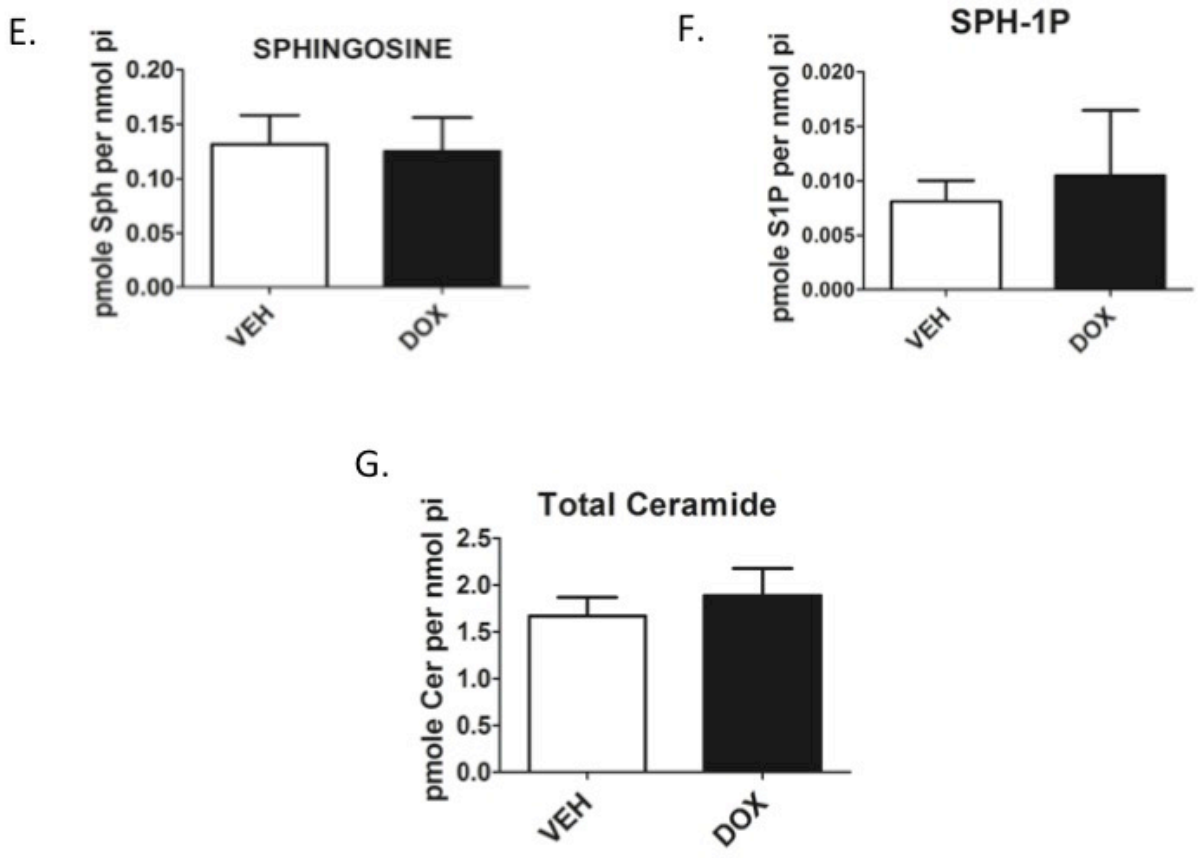

Figure 11 (continued): SK1 is deregulated in p53 mutant TNBC cells in response to doxorubicin

(E) MDA-MB-231 cells were treated with 0.8uM doxorubicin for 24h, harvested for 94phingolipidomic analysis by liquid chromatography mass spectrometry (LC/MS) and the sphingosine (E), S1P (F) and ceramide (G) was normalized to the amount of lipid phosphate for each sample (n=3).

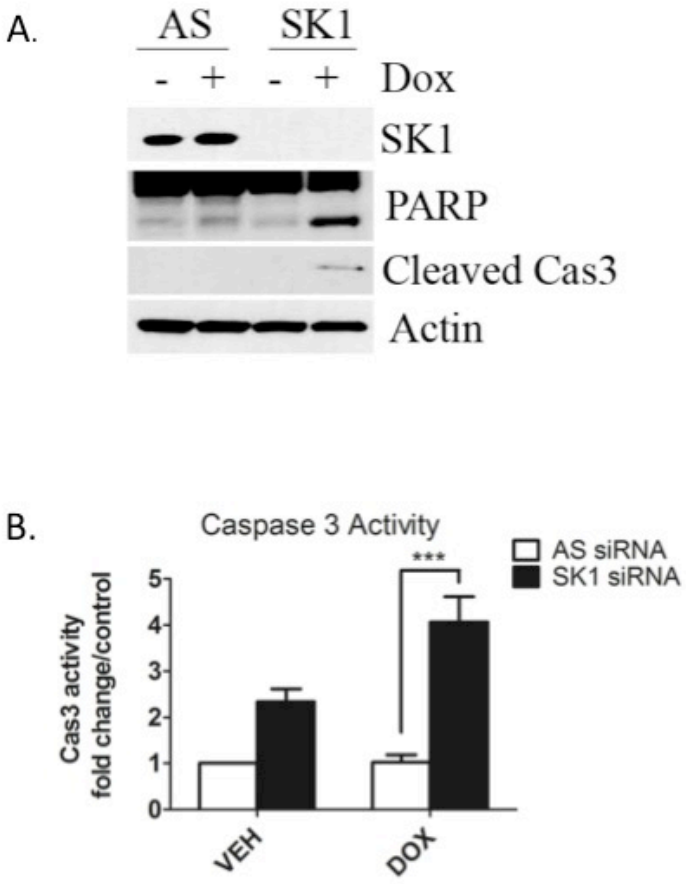

Figure 12: Effects of loss of SK1 on mutant p53 TNBC cells in response to doxorubicin

(A) MDA-MB-231 cells were transfected with SK1 siRNA (20nM). Sixty hours after transfection, cells were treated with 0.8uM doxorubicin for 24 hours and then harvested, and total cell lysate was analyzed by western blot for the proteins indicated. (E) MDA-MB-231 cells were transfected with SK1 siRNA (20nM). Sixty hours after transfection, cells were treated with 0.8uM doxorubicin for 24 hours, harvested, and Caspase 3 activity measured (n=3 ***$p<0.005$ by Two-way ANOVA)

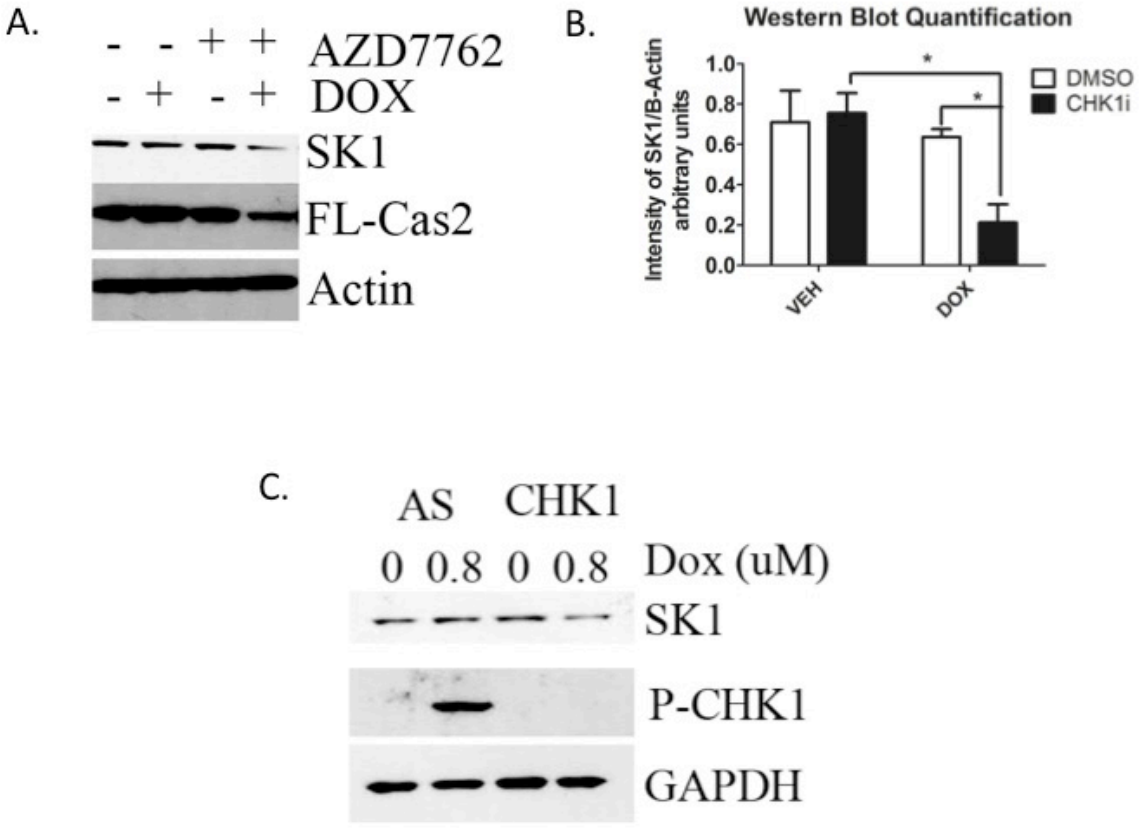

Figure 13: SK1 is downstream of the CS-pathway in mutant p53 TNBC cells in response to doxorubicin

(A) MDA-MB-231 cells were pretreated with 0.3uM CHK1 inhibitor (AZD7762) for 2 hours and then treated with 0.8uM doxorubicin for 24h hours, harvested, and total cell lysate analyzed by western blot for the proteins indicated. (B) ImageJ was used to quantify SK1 protein levels normalized to GAPDH from (A) and all replicates (n=3 *$p<0.05$ by Two-way ANOVA). (C) MDA-MB-231 cells were transfected with CHK1 siRNA (20nM). Forty-eight hours after transfection, cells were treated with 0.8uM doxorubicin for 24 hours, harvested and total cell lysate was analyzed by western blot for the proteins indicated.

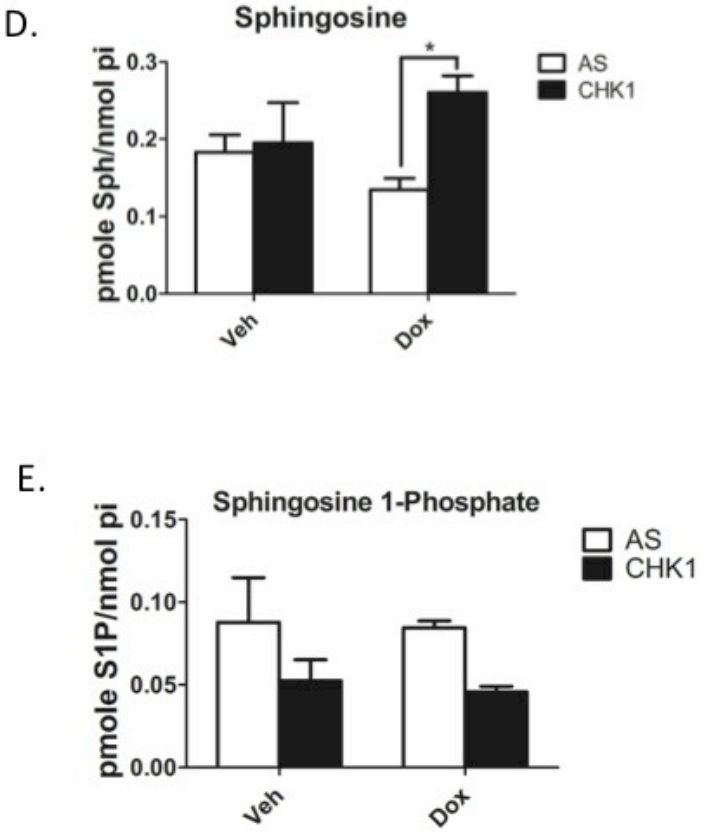

Figure 13 (continued): SK1 is downstream of the CS-pathway in mutant p53 TNBC cells in response to doxorubicin

MDA-MB-231 cells were transfected with CHK1 siRNA (20nM). Forty-eight hours after transfection, cells were treated with 0.8uM doxorubicin for 24 hours then harvested for 97phingolipidomic analysis by liquid chromatography mass spectrometry (LC/MS) to measure sphingosine (D) or S1P (E) (n=3 *$p<0.05$ by Two-way ANOVA).

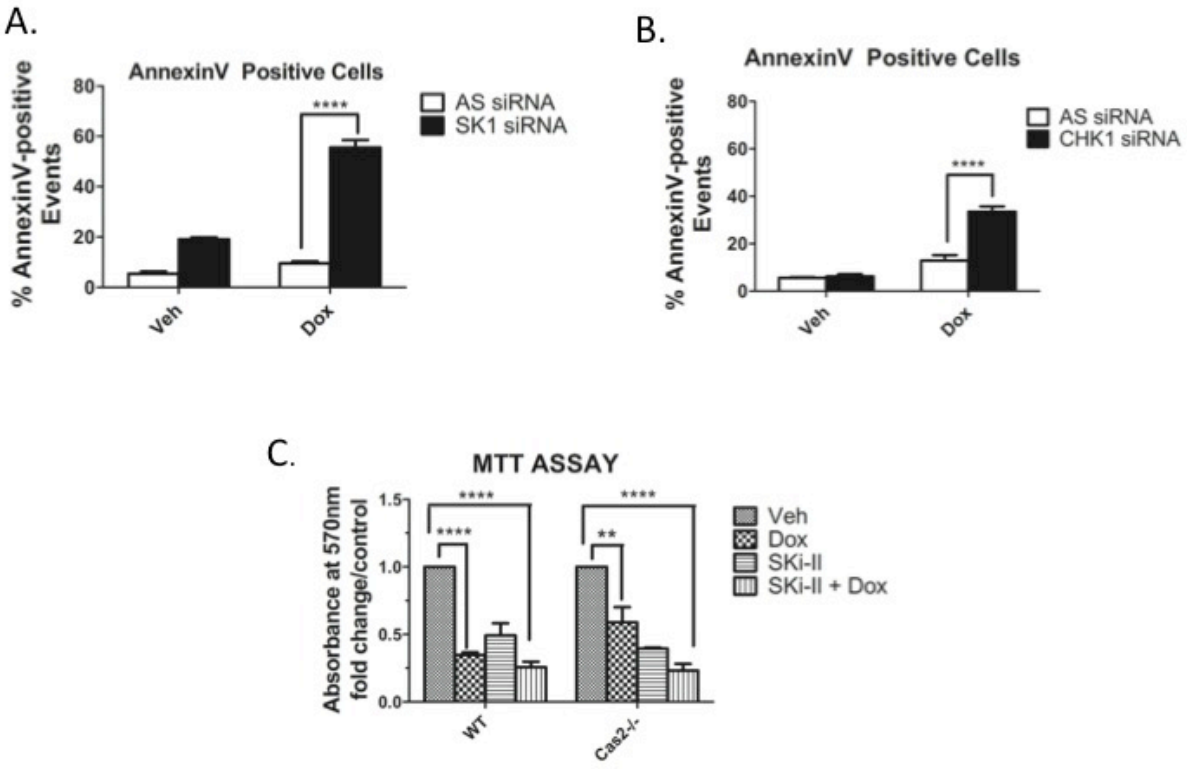

Figure 14: Loss of SK1 sensitizes mutant p53 TNBC cells to a greater extent than loss of CHK1

(A) MDA-MB-231 cells were transfected with SK1 siRNA (20nM). Sixty hours after transfection, cells were treated with 0.8uM doxorubicin for 24 hours, labeled with Annexin-V and analyzed by flow cytometry to detect apoptotic cells as described in "Materials and Methods" (n=3 ****p<0.001 by Two-way ANOVA). (B) MDA-MB-231 cells were transfected with CHK1 siRNA (20nM). Forty-eight hours after transfection, cells were treated with 0.8uM doxorubicin for 24 hours, labeled with Annexin-V and analyzed by flow cytometry to detect apoptotic cells as described in "Materials and Methods" (n=3 ****p<0.001 by Two-way ANOVA). (C) MEFs were pretreated with 10uM Ski-II for one hour followed by 0.2uM doxorubicin for 24h. MTT assay was then performed as described in "Materials and Methods" to assess cell viability.

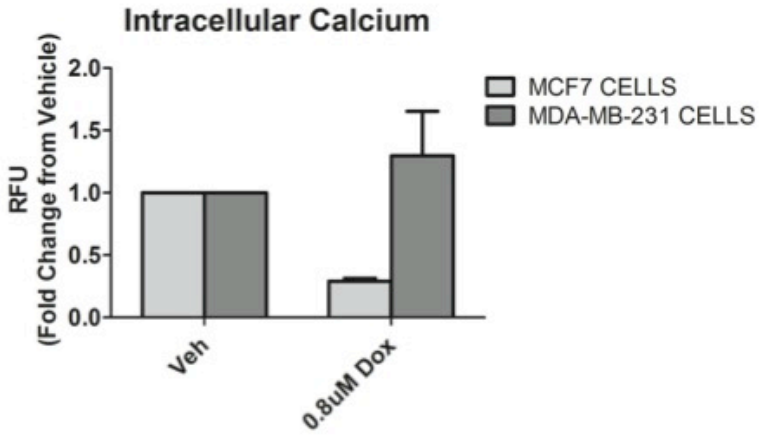

Figure 15: Doxorubicin treatment increases intracellular calcium levels in MDA-MB-231 cells

Cells were plated in a 96-well plate in triplicate followed by doxorubicin (0.8uM) for 24 hours. Following treatment Fluo-8 dye was added to the media and allowed to incubate for 1 hour. Fluorescence intensity at Ex/Em = 490/525 was measured. Results were normalized to respective vehicle controls.

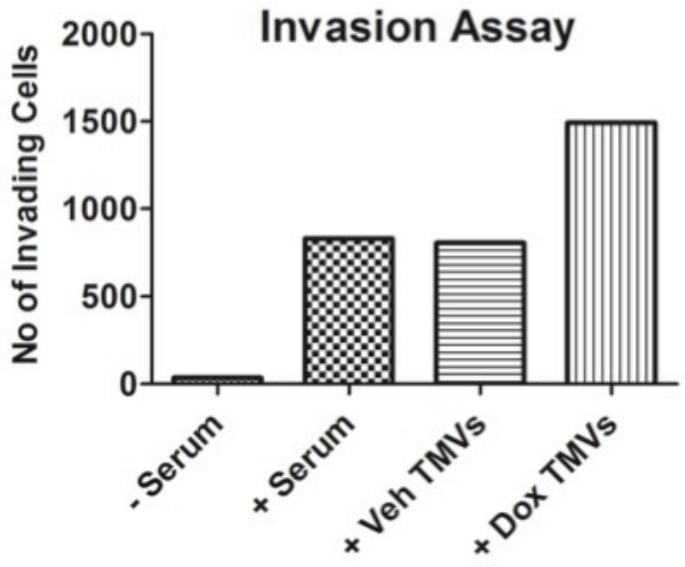

Figure 16: Doxorubicn-induced TMVs increase invasion of MCF7 cells

TMVs isolated from either vehicle or 100phingolipi treated MDA-MB-231 were co-cultured with MCF7 cells in serum-free medium for 4 hours, plated in the apical chamber of Matrigel-coated transwell inserts, and allowed to invade for 48 hours toward serum. For the negative control MCF7 cells with no TMVS were allowed to invade toward serum free media and the positive control MCF7 cells with no TMVs were allowed to invade toward serum. Invading cells were stained with fluorescent dye and counted.

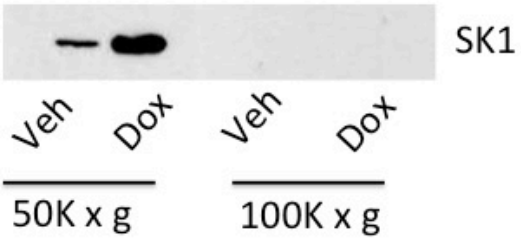

Figure 17: SK1 is enriched in doxorubicin-induced TMVs

The media from MDA-MB-231 treated with vehicle or doxorubicin for 68 hours was subjected to differential centrifugation. Pellets from the 50,000 x g and 100,000 x g spins, containing TMVs and exosomes respectively were analyzed by western blot for SK1 protein levels.

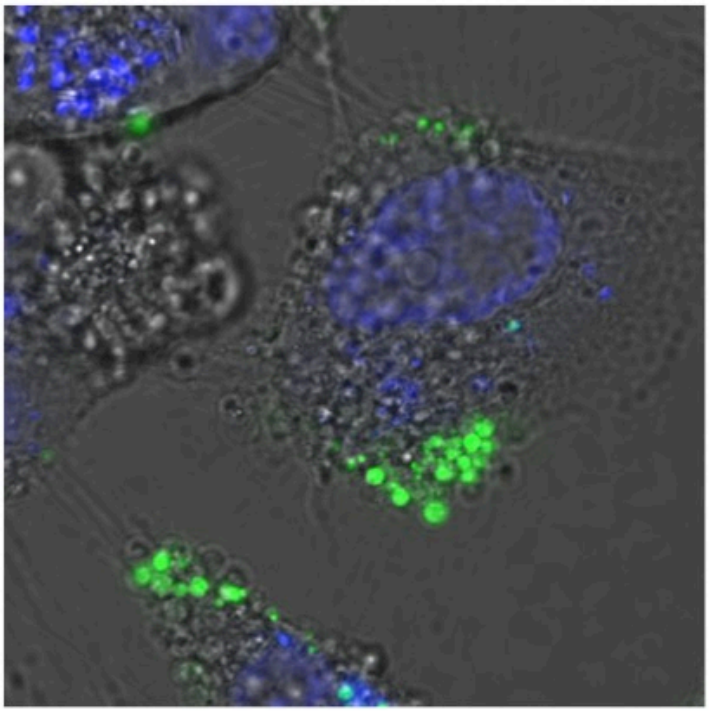

Figure 18: GFP-SK1 is found in TMVs shed from MDA-MB-231 breast cancer cells.

GFP-SK1 was overexpressed in MDA-MB-231 cells followed by doxorubicin treatment for 68 hours. Cells were then incubated with Draq5 a cell permeable dye that labels DNA for visualization (blue) and visualized by confocal microscopy.

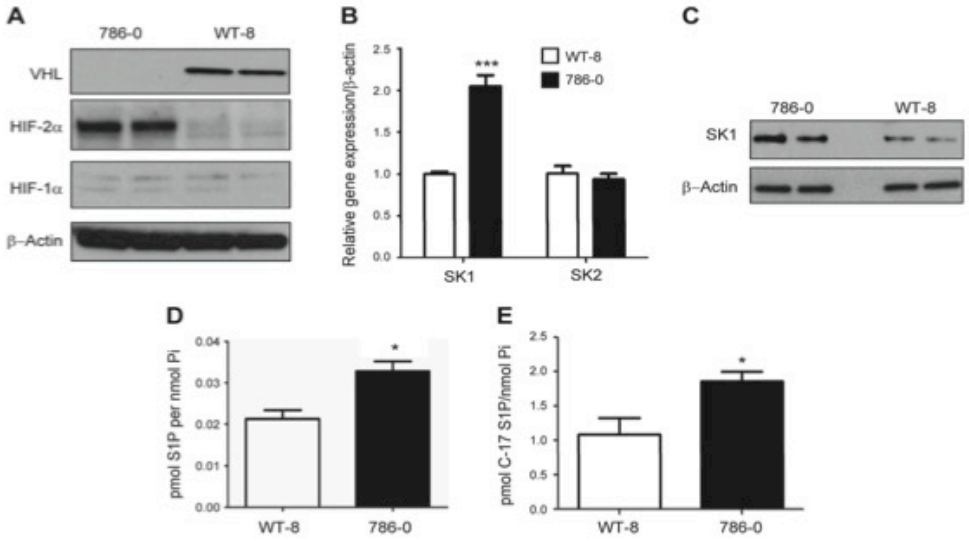

Figure 19. VHL-defective 786-0 cells showed higher expression of HIF-2a and SK1 with higher S1P levels.

(A) Proteins were extracted from VHL-defective (786-0) cells and those stably expressing VHL (WT-8) and subjected to Western blot analysis using VHL, HIF-2a, and HIF-1a antibodies; b-actin served as a protein loading control. B) Total RNA was extracted from 786-0 and WT-8 cells, and then it was reverse transcribed and used for quantitative PCR assay using SK1- and SK2-specific TaqMan probes. C) Protein samples from 786-0 and WT-8 cells were used for Western blot analysis using SK1 antibody and b-actin as a loading control. Lipids were extracted from unlabeled (D) or C17-sphingosine–labeled (E) 786-0 and WT-8 cells; S1P and C-17 S1P (C-17 S1P) were determined by mass spectrometry. Data are means of triplicate measurements and are expressed as picomole of lipid per nanomoles Pi. *P <0.05; ***P<0.001.

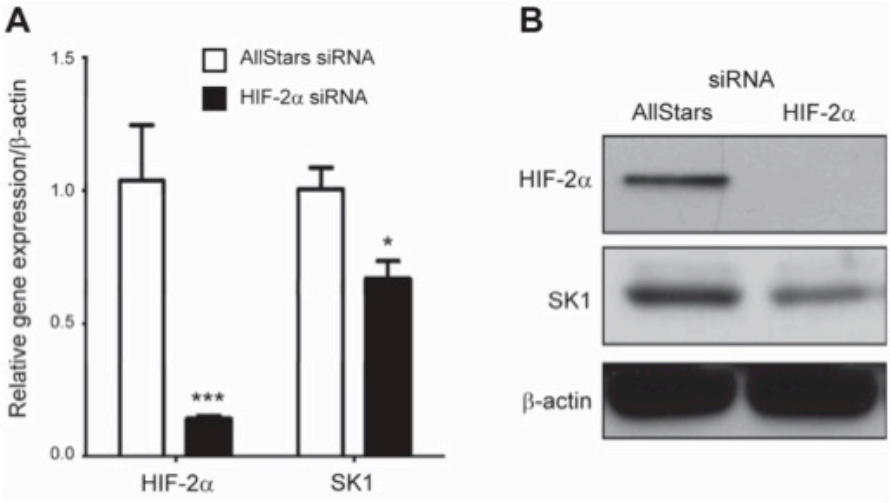

Figure 20. Knocking down of HIF-2a in 786-0 cells is associated with less SK1 expression. 786-0 cells were transfected with either AllStars negative control or HIF-2a siRNA for 48 hours, followed by RNA and protein extraction. Analyses of HIF-2a and SK1 message by quantitative PCR (A) and protein levels by Western blotting (B) were performed. *P<0.05, ***P<0.001; n=3.

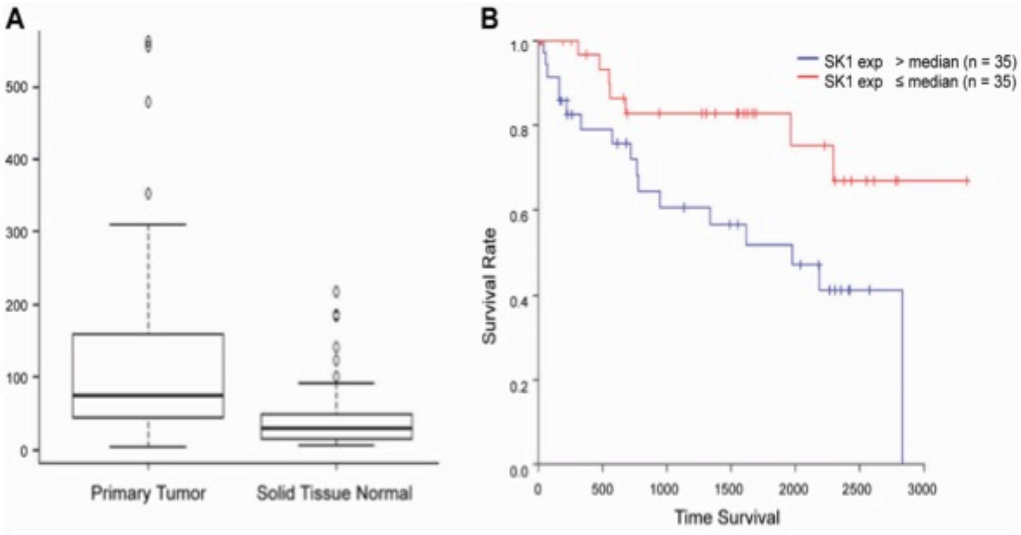

Figure 21. SK1 is highly expressed in primary tumors and associated with less survival rate in ccRCC patients.

(A) A box blot was generated from TCGA RNA seq datasets of paired normal and ccRCC tumor samples (72 samples) for SK1 gene expression, P = 0.00000457. B) Kaplan-Meier survival curve of ccRCC patients from TCGA database. Based on SK1 mRNA levels in their tumors, patients were equally divided into 2 groups (top and bottom 50% of SK1 expression); log-rank test, P=0.000000235.

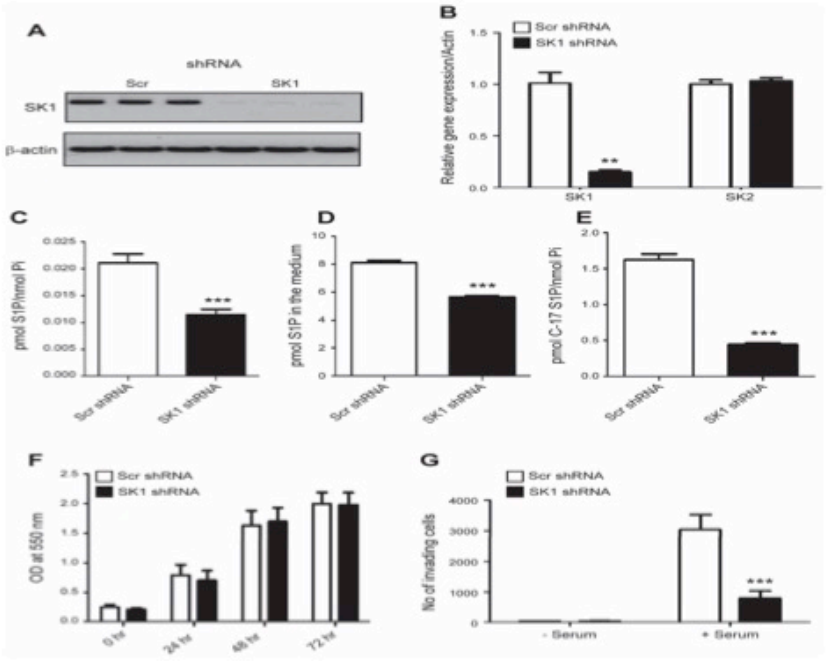

Figure 22. Down-regulation of SK1 expression does not affect proliferation but decreases the invasion of ccRCC. SK1 knockdown was achieved by introducing specific shRNA in 786-0 cells.

Knockdown was validated by quantitative PCR (A) and Western blotting (B). Silencing of SK1 was associated with a significant decrease in intracellular (C), extracellular (D), and C-17 S1P (E) levels. F) Cell proliferation was assessed by MTT assay; assay was performed in triplicate for each time point (0, 24, 48, and 72 hours). G) 786-0 cells stably expression scrambled (Scr) or SK1 shRNA were serum starved in serum-free medium for 4 hours, plated in the apical chamber of Matrigel-coated transwell inserts, and allowed to invade for 48 hours toward serum. Invading cells were stained with fluorescent dye and counted. **P<0.01, ***P<0.001; n=3.

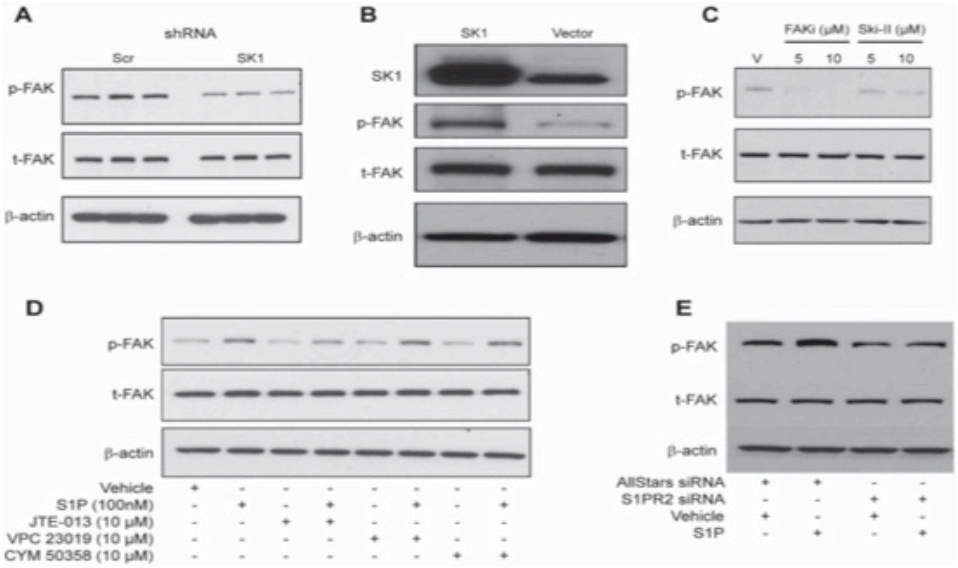

Figure 23. SK1 regulates phosphorylation of FAK in 786-0 cells through S1P-S1PR2.

(A) Protein lysates from scrambled (Scr) and SK1 shRNA stable cells were subjected to Western blot analysis for p-FAK, t-FAK, and b-actin as a loading control. B) 786-0 cells were transfected with either empty vector or SK1-expressing plasmid, followed by Western blot analysis of FAK phosphorylation. C) 786-0 cells were treated with vehicle (V), FAKi (5 and 10 mM), or sphingosine kinase inhibitor, Ski-II (5 and 10 mM final concentrations) for 24 hours followed by protein extraction and Western blotting analysis. Representative blots are shown from 3 independent experiments. D) SK1 shRNA stable cells were serum starved for 6 hours and treated with vehicle or 100 nM S1P for 10 minutes following 1-hour pretreatment with 10 mM from each S1PR2-specific antagonist, JTE-013; S1PR1/3 antagonist, VPC 23019; or S1PR4-specific antagonist, CYM 50358. pFAK, tFAK, and b-actin levels were analyzed by Western blotting. E) SK1 shRNA stable cells were transfected with AllStars negative control or S1PR2 siRNA. Cells were then serum starved and treated with vehicle or S1P for 10 minutes, and FAK phosphorylation was assessed by Western blotting

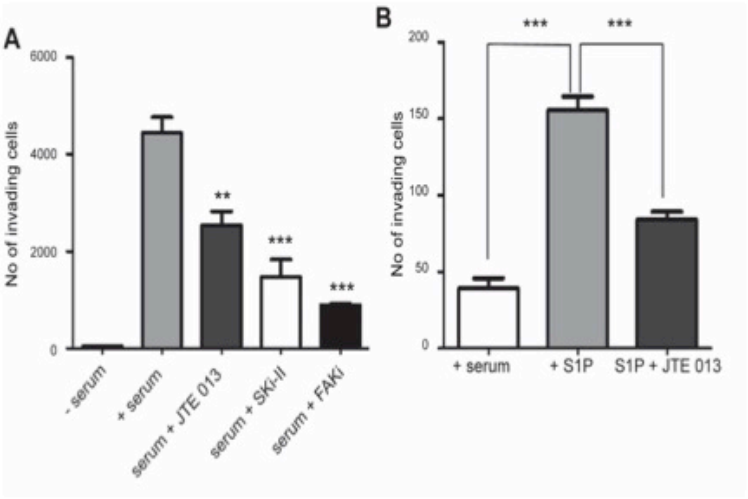

Figure 24. S1P receptor 2 antagonist (JTE013), pharmacologic inhibitors of sphingosine kinase (Ski-II) and FAK (FAKi) decreased the invasion of ccRCC cells.

(A) 786-0 cells stably expressing scrambled shRNA were serum starved in serum- free medium for 4 hours, plated in the apical chamber of Matrigel-coated transwell inserts, treated with 10 mM JTE013, 10 mM Ski-II, or 5 mM FAKi and allowed to invade for 48 hours toward serum. B) 786-0 cells stably expressing SK1 shRNA were serum starved in serum-free medium for 4 hours, plated in the apical chamber of Matrigel-coated transwell inserts with or without 10 mM JTE013, and allowed to invade for 48 hours toward serum-free medium or serum-free with S1P. Invading cells were stained with fluorescent dye and counted. *P< 0.05, **P<0.01, ***P<0.001; n=3.

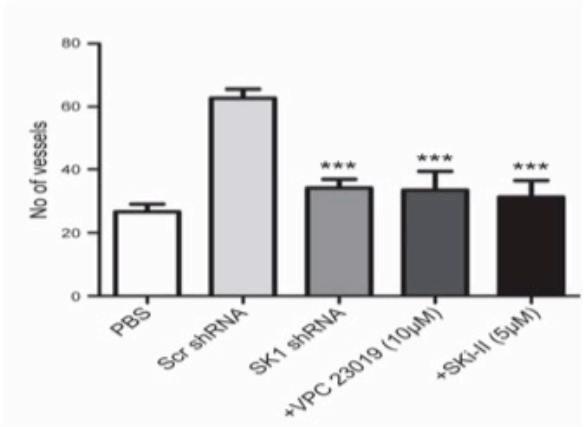

Figure 25. Down-regulation of SK1 expression is associated with less angiogenesis that is also blocked by the S1PR1/3 antagonist and Ski-II.
786-0 cells stably expressing SK1shRNA were incubated with CAM. The same was performed for cells expressing scrambled shRNA with or without 10 mM S1PR1/3 antagonist VPC23019 or inhibitor of sphingosine kinase, Ski- II, for 4 days. The membranes then were photographed, and blood vessels were counted. ***P<0.001; n = 3.

Supplemental Figures

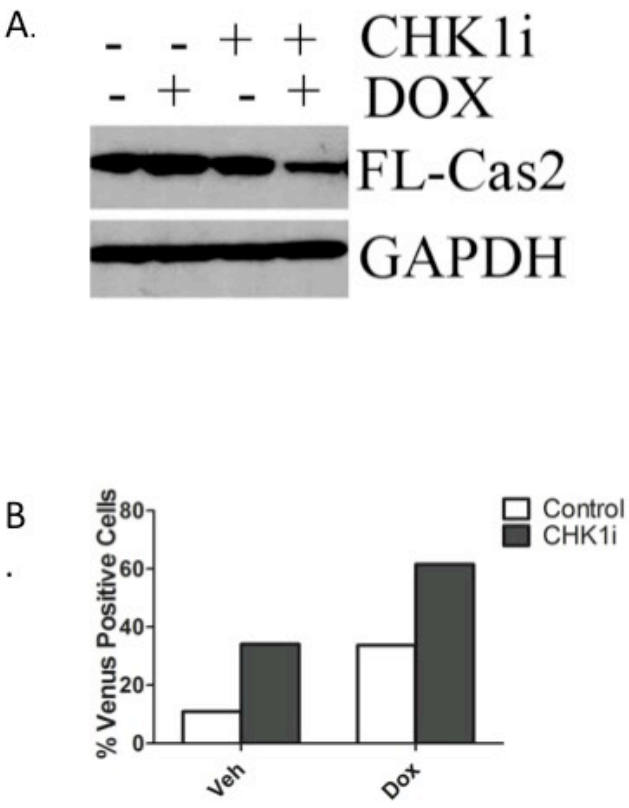

Figure S1: The CS-Pathway can be activated in wild type p53 breast cancer cells

(A) MCF7 cells were pretreated for 1 hour with 0.3uM CHK1 inhibitor (AZD7762) or DMSO followed by treatment with 0.4uM Dox or vehicle for 24 hours. Cells were then harvested in RIPA buffer and total cell lysate was analyzed by western blot for the proteins indicated. (B) MCF7 cells were transiently transfected with C2-CARD VN (500ng) and C2-CARD VC (500ng) along with pshooter.dsRed-mito (250ng) as a reporter for transfection. Twenty-four hours after transfection, cells were pretreated for 1 hour with 0.3uM CHK1 inhibitor (AZD7762) or DMSO followed by treatment with 0.4uM Dox or vehicle for 24 hours. Then the percentage of pshooter.ds.Red-mito-positive (red) cells that were Venus positive (green) was determined from a minimum of 100 cells per plate.

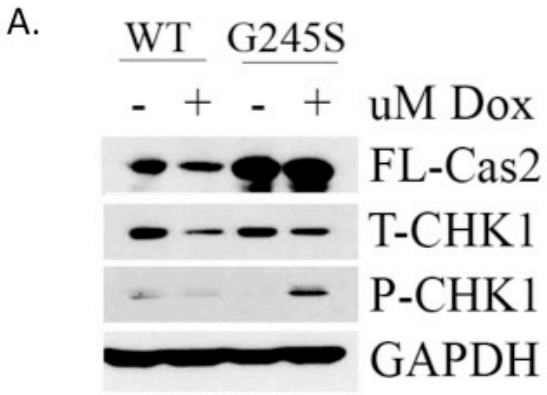

Figure S2: P53 deficiency triggers deregulation of the CHK1-Caspase 2 pathway

(A) WT or HUPK1 G245S MEFs were treated with 0.2uM Dox for 24h, harvested in RIPA buffer and total cell lysate was analyzed by western blot for the proteins indicated.

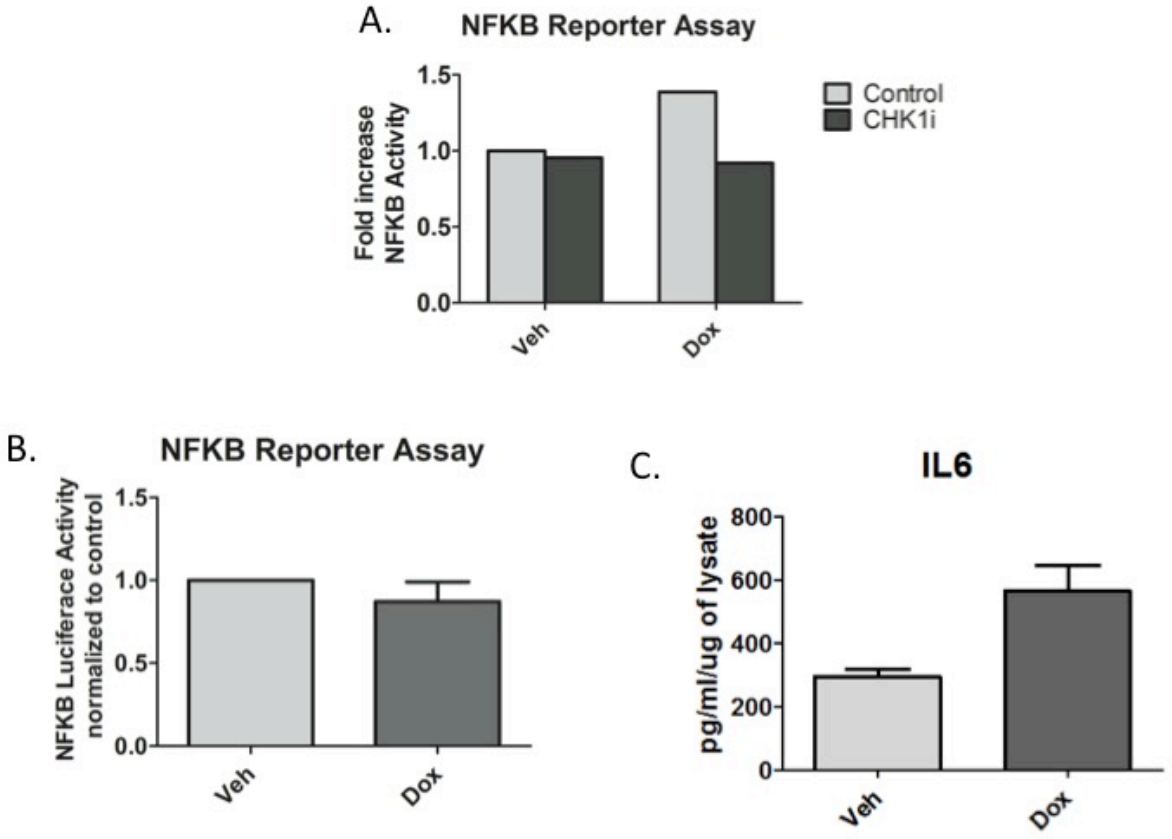

Figure S3: CHK1 levels regulate NFKB signaling in p53 deficient cells

(A) WT and HUPK1 G245S MEFs were co-transfected with 1ug of NFKB promoter-luciferase construct and V5 luciferase construct for 18 hours. MEFs were then pretreated for 1 hour with 0.3uM CHK1 inhibitor (AZD7762) or DMSO followed by treatment with 0.2uM doxorubicin for 24 hours. Luciferase and galactosidase activities were extracted and assayed as described in "Material and Methods" and measured luciferase activity was normalized to measured galactosidase activity. (B) MCF7 cells were co-transfected with 1ug of NFKB promoter-luciferase construct and V5 luciferase construct for 18 hours, followed by treatment with 0.8uM doxorubicin for 24 hours. Luciferase and galactosidase activities were extracted and assayed as described in "Material and Methods" and measured luciferase activity was normalized to measured galactosidase activity. (D) MDA-MB-231 cells were treated with 0.8uM doxorubicin for 24 hours, media was then collected and ELISA was performed to assess levels of IL6 protein in the media. Data are presented as mean ± SEM of 2 independent experiments.

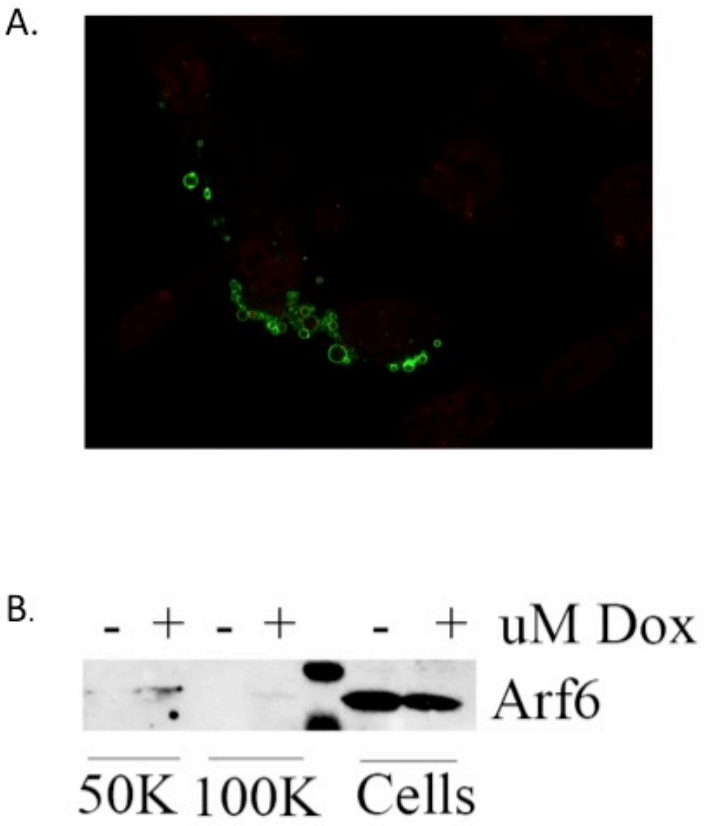

Figure S4: Doxorubicin induces the shedding of tumor-derived microvesicles containing inflammatory mediators

(A) MDA-MB-231 cells were treated 0.8uM doxorubicin for 24 hours. After 24 hours cells were stained with DRAQ5 to label all cells followed by treatment with Annexin-V and Propidium to specifically label. Images were then taken every 10 minutes for 12 hours. (B) MDA-MB-231 cells were treated 0.8uM doxorubicin for 60 hours. Cells were then harvested in RIPA buffer and media was then collected and subjected to differential centrifugation (outlined in "material and methods"). Protein was then extracted from the 50,000xg, 100,000xg pellet and cells. Lysate was analyzed by western blot for the protein indicated.

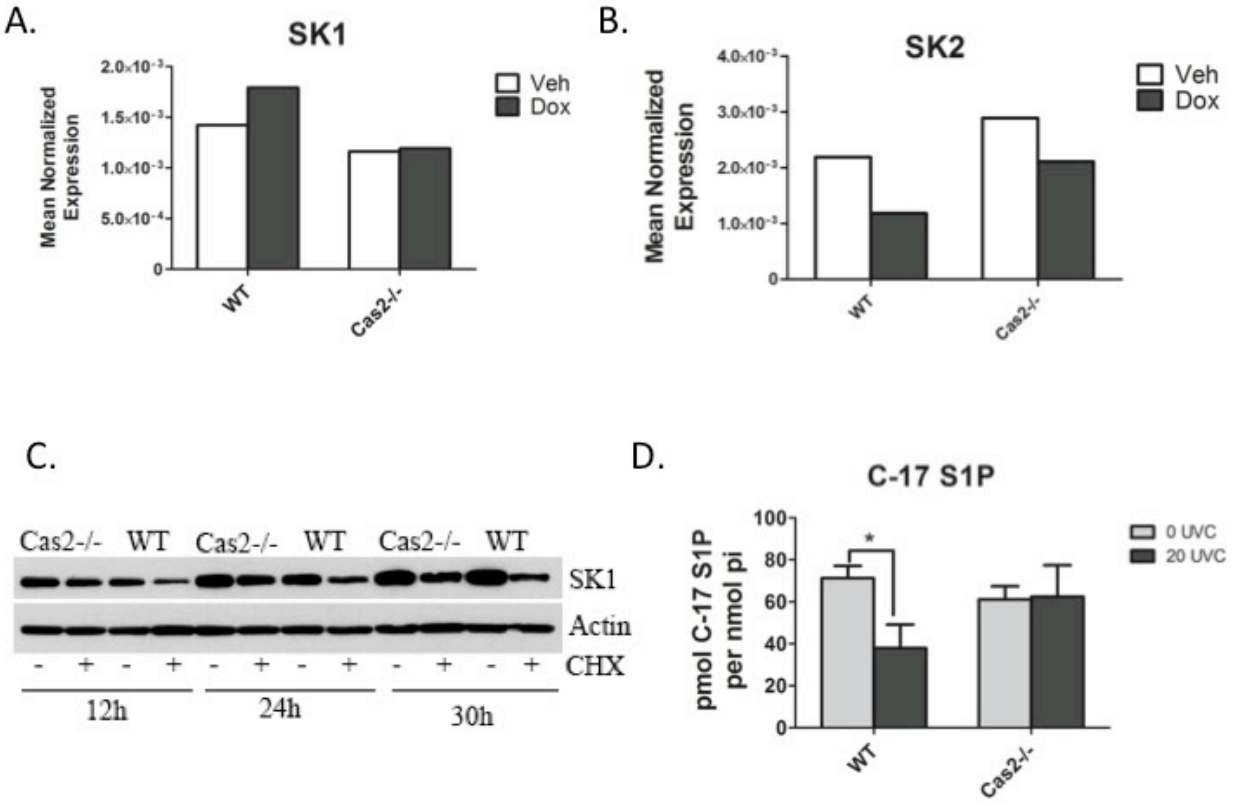

Figure S5: Caspase 2 is required for SK1 proteolysis

(A) MEFS were treated with 0.2uM doxorubicin for 24h and then harvested in RLT buffer, prepared for quantitative reverse transcriptase-PCR, with enzyme expression normalized to ß-actin expression for each reaction in triplicate. (B) MEFS were treated with 0.2uM doxorubicin for 24h and then harvested in RLT buffer, prepared for quantitative reverse transcriptase-PCR, with enzyme expression normalized to ß-actin expression for each reaction in triplicate. (C) MEFS were treated with 10uM cyclohexamide for the indicated times, harvested in RIPA buffer, and total cell lysate analyzed by western blot for the proteins indicated. (D) MEFS were treated with 0 or 20 J/m^2 for 24h and then incubated with C_{17}-sphingosine for 15 minutes. Following incubation, MEFS were harvested for 115phingolipidomic analysis by liquid chromatography mass spectrometry (LC/MS) and the C_{17}-containing S1P was normalized to the amount of lipid phosphate for each sample (n=3 *$p<0.05$ by Two-Way ANOVA).

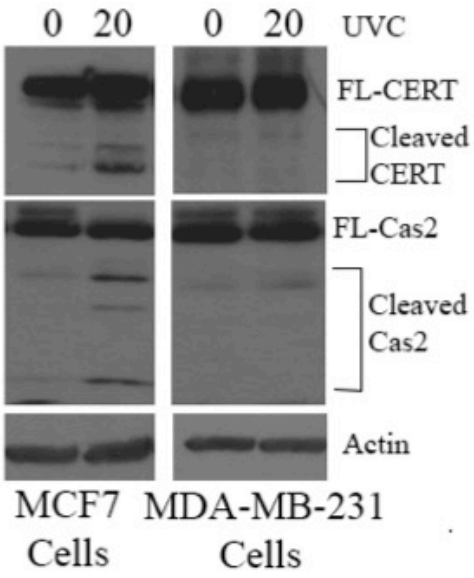

Figure S6: Caspase-2 mediated CERT proteolysis is deregulated in mutant p53 MDA-MB-231 TNBC cells

MCF7 and MDA-MB-231 cells were treated with 0 or 20J/m^2 for 24h harvested in RIPA buffer, and total cell lysate was analyzed by western blot for the proteins indicated.

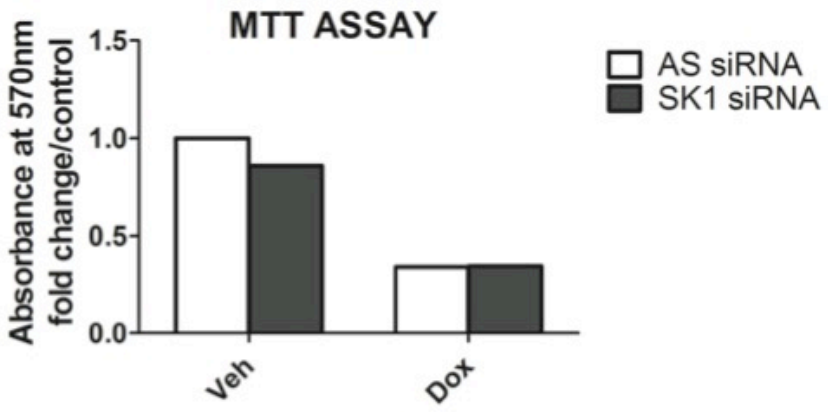

Figure S7: SK1 siRNA has no effect on doxorubicin sensitivity in MCF7 breast cancer cells

MCF7 cells were transfected with SK1 siRNA (20nM). Sixty hours after transfection, cells were treated with 0.8uM doxorubicin for 24 hours, and MTT assay was performed as in "Materials and Methods" to assess cell viability.

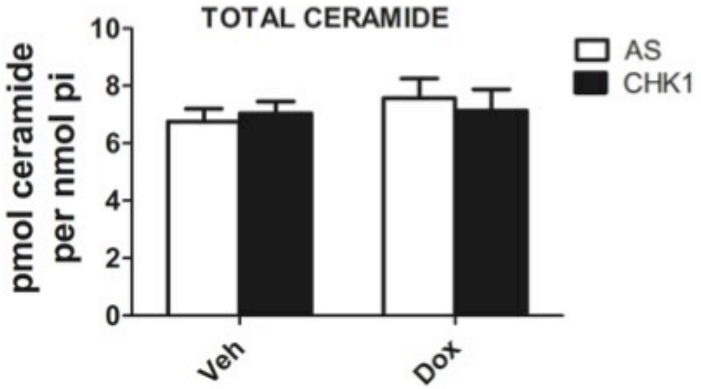

Figure S8: Activation of the CS-Pathway in mutant p53 TNBC cells does not effect ceramide levels

MDA-MB-231 cells were transfected with CHK1 siRNA (20nM). Forty-eight hours after transfection, cells were treated with 0.8uM doxorubicin and then harvested for 117phingolipidomic analysis by liquid chromatography mass spectrometry (LC/MS) to measure total ceramide (n=3).

Schemes

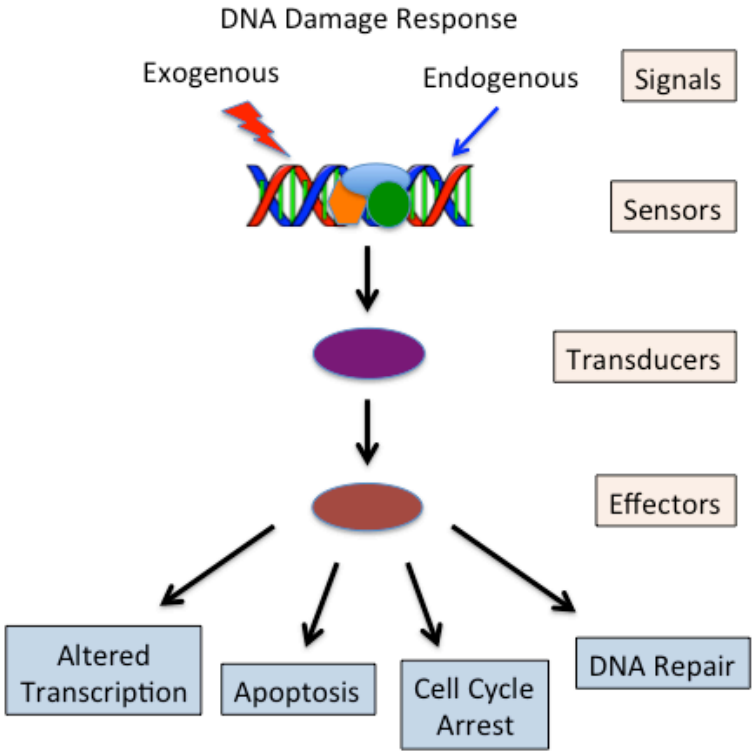

Scheme 1. The DNA damage Response

Exogenous and endogenous DNA damaging agents generate various types of lesions including DNA single- and double-strand breaks. These lesions are detected by a group proteins known collectively as sensors. Once recruited to sites of damage, sensors then recruit transducers, which act to transduce the signal via phosphorylation events of effectors. Effectors then relay these signals to initiate a myriad of biological responses including apoptosis, cell cycle arrest, DNA damage repair and altered transcription.

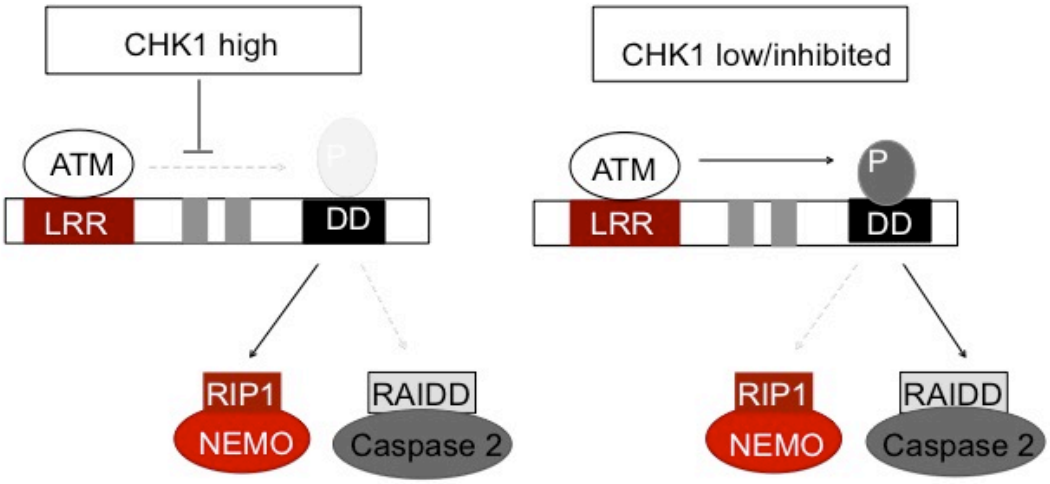

Scheme 2. The CHK1-Suppressed Pathway

The PIDDosome is required for CHK1-Suppressed (CS) cell death. CHK1 inhibits phosphorylation of PIDD by ATM on T788. Phosphorylation of PIDD by ATM recruits RAIDD and Caspase 2 leading to Caspase 2 activation and cell death.

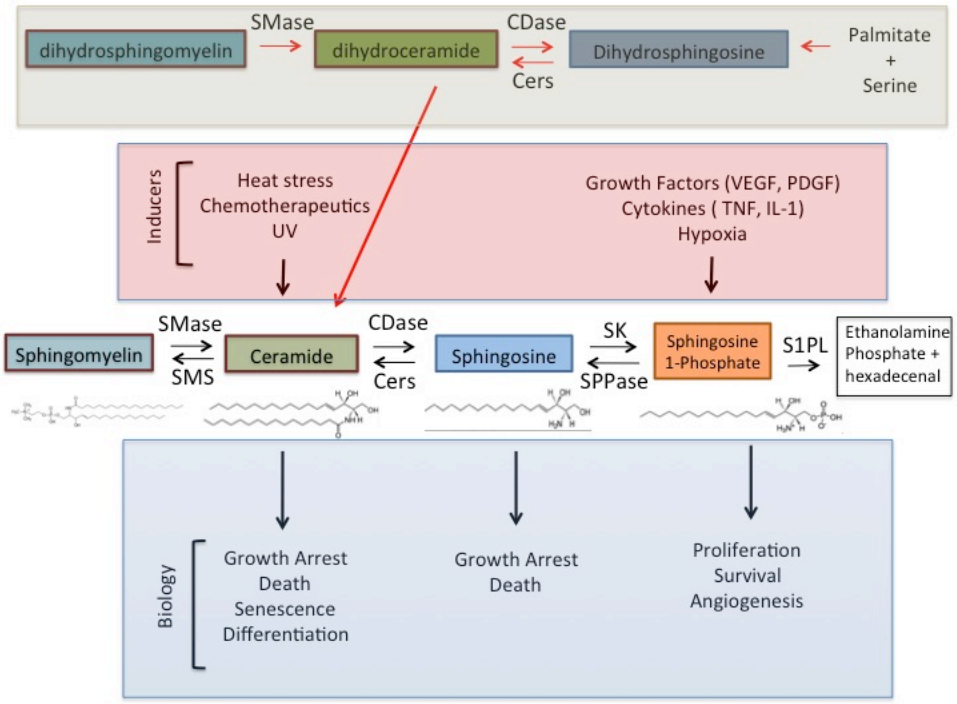

Scheme 3. Overview of Sphingolipid metabolism

Ceramide, the hub of sphingolipid metabolism can be generated several ways. De novo from the condensation of palmitate and serine or via the breakdown of sphingomyelin. Once generated, ceramide can then be converted to many other bioactive sphingolipid species. All of these reactions are carried out be a series of reactions orchestrated by the actions of highly regulated enzymes. The actions of these enzymes can be induced by a number of stimuli resulting in a myriad of biological responses.

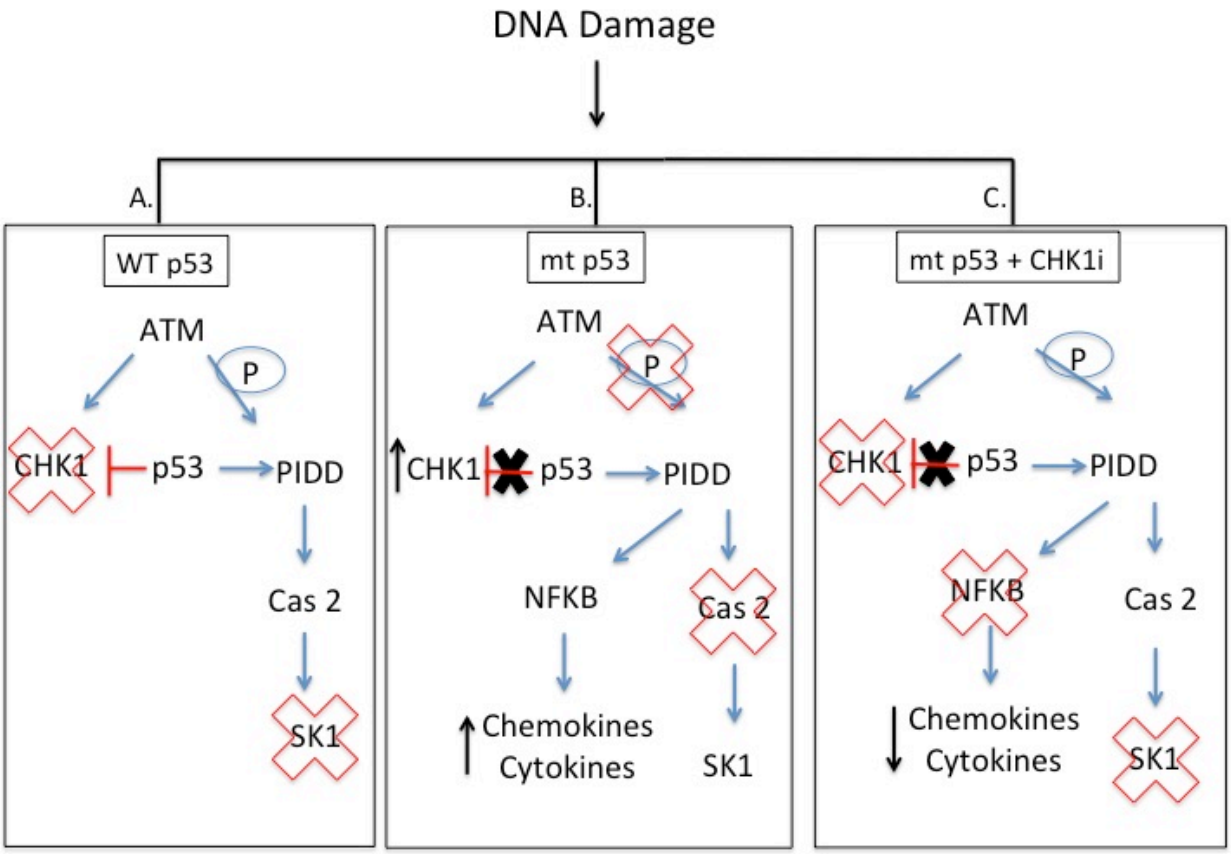

Scheme 4. **p53 regulation of the CS-pathway: Implications to NF-KB signaling and sphingolipid metabolism**

A. In response to DNA damage, wild type p53 acts as an endogenous inhibitor of CHK1 to initiate the CS-pathway and activate Caspase 2, leading to SK1 proteolysis. B. Mutant p53 cells, are deficient in the ability to down regulate CHK1 and initiate the CS-pathway, leading to SK1 persistence and NFKB activation in response to DNA damage. C. Inhibition or loss of CHK1 in mutant p53 cells, by-passes p53 to initiate the CS-pathway, leading to both activation of Caspase 2 and SK1 proteolysis and abrogation of NFKB signaling.

Tables

Sphingolipid signaling component		*Effect of DNA damage on activation/expression*	*DDR components shown to be upstream*	*DDR components shown to be downstream*
Ceramide		↑	ATM, p53, p21, Caspase-3, bcl-2	Caspase-3, PARP, p21, Rb
SMase	**nSMase2**	↑	Caspase-3, ATM, p53	
	nSMase3	↓	p53	
	ASMase	↑		Caspase-3, PARP
CerS		↑	ATM, ASMase, (bcl-2?)	Caspase-3, PARP, (bcl-2?)
CDase	**AC**	↑ (in cancer cells)	p53	?
	NC	↓	?	Rb
SK	**SK1**	↓	p53, Caspase 2, CHK1	p21, p16
	SK2	↑	?	p21
SPP1 & 2		↓	?	?
SPL		↓	p53, Caspase 2	

Table 1: Summary of current knowledge of the interactions between components of the sphingolipid pathway and the DNA damage response.

Gene	Fold Regulation	Gene	Fold Regulation	Gene	Fold Regulation	Gene	Fold Regulation	Gene	Fold Regulation	Gene	Fold Regulation
ADIPOQ	-1.9373	CCL24	-1.9381	CXCL16	-1.9373	IL17F	-3.86	IL8	-1.9427	TNFSF11	-1.9589
BMP2	-1.9942	CCL3	-1.9621	CXCL2	-1.9942	IL18	-1.9427	IL9	-1.9641	TNFSF13B	-1.9595
BMP4	-7.9218	CCL5	-4.0086	CXCL5	-7.9218	IL1A	-1.9641	LIF	-3.8498	VEGFA	-3.877
BMP6	-3.8613	CCL7	1.0194	CXCL9	-3.8613	IL1B	-3.8498	LTA	-1.934	XCL1	-1.9328
BMP7	-2.0126	CCL8	-1.952	FASLG	-2.0126	IL1RN	-1.934	LTB	1.0365	ACTB	1
C5	-1.9802	CD40LG	-1.9593	GPI	-1.9802	IL2	1.0365	MIF	1.0062	B2M	-1.9466
CCL1	1.0246	CNTF	-1.9461	IFNA2	1.0246	IL21	1.0062	MSTN	1.0494	GAPDH	-3.9306
CCL11	-1.9665	CSF1	-3.9428	IFNG	-1.9665	IL22	1.0494	NODAL	-1.9856	HPRT1	-3.8914
CCL13	1.0511	CSF2	-1.9795	IL10	1.0511	IL23A	-1.9856	OSM	-1.9564	RPLP0	-1.9516
CCL17	-1.9712	CSF3	-1.0096	IL11	-1.9712	IL24	-1.9564	PPBP	-1.9493	HGDC	1.0426
CCL18	-1.9603	CX3CL1	-1.9901	IL12A	-1.9603	IL27	-1.9493	SPP1	1.0331	RTC	1.0439
CCL19	1.0282	CXCL1	-1.9599	IL12B	1.0282	IL3	1.0331	TGFB2	-1.9256	RTC	-1.9261
CCL2	-1.945	CXCL10	-3.8706	IL13	-1.945	IL4	-1.9256	THPO	-1.9564	RTC	-1.9539
CCL20	-1.9324	CXCL11	-2.0054	IL15	-1.9324	IL5	-1.9564	TNF	-3.9446	PPC	-1.9616
CCL21	-1.9648	CXCL12	-1.9572	IL16	-1.9648	IL6	-3.9446	TNFRSF11B	-1.9593	PPC	-1.948
CCL22	-1.9616	CXCL13	1.0198	IL17A	-1.9616	IL7	-1.9593	TNFSF10	-1.9657	PPC	-1.9539

Table 2: Chemokine and cytokine mRNA array

MDA-MB-231 cells were transfected with CHK1 siRNA (20nM). Forty-eight hours after transfection, cells were treated with 0.8uM doxorubicin for 24 hours. RNA was then extracted, cDNA generated and a RT² Profiler™ PCR human Cytokines & Chemokines array was used to assess mRNA levels. Data was then analyzed using the Excel-based data analysis template provided by Qiagen. Data analysis is based on the $\Delta\Delta C_T$ method with normalization of the raw data to either housekeeping genes.

Bibliography

1. Jackson, S.P. and J. Bartek, *The DNA-damage response in human biology and disease.* Nature, 2009. **461**(7267): p. 1071-8.
2. Lindahl, T. and D.E. Barnes, *Repair of endogenous DNA damage.* Cold Spring Harb Symp Quant Biol, 2000. **65**: p. 127-33.
3. Barnes, D.E., T. Lindahl, and B. Sedgwick, *DNA repair.* Curr Opin Cell Biol, 1993. **5**(3): p. 424-33.
4. Stratton, M.R., P.J. Campbell, and P.A. Futreal, *The cancer genome.* Nature, 2009. **458**(7239): p. 719-24.
5. Halazonetis, T.D., V.G. Gorgoulis, and J. Bartek, *An oncogene-induced DNA damage model for cancer development.* Science, 2008. **319**(5868): p. 1352-5.
6. Almeida, K.H. and R.W. Sobol, *A unified view of base excision repair: lesion-dependent protein complexes regulated by post-translational modification.* DNA Repair (Amst), 2007. **6**(6): p. 695-711.
7. Caldecott, K.W., *Mammalian single-strand break repair: mechanisms and links with chromatin.* DNA Repair (Amst), 2007. **6**(4): p. 443-53.
8. Reynolds, J.J., et al., *Defective DNA ligation during short-patch single-strand break repair in ataxia oculomotor apraxia 1.* Mol Cell Biol, 2009. **29**(5): p. 1354-62.
9. Cleaver, J.E., E.T. Lam, and I. Revet, *Disorders of nucleotide excision repair: the genetic and molecular basis of heterogeneity.* Nat Rev Genet, 2009. **10**(11): p. 756-68.
10. Bohr, V.A., D.S. Okumoto, and P.C. Hanawalt, *Survival of UV-irradiated mammalian cells correlates with efficient DNA repair in an essential gene.* Proc Natl Acad Sci U S A, 1986. **83**(11): p. 3830-3.
11. Hanawalt, P.C., *Evolution of concepts in DNA repair.* Environ Mol Mutagen, 1994. **23 Suppl 24**: p. 78-85.
12. Sugasawa, K., et al., *Two-step recognition of DNA damage for mammalian nucleotide excision repair: Directional binding of the XPC complex and DNA strand scanning.* Mol Cell, 2009. **36**(4): p. 642-53.
13. de Laat, W.L., et al., *DNA structural elements required for ERCC1-XPF endonuclease activity.* J Biol Chem, 1998. **273**(14): p. 7835-42.
14. O'Donovan, A., et al., *XPG endonuclease makes the 3' incision in human DNA nucleotide excision repair.* Nature, 1994. **371**(6496): p. 432-5.
15. Sijbers, A.M., et al., *Xeroderma pigmentosum group F caused by a defect in a structure-specific DNA repair endonuclease.* Cell, 1996. **86**(5): p. 811-22.
16. Ogi, T., et al., *Three DNA polymerases, recruited by different mechanisms, carry out NER repair synthesis in human cells.* Mol Cell, 2010. **37**(5): p. 714-27.
17. Moser, J., et al., *Sealing of chromosomal DNA nicks during nucleotide excision repair requires XRCC1 and DNA ligase III alpha in a cell-cycle-specific manner.* Mol Cell, 2007. **27**(2): p. 311-23.
18. San Filippo, J., P. Sung, and H. Klein, *Mechanism of eukaryotic homologous recombination.* Annu Rev Biochem, 2008. **77**: p. 229-57.
19. de Jager, M., et al., *Human Rad50/Mre11 is a flexible complex that can tether DNA ends.* Mol Cell, 2001. **8**(5): p. 1129-35.
20. Limbo, O., et al., *Ctp1 is a cell-cycle-regulated protein that functions with Mre11 complex to control double-strand break repair by homologous recombination.* Mol Cell, 2007. **28**(1): p. 134-46.

21. Sartori, A.A., et al., *Human CtIP promotes DNA end resection.* Nature, 2007. **450**(7169): p. 509-14.
22. Wyman, C., D. Ristic, and R. Kanaar, *Homologous recombination-mediated double-strand break repair.* DNA Repair (Amst), 2004. **3**(8-9): p. 827-33.
23. Lieber, M.R., *The mechanism of human nonhomologous DNA end joining.* J Biol Chem, 2008. **283**(1): p. 1-5.
24. Helleday, T., et al., *DNA double-strand break repair: from mechanistic understanding to cancer treatment.* DNA Repair (Amst), 2007. **6**(7): p. 923-35.
25. Mukherjee, B., et al., *DNA-PK phosphorylates histone H2AX during apoptotic DNA fragmentation in mammalian cells.* DNA Repair (Amst), 2006. **5**(5): p. 575-90.
26. van Heemst, D., et al., *End-joining of blunt DNA double-strand breaks in mammalian fibroblasts is precise and requires DNA-PK and XRCC4.* DNA Repair (Amst), 2004. **3**(1): p. 43-50.
27. Zhou, B.B. and S.J. Elledge, *The DNA damage response: putting checkpoints in perspective.* Nature, 2000. **408**(6811): p. 433-9.
28. Bernstein, C., et al., *DNA repair/pro-apoptotic dual-role proteins in five major DNA repair pathways: fail-safe protection against carcinogenesis.* Mutat Res, 2002. **511**(2): p. 145-78.
29. Elledge, S.J., *Cell cycle checkpoints: preventing an identity crisis.* Science, 1996. **274**(5293): p. 1664-72.
30. Bartek, J. and J. Lukas, *DNA damage checkpoints: from initiation to recovery or adaptation.* Curr Opin Cell Biol, 2007. **19**(2): p. 238-45.
31. Shiloh, Y., *ATM and related protein kinases: safeguarding genome integrity.* Nat Rev Cancer, 2003. **3**(3): p. 155-68.
32. Uziel, T., et al., *Requirement of the MRN complex for ATM activation by DNA damage.* EMBO J, 2003. **22**(20): p. 5612-21.
33. Kim, S.T., et al., *Substrate specificities and identification of putative substrates of ATM kinase family members.* J Biol Chem, 1999. **274**(53): p. 37538-43.
34. Savitsky, K., et al., *A single ataxia telangiectasia gene with a product similar to PI-3 kinase.* Science, 1995. **268**(5218): p. 1749-53.
35. Zou, L. and S.J. Elledge, *Sensing DNA damage through ATRIP recognition of RPA-ssDNA complexes.* Science, 2003. **300**(5625): p. 1542-8.
36. Brown, E.J. and D. Baltimore, *ATR disruption leads to chromosomal fragmentation and early embryonic lethality.* Genes Dev, 2000. **14**(4): p. 397-402.
37. de Klein, A., et al., *Targeted disruption of the cell-cycle checkpoint gene ATR leads to early embryonic lethality in mice.* Curr Biol, 2000. **10**(8): p. 479-82.
38. Smith, J., et al., *The ATM-Chk2 and ATR-Chk1 pathways in DNA damage signaling and cancer.* Adv Cancer Res, 2010. **108**: p. 73-112.
39. Goto, H., K. Kasahara, and M. Inagaki, *Novel insights into chk1 regulation by phosphorylation.* Cell Struct Funct, 2015. **40**(1): p. 43-50.
40. Liu, Q., et al., *Chk1 is an essential kinase that is regulated by Atr and required for the G(2)/M DNA damage checkpoint.* Genes Dev, 2000. **14**(12): p. 1448-59.
41. Takai, H., et al., *Aberrant cell cycle checkpoint function and early embryonic death in Chk1(-/-) mice.* Genes Dev, 2000. **14**(12): p. 1439-47.

42. Ahn, J.Y., et al., *Threonine 68 phosphorylation by ataxia telangiectasia mutated is required for efficient activation of Chk2 in response to ionizing radiation.* Cancer Res, 2000. **60**(21): p. 5934-6.
43. Bell, D.W., et al., *Heterozygous germ line hCHK2 mutations in Li-Fraumeni syndrome.* Science, 1999. **286**(5449): p. 2528-31.
44. Meijers-Heijboer, H., et al., *Low-penetrance susceptibility to breast cancer due to CHEK2(*)1100delC in noncarriers of BRCA1 or BRCA2 mutations.* Nat Genet, 2002. **31**(1): p. 55-9.
45. Gatei, M., et al., *Ataxia-telangiectasia-mutated (ATM) and NBS1-dependent phosphorylation of Chk1 on Ser-317 in response to ionizing radiation.* J Biol Chem, 2003. **278**(17): p. 14806-11.
46. Sorensen, C.S., et al., *Chk1 regulates the S phase checkpoint by coupling the physiological turnover and ionizing radiation-induced accelerated proteolysis of Cdc25A.* Cancer Cell, 2003. **3**(3): p. 247-58.
47. Vogelstein, B., D. Lane, and A.J. Levine, *Surfing the p53 network.* Nature, 2000. **408**(6810): p. 307-10.
48. el-Deiry, W.S., et al., *WAF1, a potential mediator of p53 tumor suppression.* Cell, 1993. **75**(4): p. 817-25.
49. Wang, L., et al., *Analyses of p53 target genes in the human genome by bioinformatic and microarray approaches.* J Biol Chem, 2001. **276**(47): p. 43604-10.
50. Alarcon-Vargas, D. and Z. Ronai, *p53-Mdm2--the affair that never ends.* Carcinogenesis, 2002. **23**(4): p. 541-7.
51. Harris, S.L. and A.J. Levine, *The p53 pathway: positive and negative feedback loops.* Oncogene, 2005. **24**(17): p. 2899-908.
52. Sakaguchi, K., et al., *DNA damage activates p53 through a phosphorylation-acetylation cascade.* Genes Dev, 1998. **12**(18): p. 2831-41.
53. Guardavaccaro, D. and M. Pagano, *Stabilizers and destabilizers controlling cell cycle oscillators.* Mol Cell, 2006. **22**(1): p. 1-4.
54. Brugarolas, J., et al., *Radiation-induced cell cycle arrest compromised by p21 deficiency.* Nature, 1995. **377**(6549): p. 552-7.
55. Deng, C., et al., *Mice lacking p21CIP1/WAF1 undergo normal development, but are defective in G1 checkpoint control.* Cell, 1995. **82**(4): p. 675-84.
56. Clarke, A.R., et al., *Thymocyte apoptosis induced by p53-dependent and independent pathways.* Nature, 1993. **362**(6423): p. 849-52.
57. Lowe, S.W., et al., *p53 is required for radiation-induced apoptosis in mouse thymocytes.* Nature, 1993. **362**(6423): p. 847-9.
58. Merritt, A.J., et al., *The role of p53 in spontaneous and radiation-induced apoptosis in the gastrointestinal tract of normal and p53-deficient mice.* Cancer Res, 1994. **54**(3): p. 614-7.
59. Strasser, A., et al., *DNA damage can induce apoptosis in proliferating lymphoid cells via p53-independent mechanisms inhibitable by Bcl-2.* Cell, 1994. **79**(2): p. 329-39.
60. Muller, M., et al., *The role of p53 and the CD95 (APO-1/Fas) death system in chemotherapy-induced apoptosis.* Eur Cytokine Netw, 1998. **9**(4): p. 685-6.
61. Wu, G.S., et al., *KILLER/DR5 is a DNA damage-inducible p53-regulated death receptor gene.* Nat Genet, 1997. **17**(2): p. 141-3.

62. McIlwain, D.R., T. Berger, and T.W. Mak, *Caspase functions in cell death and disease.* Cold Spring Harb Perspect Biol, 2013. **5**(4): p. a008656.
63. Adams, J.M. and S. Cory, *The Bcl-2 protein family: arbiters of cell survival.* Science, 1998. **281**(5381): p. 1322-6.
64. Miyashita, T. and J.C. Reed, *Tumor suppressor p53 is a direct transcriptional activator of the human bax gene.* Cell, 1995. **80**(2): p. 293-9.
65. Nakano, K. and K.H. Vousden, *PUMA, a novel proapoptotic gene, is induced by p53.* Mol Cell, 2001. **7**(3): p. 683-94.
66. Yu, J., et al., *PUMA induces the rapid apoptosis of colorectal cancer cells.* Mol Cell, 2001. **7**(3): p. 673-82.
67. Oda, E., et al., *Noxa, a BH3-only member of the Bcl-2 family and candidate mediator of p53-induced apoptosis.* Science, 2000. **288**(5468): p. 1053-8.
68. Oda, K., et al., *p53AIP1, a potential mediator of p53-dependent apoptosis, and its regulation by Ser-46-phosphorylated p53.* Cell, 2000. **102**(6): p. 849-62.
69. Lin, Y., W. Ma, and S. Benchimol, *Pidd, a new death-domain-containing protein, is induced by p53 and promotes apoptosis.* Nat Genet, 2000. **26**(1): p. 122-7.
70. Tinel, A. and J. Tschopp, *The PIDDosome, a protein complex implicated in activation of caspase-2 in response to genotoxic stress.* Science, 2004. **304**(5672): p. 843-6.
71. Moroni, M.C., et al., *Apaf-1 is a transcriptional target for E2F and p53.* Nat Cell Biol, 2001. **3**(6): p. 552-8.
72. Zou, H., et al., *An APAF-1.cytochrome c multimeric complex is a functional apoptosome that activates procaspase-9.* J Biol Chem, 1999. **274**(17): p. 11549-56.
73. MacLachlan, T.K. and W.S. El-Deiry, *Apoptotic threshold is lowered by p53 transactivation of caspase-6.* Proc Natl Acad Sci U S A, 2002. **99**(14): p. 9492-7.
74. Zhang, Y. and T. Hunter, *Roles of Chk1 in cell biology and cancer therapy.* Int J Cancer, 2014. **134**(5): p. 1013-23.
75. Ma, C.X., et al., *Targeting Chk1 in p53-deficient triple-negative breast cancer is therapeutically beneficial in human-in-mouse tumor models.* J Clin Invest, 2012. **122**(4): p. 1541-52.
76. Golding, S.E., et al., *Improved ATM kinase inhibitor KU-60019 radiosensitizes glioma cells, compromises insulin, AKT and ERK prosurvival signaling, and inhibits migration and invasion.* Mol Cancer Ther, 2009. **8**(10): p. 2894-902.
77. Fokas, E., et al., *Targeting ATR in vivo using the novel inhibitor VE-822 results in selective sensitization of pancreatic tumors to radiation.* Cell Death Dis, 2012. **3**: p. e441.
78. Prevo, R., et al., *The novel ATR inhibitor VE-821 increases sensitivity of pancreatic cancer cells to radiation and chemotherapy.* Cancer Biol Ther, 2012. **13**(11): p. 1072-81.
79. Ma, C.X., J.W. Janetka, and H. Piwnica-Worms, *Death by releasing the breaks: CHK1 inhibitors as cancer therapeutics.* Trends Mol Med, 2011. **17**(2): p. 88-96.
80. Garrett, M.D. and I. Collins, *Anticancer therapy with checkpoint inhibitors: what, where and when?* Trends Pharmacol Sci, 2011. **32**(5): p. 308-16.
81. Takahashi, I., et al., *UCN-01 and UCN-02, new selective inhibitors of protein kinase C. II. Purification, physico-chemical properties, structural determination and biological activities.* J Antibiot (Tokyo), 1989. **42**(4): p. 571-6.
82. Graves, P.R., et al., *The Chk1 protein kinase and the Cdc25C regulatory pathways are targets of the anticancer agent UCN-01.* J Biol Chem, 2000. **275**(8): p. 5600-5.

83. Zhao, B., et al., *Structural basis for Chk1 inhibition by UCN-01.* J Biol Chem, 2002. **277**(48): p. 46609-15.
84. Carrassa, L. and G. Damia, *Unleashing Chk1 in cancer therapy.* Cell Cycle, 2011. **10**(13): p. 2121-8.
85. McNeely, S., R. Beckmann, and A.K. Bence Lin, *CHEK again: revisiting the development of CHK1 inhibitors for cancer therapy.* Pharmacol Ther, 2014. **142**(1): p. 1-10.
86. Montano, R., et al., *Sensitization of human cancer cells to gemcitabine by the Chk1 inhibitor MK-8776: cell cycle perturbation and impact of administration schedule in vitro and in vivo.* BMC Cancer, 2013. **13**: p. 604.
87. Thompson, R. and A. Eastman, *The cancer therapeutic potential of Chk1 inhibitors: how mechanistic studies impact on clinical trial design.* Br J Clin Pharmacol, 2013. **76**(3): p. 358-69.
88. De Witt Hamer, P.C., et al., *WEE1 kinase targeting combined with DNA-damaging cancer therapy catalyzes mitotic catastrophe.* Clin Cancer Res, 2011. **17**(13): p. 4200-7.
89. Bryant, C., R. Rawlinson, and A.J. Massey, *Chk1 inhibition as a novel therapeutic strategy for treating triple-negative breast and ovarian cancers.* BMC Cancer, 2014. **14**: p. 570.
90. Bryant, C., K. Scriven, and A.J. Massey, *Inhibition of the checkpoint kinase Chk1 induces DNA damage and cell death in human Leukemia and Lymphoma cells.* Mol Cancer, 2014. **13**: p. 147.
91. Kim, M.K., J. James, and C.M. Annunziata, *Topotecan synergizes with CHEK1 (CHK1) inhibitor to induce apoptosis in ovarian cancer cells.* BMC Cancer, 2015. **15**(1): p. 196.
92. Ma, Z., et al., *The Chk1 inhibitor AZD7762 sensitises p53 mutant breast cancer cells to radiation in vitro and in vivo.* Mol Med Rep, 2012. **6**(4): p. 897-903.
93. Castedo, M., et al., *Cell death by mitotic catastrophe: a molecular definition.* Oncogene, 2004. **23**(16): p. 2825-37.
94. Sidi, S., et al., *Chk1 suppresses a caspase-2 apoptotic response to DNA damage that bypasses p53, Bcl-2, and caspase-3.* Cell, 2008. **133**(5): p. 864-77.
95. Hannun, Y.A., C. Luberto, and K.M. Argraves, *Enzymes of sphingolipid metabolism: from modular to integrative signaling.* Biochemistry, 2001. **40**(16): p. 4893-903.
96. Mathias, S., L.A. Pena, and R.N. Kolesnick, *Signal transduction of stress via ceramide.* Biochem J, 1998. **335 (Pt 3)**: p. 465-80.
97. Reynolds, C.P., B.J. Maurer, and R.N. Kolesnick, *Ceramide synthesis and metabolism as a target for cancer therapy.* Cancer Lett, 2004. **206**(2): p. 169-80.
98. Gault, C.R. and L.M. Obeid, *Still benched on its way to the bedside: sphingosine kinase 1 as an emerging target in cancer chemotherapy.* Crit Rev Biochem Mol Biol, 2011. **46**(4): p. 342-51.
99. Hannun, Y.A. and L.M. Obeid, *Principles of bioactive lipid signalling: lessons from sphingolipids.* Nat Rev Mol Cell Biol, 2008. **9**(2): p. 139-50.
100. Marchesini, N., J.A. Jones, and Y.A. Hannun, *Confluence induced threonine41/serine45 phospho-beta-catenin dephosphorylation via ceramide-mediated activation of PP1cgamma.* Biochim Biophys Acta, 2007. **1771**(12): p. 1418-28.

101. Milhas, D., C.J. Clarke, and Y.A. Hannun, *Sphingomyelin metabolism at the plasma membrane: implications for bioactive sphingolipids.* FEBS Lett, 2010. **584**(9): p. 1887-94.
102. Tani, M. and Y.A. Hannun, *Analysis of membrane topology of neutral sphingomyelinase 2.* FEBS Lett, 2007. **581**(7): p. 1323-8.
103. Hofmann, K., et al., *Cloning and characterization of the mammalian brain-specific, Mg2+-dependent neutral sphingomyelinase.* Proc Natl Acad Sci U S A, 2000. **97**(11): p. 5895-900.
104. Wu, B.X., et al., *Identification of novel anionic phospholipid binding domains in neutral sphingomyelinase 2 with selective binding preference.* J Biol Chem, 2011. **286**(25): p. 22362-71.
105. Clarke, C.J., T.G. Truong, and Y.A. Hannun, *Role for neutral sphingomyelinase-2 in tumor necrosis factor alpha-stimulated expression of vascular cell adhesion molecule-1 (VCAM) and intercellular adhesion molecule-1 (ICAM) in lung epithelial cells: p38 MAPK is an upstream regulator of nSMase2.* J Biol Chem, 2007. **282**(2): p. 1384-96.
106. Filosto, S., et al., *Neutral sphingomyelinase 2: a novel target in cigarette smoke-induced apoptosis and lung injury.* Am J Respir Cell Mol Biol, 2011. **44**(3): p. 350-60.
107. Goldkorn, T. and S. Filosto, *Lung injury and cancer: Mechanistic insights into ceramide and EGFR signaling under cigarette smoke.* Am J Respir Cell Mol Biol, 2010. **43**(3): p. 259-68.
108. Khavandgar, Z., et al., *A cell-autonomous requirement for neutral sphingomyelinase 2 in bone mineralization.* J Cell Biol, 2011. **194**(2): p. 277-89.
109. Kim, W.J., et al., *Mutations in the neutral sphingomyelinase gene SMPD3 implicate the ceramide pathway in human leukemias.* Blood, 2008. **111**(9): p. 4716-22.
110. Jenkins, R.W., D. Canals, and Y.A. Hannun, *Roles and regulation of secretory and lysosomal acid sphingomyelinase.* Cell Signal, 2009. **21**(6): p. 836-46.
111. Schissel, S.L., et al., *Zn2+-stimulated sphingomyelinase is secreted by many cell types and is a product of the acid sphingomyelinase gene.* J Biol Chem, 1996. **271**(31): p. 18431-6.
112. Schuchman, E.H., *The pathogenesis and treatment of acid sphingomyelinase-deficient Niemann-Pick disease.* J Inherit Metab Dis, 2007. **30**(5): p. 654-63.
113. Vit, J.P. and F. Rosselli, *Role of the ceramide-signaling pathways in ionizing radiation-induced apoptosis.* Oncogene, 2003. **22**(54): p. 8645-52.
114. Doehner, W., et al., *Secretory sphingomyelinase is upregulated in chronic heart failure: a second messenger system of immune activation relates to body composition, muscular functional capacity, and peripheral blood flow.* Eur Heart J, 2007. **28**(7): p. 821-8.
115. Gorska, M., E. Baranczuk, and A. Dobrzyn, *Secretory Zn2+-dependent sphingomyelinase activity in the serum of patients with type 2 diabetes is elevated.* Horm Metab Res, 2003. **35**(8): p. 506-7.
116. Tabas, I., *Secretory sphingomyelinase.* Chem Phys Lipids, 1999. **102**(1-2): p. 123-30.
117. Schuchman, E.H., *Acid sphingomyelinase, cell membranes and human disease: lessons from Niemann-Pick disease.* FEBS Lett, 2010. **584**(9): p. 1895-900.
118. Smith, E.L. and E.H. Schuchman, *Acid sphingomyelinase overexpression enhances the antineoplastic effects of irradiation in vitro and in vivo.* Mol Ther, 2008. **16**(9): p. 1565-71.

119. Duan, R.D., *Alkaline sphingomyelinase: an old enzyme with novel implications.* Biochim Biophys Acta, 2006. **1761**(3): p. 281-91.
120. Zhang, Y., et al., *Crucial role of alkaline sphingomyelinase in sphingomyelin digestion: a study on enzyme knockout mice.* J Lipid Res, 2011. **52**(4): p. 771-81.
121. Duan, R.D., et al., *Identification of human intestinal alkaline sphingomyelinase as a novel ecto-enzyme related to the nucleotide phosphodiesterase family.* J Biol Chem, 2003. **278**(40): p. 38528-36.
122. Sribney, M., *Enzymatic synthesis of ceramide.* Biochim Biophys Acta, 1966. **125**(3): p. 542-7.
123. Mizutani, Y., A. Kihara, and Y. Igarashi, *Mammalian Lass6 and its related family members regulate synthesis of specific ceramides.* Biochem J, 2005. **390**(Pt 1): p. 263-71.
124. Stiban, J., R. Tidhar, and A.H. Futerman, *Ceramide synthases: roles in cell physiology and signaling.* Adv Exp Med Biol, 2010. **688**: p. 60-71.
125. Hirschberg, K., J. Rodger, and A.H. Futerman, *The long-chain sphingoid base of sphingolipids is acylated at the cytosolic surface of the endoplasmic reticulum in rat liver.* Biochem J, 1993. **290 (Pt 3)**: p. 751-7.
126. Mandon, E.C., et al., *Subcellular localization and membrane topology of serine palmitoyltransferase, 3-dehydrosphinganine reductase, and sphinganine N-acyltransferase in mouse liver.* J Biol Chem, 1992. **267**(16): p. 11144-8.
127. Cifone, M.G., et al., *Apoptotic signaling through CD95 (Fas/Apo-1) activates an acidic sphingomyelinase.* J Exp Med, 1994. **180**(4): p. 1547-52.
128. Haimovitz-Friedman, A., et al., *Ionizing radiation acts on cellular membranes to generate ceramide and initiate apoptosis.* J Exp Med, 1994. **180**(2): p. 525-35.
129. Jarvis, W.D., et al., *Attenuation of ceramide-induced apoptosis by diglyceride in human myeloid leukemia cells.* J Biol Chem, 1994. **269**(50): p. 31685-92.
130. Obeid, L.M., et al., *Programmed cell death induced by ceramide.* Science, 1993. **259**(5102): p. 1769-71.
131. Jaffrezou, J.P., et al., *Daunorubicin-induced apoptosis: triggering of ceramide generation through sphingomyelin hydrolysis.* EMBO J, 1996. **15**(10): p. 2417-24.
132. Santana, P., et al., *Acid sphingomyelinase-deficient human lymphoblasts and mice are defective in radiation-induced apoptosis.* Cell, 1996. **86**(2): p. 189-99.
133. Bose, R., et al., *Ceramide synthase mediates daunorubicin-induced apoptosis: an alternative mechanism for generating death signals.* Cell, 1995. **82**(3): p. 405-14.
134. Liao, W.C., et al., *Ataxia telangiectasia-mutated gene product inhibits DNA damage-induced apoptosis via ceramide synthase.* J Biol Chem, 1999. **274**(25): p. 17908-17.
135. Min, J., et al., *(Dihydro)ceramide synthase 1 regulated sensitivity to cisplatin is associated with the activation of p38 mitogen-activated protein kinase and is abrogated by sphingosine kinase 1.* Mol Cancer Res, 2007. **5**(8): p. 801-12.
136. Dbaibo, G.S., et al., *p53-dependent ceramide response to genotoxic stress.* J Clin Invest, 1998. **102**(2): p. 329-39.
137. Sawada, M., et al., *p53 regulates ceramide formation by neutral sphingomyelinase through reactive oxygen species in human glioma cells.* Oncogene, 2001. **20**(11): p. 1368-78.

138. Corcoran, C.A., et al., *Neutral sphingomyelinase-3 is a DNA damage and nongenotoxic stress-regulated gene that is deregulated in human malignancies.* Mol Cancer Res, 2008. **6**(5): p. 795-807.
139. Ravid, T., et al., *Ceramide accumulation precedes caspase-3 activation during apoptosis of A549 human lung adenocarcinoma cells.* Am J Physiol Lung Cell Mol Physiol, 2003. **284**(6): p. L1082-92.
140. Takeda, Y., et al., *Ceramide generation in nitric oxide-induced apoptosis. Activation of magnesium-dependent neutral sphingomyelinase via caspase-3.* J Biol Chem, 1999. **274**(15): p. 10654-60.
141. Mullen, T.D., et al., *Ceramide synthase-dependent ceramide generation and programmed cell death: involvement of salvage pathway in regulating postmitochondrial events.* J Biol Chem, 2011. **286**(18): p. 15929-42.
142. Metkar, S.S., et al., *Ceramide-induced apoptosis in fas-resistant Hodgkin's disease cell lines is caspase independent.* Exp Cell Res, 2000. **255**(1): p. 18-29.
143. Dasika, G.K., et al., *DNA damage-induced cell cycle checkpoints and DNA strand break repair in development and tumorigenesis.* Oncogene, 1999. **18**(55): p. 7883-99.
144. Dbaibo, G.S., et al., *Retinoblastoma gene product as a downstream target for a ceramide-dependent pathway of growth arrest.* Proc Natl Acad Sci U S A, 1995. **92**(5): p. 1347-51.
145. Jayadev, S., et al., *Role for ceramide in cell cycle arrest.* J Biol Chem, 1995. **270**(5): p. 2047-52.
146. Phillips, D.C., et al., *Ceramide-induced G2 arrest in rhabdomyosarcoma (RMS) cells requires p21Cip1/Waf1 induction and is prevented by MDM2 overexpression.* Cell Death Differ, 2007. **14**(10): p. 1780-91.
147. Kastan, M.B., et al., *A mammalian cell cycle checkpoint pathway utilizing p53 and GADD45 is defective in ataxia-telangiectasia.* Cell, 1992. **71**(4): p. 587-97.
148. Zhang, J., et al., *Bcl-2 interrupts the ceramide-mediated pathway of cell death.* Proc Natl Acad Sci U S A, 1996. **93**(11): p. 5325-8.
149. Koch, J., et al., *Molecular cloning and characterization of a full-length complementary DNA encoding human acid ceramidase. Identification Of the first molecular lesion causing Farber disease.* J Biol Chem, 1996. **271**(51): p. 33110-5.
150. Lansmann, S., et al., *Purification of acid sphingomyelinase from human placenta: characterization and N-terminal sequence.* FEBS Lett, 1996. **399**(3): p. 227-31.
151. Momoi, T., Y. Ben-Yoseph, and H.L. Nadler, *Substrate-specificities of acid and alkaline ceramidases in fibroblasts from patients with Farber disease and controls.* Biochem J, 1982. **205**(2): p. 419-25.
152. Jameson, R.A., P.J. Holt, and J.H. Keen, *Farber's disease (lysosomal acid ceramidase deficiency).* Ann Rheum Dis, 1987. **46**(7): p. 559-61.
153. Burek, C., et al., *The role of ceramide in receptor- and stress-induced apoptosis studied in acidic ceramidase-deficient Farber disease cells.* Oncogene, 2001. **20**(45): p. 6493-502.
154. Segui, B., et al., *Stress-induced apoptosis is not mediated by endolysosomal ceramide.* FASEB J, 2000. **14**(1): p. 36-47.

155. Norris, J.S., et al., *Combined therapeutic use of AdGFPFasL and small molecule inhibitors of ceramide metabolism in prostate and head and neck cancers: a status report.* Cancer Gene Ther, 2006. **13**(12): p. 1045-51.
156. Seelan, R.S., et al., *Human acid ceramidase is overexpressed but not mutated in prostate cancer.* Genes Chromosomes Cancer, 2000. **29**(2): p. 137-46.
157. Saad, A.F., et al., *The functional effects of acid ceramidase overexpression in prostate cancer progression and resistance to chemotherapy.* Cancer Biol Ther, 2007. **6**(9): p. 1455-60.
158. Hara, S., et al., *p53-Independent ceramide formation in human glioma cells during gamma-radiation-induced apoptosis.* Cell Death Differ, 2004. **11**(8): p. 853-61.
159. Cheng, J.C., et al., *Radiation-induced acid ceramidase confers prostate cancer resistance and tumor relapse.* J Clin Invest, 2013. **123**(10): p. 4344-58.
160. Mao, C. and L.M. Obeid, *Ceramidases: regulators of cellular responses mediated by ceramide, sphingosine, and sphingosine-1-phosphate.* Biochim Biophys Acta, 2008. **1781**(9): p. 424-34.
161. Tani, M., H. Iida, and M. Ito, *O-glycosylation of mucin-like domain retains the neutral ceramidase on the plasma membranes as a type II integral membrane protein.* J Biol Chem, 2003. **278**(12): p. 10523-30.
162. El Bawab, S., et al., *Molecular cloning and characterization of a human mitochondrial ceramidase.* J Biol Chem, 2000. **275**(28): p. 21508-13.
163. Kono, M., et al., *Neutral ceramidase encoded by the Asah2 gene is essential for the intestinal degradation of sphingolipids.* J Biol Chem, 2006. **281**(11): p. 7324-31.
164. Ohlsson, L., et al., *Purification and characterization of human intestinal neutral ceramidase.* Biochimie, 2007. **89**(8): p. 950-60.
165. Wu, B.X., Y.H. Zeidan, and Y.A. Hannun, *Downregulation of neutral ceramidase by gemcitabine: Implications for cell cycle regulation.* Biochim Biophys Acta, 2009. **1791**(8): p. 730-9.
166. Huwiler, A., J. Pfeilschifter, and H. van den Bosch, *Nitric oxide donors induce stress signaling via ceramide formation in rat renal mesangial cells.* J Biol Chem, 1999. **274**(11): p. 7190-5.
167. Franzen, R., et al., *Nitric oxide induces degradation of the neutral ceramidase in rat renal mesangial cells and is counterregulated by protein kinase C.* J Biol Chem, 2002. **277**(48): p. 46184-90.
168. Franzen, R., J. Pfeilschifter, and A. Huwiler, *Nitric oxide induces neutral ceramidase degradation by the ubiquitin/proteasome complex in renal mesangial cell cultures.* FEBS Lett, 2002. **532**(3): p. 441-4.
169. Pyne, N.J., et al., *The role of sphingosine 1-phosphate in inflammation and cancer.* Adv Biol Regul, 2014. **54**: p. 121-9.
170. Nagahashi, M., et al., *Sphingosine-1-phosphate in chronic intestinal inflammation and cancer.* Adv Biol Regul, 2014. **54**: p. 112-20.
171. van Koppen, C., et al., *Activation of a high affinity Gi protein-coupled plasma membrane receptor by sphingosine-1-phosphate.* J Biol Chem, 1996. **271**(4): p. 2082-7.
172. Pitson, S.M., *Regulation of sphingosine kinase and sphingolipid signaling.* Trends Biochem Sci, 2011. **36**(2): p. 97-107.

173. Siow, D.L., et al., *Sphingosine kinase localization in the control of sphingolipid metabolism.* Adv Enzyme Regul, 2011. **51**(1): p. 229-44.
174. Pitson, S.M., et al., *Activation of sphingosine kinase 1 by ERK1/2-mediated phosphorylation.* EMBO J, 2003. **22**(20): p. 5491-500.
175. Ancellin, N., et al., *Extracellular export of sphingosine kinase-1 enzyme. Sphingosine 1-phosphate generation and the induction of angiogenic vascular maturation.* J Biol Chem, 2002. **277**(8): p. 6667-75.
176. Inagaki, Y., et al., *Identification of functional nuclear export sequences in human sphingosine kinase 1.* Biochem Biophys Res Commun, 2003. **311**(1): p. 168-73.
177. Johnson, K.R., et al., *PKC-dependent activation of sphingosine kinase 1 and translocation to the plasma membrane. Extracellular release of sphingosine-1-phosphate induced by phorbol 12-myristate 13-acetate (PMA).* J Biol Chem, 2002. **277**(38): p. 35257-62.
178. Delon, C., et al., *Sphingosine kinase 1 is an intracellular effector of phosphatidic acid.* J Biol Chem, 2004. **279**(43): p. 44763-74.
179. Johnson, K.R., et al., *Immunohistochemical distribution of sphingosine kinase 1 in normal and tumor lung tissue.* J Histochem Cytochem, 2005. **53**(9): p. 1159-66.
180. Kawamori, T., et al., *Sphingosine kinase 1 is up-regulated in colon carcinogenesis.* FASEB J, 2006. **20**(2): p. 386-8.
181. Rosa, R., et al., *Sphingosine kinase 1 overexpression contributes to cetuximab resistance in human colorectal cancer models.* Clin Cancer Res, 2013. **19**(1): p. 138-47.
182. Shida, D., et al., *Targeting SphK1 as a new strategy against cancer.* Curr Drug Targets, 2008. **9**(8): p. 662-73.
183. Taha, T.A., et al., *Down-regulation of sphingosine kinase-1 by DNA damage: dependence on proteases and p53.* J Biol Chem, 2004. **279**(19): p. 20546-54.
184. Kessis, T.D., et al., *Human papillomavirus 16 E6 expression disrupts the p53-mediated cellular response to DNA damage.* Proc Natl Acad Sci U S A, 1993. **90**(9): p. 3988-92.
185. Heffernan-Stroud, L.A., et al., *Defining a role for sphingosine kinase 1 in p53-dependent tumors.* Oncogene, 2012. **31**(9): p. 1166-75.
186. Soussi, T., *p53 alterations in human cancer: more questions than answers.* Oncogene, 2007. **26**(15): p. 2145-56.
187. Soussi, T. and K.G. Wiman, *Shaping genetic alterations in human cancer: the p53 mutation paradigm.* Cancer Cell, 2007. **12**(4): p. 303-12.
188. Weisz, L., M. Oren, and V. Rotter, *Transcription regulation by mutant p53.* Oncogene, 2007. **26**(15): p. 2202-11.
189. Ando, K., et al., *PIDD death-domain phosphorylation by ATM controls prodeath versus prosurvival PIDDosome signaling.* Mol Cell, 2012. **47**(5): p. 681-93.
190. Liu, H., et al., *Molecular cloning and functional characterization of a novel mammalian sphingosine kinase type 2 isoform.* J Biol Chem, 2000. **275**(26): p. 19513-20.
191. Igarashi, N., et al., *Sphingosine kinase 2 is a nuclear protein and inhibits DNA synthesis.* J Biol Chem, 2003. **278**(47): p. 46832-9.
192. Sankala, H.M., et al., *Involvement of sphingosine kinase 2 in p53-independent induction of p21 by the chemotherapeutic drug doxorubicin.* Cancer Res, 2007. **67**(21): p. 10466-74.

193. Maceyka, M., et al., *SphK1 and SphK2, sphingosine kinase isoenzymes with opposing functions in sphingolipid metabolism.* J Biol Chem, 2005. **280**(44): p. 37118-29.
194. Pyne, S., et al., *Lipid phosphate phosphatases and lipid phosphate signalling.* Biochem Soc Trans, 2005. **33**(Pt 6): p. 1370-4.
195. Mandala, S.M., et al., *Molecular cloning and characterization of a lipid phosphohydrolase that degrades sphingosine-1- phosphate and induces cell death.* Proc Natl Acad Sci U S A, 2000. **97**(14): p. 7859-64.
196. Mandala, S.M., et al., *Sphingoid base 1-phosphate phosphatase: a key regulator of sphingolipid metabolism and stress response.* Proc Natl Acad Sci U S A, 1998. **95**(1): p. 150-5.
197. Ogawa, C., et al., *Identification and characterization of a novel human sphingosine-1-phosphate phosphohydrolase, hSPP2.* J Biol Chem, 2003. **278**(2): p. 1268-72.
198. Ikeda, M., A. Kihara, and Y. Igarashi, *Sphingosine-1-phosphate lyase SPL is an endoplasmic reticulum-resident, integral membrane protein with the pyridoxal 5'-phosphate binding domain exposed to the cytosol.* Biochem Biophys Res Commun, 2004. **325**(1): p. 338-43.
199. Le Stunff, H., et al., *Sphingosine-1-phosphate phosphohydrolase in regulation of sphingolipid metabolism and apoptosis.* J Cell Biol, 2002. **158**(6): p. 1039-49.
200. Le Stunff, H., et al., *Recycling of sphingosine is regulated by the concerted actions of sphingosine-1-phosphate phosphohydrolase 1 and sphingosine kinase 2.* J Biol Chem, 2007. **282**(47): p. 34372-80.
201. Johnson, K.R., et al., *Role of human sphingosine-1-phosphate phosphatase 1 in the regulation of intra- and extracellular sphingosine-1-phosphate levels and cell viability.* J Biol Chem, 2003. **278**(36): p. 34541-7.
202. Oskouian, B., et al., *Sphingosine-1-phosphate lyase potentiates apoptosis via p53- and p38-dependent pathways and is down-regulated in colon cancer.* Proc Natl Acad Sci U S A, 2006. **103**(46): p. 17384-9.
203. Kolesnick, R. and Z. Fuks, *Radiation and ceramide-induced apoptosis.* Oncogene, 2003. **22**(37): p. 5897-906.
204. Ossina, N.K., et al., *Interferon-gamma modulates a p53-independent apoptotic pathway and apoptosis-related gene expression.* J Biol Chem, 1997. **272**(26): p. 16351-7.
205. Wichmann, A., B. Jaklevic, and T.T. Su, *Ionizing radiation induces caspase-dependent but Chk2- and p53-independent cell death in Drosophila melanogaster.* Proc Natl Acad Sci U S A, 2006. **103**(26): p. 9952-7.
206. Patil, M., N. Pabla, and Z. Dong, *Checkpoint kinase 1 in DNA damage response and cell cycle regulation.* Cell Mol Life Sci, 2013. **70**(21): p. 4009-21.
207. Janssens, S., et al., *PIDD mediates NF-kappaB activation in response to DNA damage.* Cell, 2005. **123**(6): p. 1079-92.
208. Baltimore, D., *NF-kappaB is 25.* Nat Immunol, 2011. **12**(8): p. 683-5.
209. Wu, Z.H., A. Mabb, and S. Miyamoto, *PIDD: a switch hitter.* Cell, 2005. **123**(6): p. 980-2.
210. Shieh, S.Y., et al., *The human homologs of checkpoint kinases Chk1 and Cds1 (Chk2) phosphorylate p53 at multiple DNA damage-inducible sites.* Genes Dev, 2000. **14**(3): p. 289-300.

211. Gottifredi, V., et al., *p53 down-regulates CHK1 through p21 and the retinoblastoma protein.* Mol Cell Biol, 2001. **21**(4): p. 1066-76.
212. Lezina, L., et al., *miR-16 and miR-26a target checkpoint kinases Wee1 and Chk1 in response to p53 activation by genotoxic stress.* Cell Death Dis, 2013. **4**: p. e953.
213. Al-Kaabi, M.M., et al., *Checkpoint kinase1 (CHK1) is an important biomarker in breast cancer having a role in chemotherapy response.* Br J Cancer, 2015. **112**(5): p. 901-911.
214. Zhang, Y.W., et al., *The F box protein Fbx6 regulates Chk1 stability and cellular sensitivity to replication stress.* Mol Cell, 2009. **35**(4): p. 442-53.
215. Bouchier-Hayes, L. and D.R. Green, *Real time with caspase-2.* Cell Cycle, 2010. **9**(1): p. 12-3.
216. Bouchier-Hayes, L., et al., *Characterization of cytoplasmic caspase-2 activation by induced proximity.* Mol Cell, 2009. **35**(6): p. 830-40.
217. Carey, L.A., et al., *Race, breast cancer subtypes, and survival in the Carolina Breast Cancer Study.* JAMA, 2006. **295**(21): p. 2492-502.
218. Grivennikov, S.I., F.R. Greten, and M. Karin, *Immunity, inflammation, and cancer.* Cell, 2010. **140**(6): p. 883-99.
219. D'Souza-Schorey, C. and J.W. Clancy, *Tumor-derived microvesicles: shedding light on novel microenvironment modulators and prospective cancer biomarkers.* Genes Dev, 2012. **26**(12): p. 1287-99.
220. Raposo, G. and W. Stoorvogel, *Extracellular vesicles: exosomes, microvesicles, and friends.* J Cell Biol, 2013. **200**(4): p. 373-83.
221. Muralidharan-Chari, V., et al., *Microvesicles: mediators of extracellular communication during cancer progression.* J Cell Sci, 2010. **123**(Pt 10): p. 1603-11.
222. Martins, V.R., M.S. Dias, and P. Hainaut, *Tumor-cell-derived microvesicles as carriers of molecular information in cancer.* Curr Opin Oncol, 2013. **25**(1): p. 66-75.
223. Fridman, J.S. and S.W. Lowe, *Control of apoptosis by p53.* Oncogene, 2003. **22**(56): p. 9030-40.
224. Speidel, D., *Transcription-independent p53 apoptosis: an alternative route to death.* Trends Cell Biol, 2010. **20**(1): p. 14-24.
225. Harris, C.C., *p53: at the crossroads of molecular carcinogenesis and risk assessment.* Science, 1993. **262**(5142): p. 1980-1.
226. Dai, Y. and S. Grant, *New insights into checkpoint kinase 1 in the DNA damage response signaling network.* Clin Cancer Res, 2010. **16**(2): p. 376-83.
227. Reinhardt, H.C. and M.B. Yaffe, *Kinases that control the cell cycle in response to DNA damage: Chk1, Chk2, and MK2.* Curr Opin Cell Biol, 2009. **21**(2): p. 245-55.
228. Cooks, T., et al., *Mutant p53 prolongs NF-kappaB activation and promotes chronic inflammation and inflammation-associated colorectal cancer.* Cancer Cell, 2013. **23**(5): p. 634-46.
229. Dalmases, A., et al., *Deficiency in p53 is required for doxorubicin induced transcriptional activation of NF-small ka, CyrillicB target genes in human breast cancer.* Oncotarget, 2014. **5**(1): p. 196-210.
230. Blancafort, P., D.J. Segal, and C.F. Barbas, 3rd, *Designing transcription factor architectures for drug discovery.* Mol Pharmacol, 2004. **66**(6): p. 1361-71.
231. Giusti, I., S. D'Ascenzo, and V. Dolo, *Microvesicles as potential ovarian cancer biomarkers.* Biomed Res Int, 2013. **2013**: p. 703048.

232. Tapia, M.A., et al., *Inhibition of the canonical IKK/NF kappa B pathway sensitizes human cancer cells to doxorubicin.* Cell Cycle, 2007. **6**(18): p. 2284-92.
233. Pyne, N.J. and S. Pyne, *Sphingosine 1-phosphate and cancer.* Nat Rev Cancer, 2010. **10**(7): p. 489-503.
234. Kawamori, T., et al., *Role for sphingosine kinase 1 in colon carcinogenesis.* FASEB J, 2009. **23**(2): p. 405-14.
235. Akao, Y., et al., *High expression of sphingosine kinase 1 and S1P receptors in chemotherapy-resistant prostate cancer PC3 cells and their camptothecin-induced up-regulation.* Biochem Biophys Res Commun, 2006. **342**(4): p. 1284-90.
236. Bayerl, M.G., et al., *Sphingosine kinase 1 protein and mRNA are overexpressed in non-Hodgkin lymphomas and are attractive targets for novel pharmacological interventions.* Leuk Lymphoma, 2008. **49**(5): p. 948-54.
237. Long, J.S., et al., *Sphingosine kinase 1 induces tolerance to human epidermal growth factor receptor 2 and prevents formation of a migratory phenotype in response to sphingosine 1-phosphate in estrogen receptor-positive breast cancer cells.* Mol Cell Biol, 2010. **30**(15): p. 3827-41.
238. Pchejetski, D., et al., *Chemosensitizing effects of sphingosine kinase-1 inhibition in prostate cancer cell and animal models.* Mol Cancer Ther, 2008. **7**(7): p. 1836-45.
239. Watson, C., et al., *High expression of sphingosine 1-phosphate receptors, S1P1 and S1P3, sphingosine kinase 1, and extracellular signal-regulated kinase-1/2 is associated with development of tamoxifen resistance in estrogen receptor-positive breast cancer patients.* Am J Pathol, 2010. **177**(5): p. 2205-15.
240. Pereira, N.A. and Z. Song, *Some commonly used caspase substrates and inhibitors lack the specificity required to monitor individual caspase activity.* Biochem Biophys Res Commun, 2008. **377**(3): p. 873-7.
241. Haupt, S., et al., *Apoptosis - the p53 network.* J Cell Sci, 2003. **116**(Pt 20): p. 4077-85.
242. Schuler, M., et al., *p53 induces apoptosis by caspase activation through mitochondrial cytochrome c release.* J Biol Chem, 2000. **275**(10): p. 7337-42.
243. Fava, L.L., et al., *Caspase-2 at a glance.* J Cell Sci, 2012. **125**(Pt 24): p. 5911-5.
244. Bergeron, L., et al., *Defects in regulation of apoptosis in caspase-2-deficient mice.* Genes Dev, 1998. **12**(9): p. 1304-14.
245. Kumar, S., *Caspase function in programmed cell death.* Cell Death Differ, 2007. **14**(1): p. 32-43.
246. Lowe, S.W., et al., *p53 status and the efficacy of cancer therapy in vivo.* Science, 1994. **266**(5186): p. 807-10.
247. Levine, A.J. and M. Oren, *The first 30 years of p53: growing ever more complex.* Nat Rev Cancer, 2009. **9**(10): p. 749-58.
248. Brosh, R. and V. Rotter, *When mutants gain new powers: news from the mutant p53 field.* Nat Rev Cancer, 2009. **9**(10): p. 701-13.
249. Canals, D., et al., *Differential effects of ceramide and sphingosine 1-phosphate on ERM phosphorylation: probing sphingolipid signaling at the outer plasma membrane.* J Biol Chem, 2010. **285**(42): p. 32476-85.
250. Wang, S., et al., *Doxorubicin induces apoptosis in normal and tumor cells via distinctly different mechanisms. intermediacy of H(2)O(2)- and p53-dependent pathways.* J Biol Chem, 2004. **279**(24): p. 25535-43.

251. Panaretakis, T., et al., *Doxorubicin requires the sequential activation of caspase-2, protein kinase Cdelta, and c-Jun NH2-terminal kinase to induce apoptosis.* Mol Biol Cell, 2005. **16**(8): p. 3821-31.
252. Hannun, Y.A. and L.M. Obeid, *Many ceramides.* J Biol Chem, 2011. **286**(32): p. 27855-62.
253. Chandran, S. and C.E. Machamer, *Inactivation of ceramide transfer protein during pro-apoptotic stress by Golgi disassembly and caspase cleavage.* Biochem J, 2012. **442**(2): p. 391-401.
254. Dent, P., et al., *CHK1 inhibitors in combination chemotherapy: thinking beyond the cell cycle.* Mol Interv, 2011. **11**(2): p. 133-40.
255. Johnson, E.S., et al., *Metabolomic profiling reveals a role for caspase-2 in lipoapoptosis.* J Biol Chem, 2013. **288**(20): p. 14463-75.
256. Wilson, C.H., et al., *Age-related proteostasis and metabolic alterations in Caspase-2-deficient mice.* Cell Death Dis, 2015. **6**: p. e1597.
257. Song, T., et al., *miR-708 promotes the development of bladder carcinoma via direct repression of Caspase-2.* J Cancer Res Clin Oncol, 2013. **139**(7): p. 1189-98.
258. Meng, X.D., et al., *Increased SPHK1 expression is associated with poor prognosis in bladder cancer.* Tumour Biol, 2014. **35**(3): p. 2075-80.
259. Oliver, T.G., et al., *Caspase-2-mediated cleavage of Mdm2 creates a p53-induced positive feedback loop.* Mol Cell, 2011. **43**(1): p. 57-71.
260. Weldon, C.B., et al., *NF-kappa B-mediated chemoresistance in breast cancer cells.* Surgery, 2001. **130**(2): p. 143-50.
261. DiDonato, J.A., F. Mercurio, and M. Karin, *NF-kappaB and the link between inflammation and cancer.* Immunol Rev, 2012. **246**(1): p. 379-400.
262. Tornatore, L., et al., *Cancer-selective targeting of the NF-kappaB survival pathway with GADD45beta/MKK7 inhibitors.* Cancer Cell, 2014. **26**(4): p. 495-508.
263. Baj-Krzyworzeka, M., et al., *Tumour-derived microvesicles carry several surface determinants and mRNA of tumour cells and transfer some of these determinants to monocytes.* Cancer Immunol Immunother, 2006. **55**(7): p. 808-18.
264. Cocucci, E., G. Racchetti, and J. Meldolesi, *Shedding microvesicles: artefacts no more.* Trends Cell Biol, 2009. **19**(2): p. 43-51.
265. Ratajczak, J., et al., *Membrane-derived microvesicles: important and underappreciated mediators of cell-to-cell communication.* Leukemia, 2006. **20**(9): p. 1487-95.
266. Del Conde, I., et al., *Tissue-factor-bearing microvesicles arise from lipid rafts and fuse with activated platelets to initiate coagulation.* Blood, 2005. **106**(5): p. 1604-11.
267. Muralidharan-Chari, V., et al., *ARF6-regulated shedding of tumor cell-derived plasma membrane microvesicles.* Curr Biol, 2009. **19**(22): p. 1875-85.
268. Crawford, S., et al., *Effect of increased extracellular ca on microvesicle production and tumor spheroid formation.* Cancer Microenviron, 2010. **4**(1): p. 93-103.
269. Pilzer, D., et al., *Emission of membrane vesicles: roles in complement resistance, immunity and cancer.* Springer Semin Immunopathol, 2005. **27**(3): p. 375-87.
270. Savina, A., et al., *Rab11 promotes docking and fusion of multivesicular bodies in a calcium-dependent manner.* Traffic, 2005. **6**(2): p. 131-43.

271. Al-Nedawi, K., et al., *Endothelial expression of autocrine VEGF upon the uptake of tumor-derived microvesicles containing oncogenic EGFR.* Proc Natl Acad Sci U S A, 2009. **106**(10): p. 3794-9.
272. Al-Nedawi, K., B. Meehan, and J. Rak, *Microvesicles: messengers and mediators of tumor progression.* Cell Cycle, 2009. **8**(13): p. 2014-8.
273. Antonyak, M.A., et al., *Cancer cell-derived microvesicles induce transformation by transferring tissue transglutaminase and fibronectin to recipient cells.* Proc Natl Acad Sci U S A, 2011. **108**(12): p. 4852-7.
274. Chipuk, J.E. and D.R. Green, *How do BCL-2 proteins induce mitochondrial outer membrane permeabilization?* Trends Cell Biol, 2008. **18**(4): p. 157-64.
275. Goldstein, J.C., et al., *The coordinate release of cytochrome c during apoptosis is rapid, complete and kinetically invariant.* Nat Cell Biol, 2000. **2**(3): p. 156-62.
276. Von Ahsen, O., et al., *The 'harmless' release of cytochrome c.* Cell Death Differ, 2000. **7**(12): p. 1192-9.
277. Rini, B.I., S.C. Campbell, and B. Escudier, *Renal cell carcinoma.* Lancet, 2009. **373**(9669): p. 1119-32.
278. Gnarra, J.R., et al., *Mutations of the VHL tumour suppressor gene in renal carcinoma.* Nat Genet, 1994. **7**(1): p. 85-90.
279. Schraml, P., et al., *VHL mutations and their correlation with tumour cell proliferation, microvessel density, and patient prognosis in clear cell renal cell carcinoma.* J Pathol, 2002. **196**(2): p. 186-93.
280. Herman, J.G., et al., *Silencing of the VHL tumor-suppressor gene by DNA methylation in renal carcinoma.* Proc Natl Acad Sci U S A, 1994. **91**(21): p. 9700-4.
281. Cockman, M.E., et al., *Hypoxia inducible factor-alpha binding and ubiquitylation by the von Hippel-Lindau tumor suppressor protein.* J Biol Chem, 2000. **275**(33): p. 25733-41.
282. Maxwell, P.H., et al., *The tumour suppressor protein VHL targets hypoxia-inducible factors for oxygen-dependent proteolysis.* Nature, 1999. **399**(6733): p. 271-5.
283. Keith, B., R.S. Johnson, and M.C. Simon, *HIF1alpha and HIF2alpha: sibling rivalry in hypoxic tumour growth and progression.* Nat Rev Cancer, 2012. **12**(1): p. 9-22.
284. Kondo, K., et al., *Inhibition of HIF2alpha is sufficient to suppress pVHL-defective tumor growth.* PLoS Biol, 2003. **1**(3): p. E83.
285. Raval, R.R., et al., *Contrasting properties of hypoxia-inducible factor 1 (HIF-1) and HIF-2 in von Hippel-Lindau-associated renal cell carcinoma.* Mol Cell Biol, 2005. **25**(13): p. 5675-86.
286. Zimmer, M., et al., *Inhibition of hypoxia-inducible factor is sufficient for growth suppression of VHL-/- tumors.* Mol Cancer Res, 2004. **2**(2): p. 89-95.
287. Hu, C.J., et al., *Differential roles of hypoxia-inducible factor 1alpha (HIF-1alpha) and HIF-2alpha in hypoxic gene regulation.* Mol Cell Biol, 2003. **23**(24): p. 9361-74.
288. Wang, V., et al., *Differential gene up-regulation by hypoxia-inducible factor-1alpha and hypoxia-inducible factor-2alpha in HEK293T cells.* Cancer Res, 2005. **65**(8): p. 3299-306.
289. Gordan, J.D., et al., *HIF-2alpha promotes hypoxic cell proliferation by enhancing c-myc transcriptional activity.* Cancer Cell, 2007. **11**(4): p. 335-47.
290. Anelli, V., et al., *Sphingosine kinase 1 is up-regulated during hypoxia in U87MG glioma cells. Role of hypoxia-inducible factors 1 and 2.* J Biol Chem, 2008. **283**(6): p. 3365-75.

291. Pitson, S.M., et al., *Human sphingosine kinase: purification, molecular cloning and characterization of the native and recombinant enzymes.* Biochem J, 2000. **350 Pt 2**: p. 429-41.
292. Wattenberg, B.W., *Role of sphingosine kinase localization in sphingolipid signaling.* World J Biol Chem, 2010. **1**(12): p. 362-8.
293. Orr Gandy, K.A. and L.M. Obeid, *Targeting the sphingosine kinase/sphingosine 1-phosphate pathway in disease: review of sphingosine kinase inhibitors.* Biochim Biophys Acta, 2013. **1831**(1): p. 157-66.
294. Taha, T.A., et al., *Loss of sphingosine kinase-1 activates the intrinsic pathway of programmed cell death: modulation of sphingolipid levels and the induction of apoptosis.* FASEB J, 2006. **20**(3): p. 482-4.
295. Gao, P. and C.D. Smith, *Ablation of sphingosine kinase-2 inhibits tumor cell proliferation and migration.* Mol Cancer Res, 2011. **9**(11): p. 1509-19.
296. Chumanevich, A.A., et al., *Suppression of colitis-driven colon cancer in mice by a novel small molecule inhibitor of sphingosine kinase.* Carcinogenesis, 2010. **31**(10): p. 1787-93.
297. Ruckhaberle, E., et al., *Microarray analysis of altered sphingolipid metabolism reveals prognostic significance of sphingosine kinase 1 in breast cancer.* Breast Cancer Res Treat, 2008. **112**(1): p. 41-52.
298. Zhuge, Y.H., H.Q. Tao, and Y.Y. Wang, *[Relationship between sphingosine kinase 1 expression and tumor invasion, metastasis and prognosis in gastric cancer].* Zhonghua Yi Xue Za Zhi, 2011. **91**(39): p. 2765-8.
299. Guan, H., et al., *Sphingosine kinase 1 is overexpressed and promotes proliferation in human thyroid cancer.* Mol Endocrinol, 2011. **25**(11): p. 1858-66.
300. Facchinetti, M.M., et al., *The expression of sphingosine kinase-1 in head and neck carcinoma.* Cells Tissues Organs, 2010. **192**(5): p. 314-24.
301. Orr Gandy, K.A., et al., *Epidermal growth factor-induced cellular invasion requires sphingosine-1-phosphate/sphingosine-1-phosphate 2 receptor-mediated ezrin activation.* FASEB J, 2013. **27**(8): p. 3155-66.
302. Kitatani, K., J. Idkowiak-Baldys, and Y.A. Hannun, *Mechanism of inhibition of sequestration of protein kinase C alpha/betaII by ceramide. Roles of ceramide-activated protein phosphatases and phosphorylation/dephosphorylation of protein kinase C alpha/betaII on threonine 638/641.* J Biol Chem, 2007. **282**(28): p. 20647-56.
303. Van Veldhoven, P.P. and R.M. Bell, *Effect of harvesting methods, growth conditions and growth phase on diacylglycerol levels in cultured human adherent cells.* Biochim Biophys Acta, 1988. **959**(2): p. 185-96.
304. Bligh, E.G. and W.J. Dyer, *A rapid method of total lipid extraction and purification.* Can J Biochem Physiol, 1959. **37**(8): p. 911-7.
305. Vadas, M., et al., *The role of sphingosine kinase 1 in cancer: oncogene or non-oncogene addiction?* Biochim Biophys Acta, 2008. **1781**(9): p. 442-7.
306. Kohno, M., et al., *Intracellular role for sphingosine kinase 1 in intestinal adenoma cell proliferation.* Mol Cell Biol, 2006. **26**(19): p. 7211-23.
307. Schwock, J., N. Dhani, and D.W. Hedley, *Targeting focal adhesion kinase signaling in tumor growth and metastasis.* Expert Opin Ther Targets, 2010. **14**(1): p. 77-94.

308. French, K.J., et al., *Discovery and evaluation of inhibitors of human sphingosine kinase.* Cancer Res, 2003. **63**(18): p. 5962-9.
309. Golubovskaya, V.M., et al., *A small molecule inhibitor, 1,2,4,5-benzenetetraamine tetrahydrochloride, targeting the y397 site of focal adhesion kinase decreases tumor growth.* J Med Chem, 2008. **51**(23): p. 7405-16.
310. Cingolani, F., et al., *Inhibition of dihydroceramide desaturase activity by the sphingosine kinase inhibitor SKI II.* J Lipid Res, 2014. **55**(8): p. 1711-1720.
311. Tolan, D., et al., *Assessment of the extracellular and intracellular actions of sphingosine 1-phosphate by using the p42/p44 mitogen-activated protein kinase cascade as a model.* Cell Signal, 1999. **11**(5): p. 349-54.
312. Baldewijns, M.M., et al., *VHL and HIF signalling in renal cell carcinogenesis.* J Pathol, 2010. **221**(2): p. 125-38.
313. Pitson, S.M., J.A. Powell, and C.S. Bonder, *Regulation of sphingosine kinase in hematological malignancies and other cancers.* Anticancer Agents Med Chem, 2011. **11**(9): p. 799-809.
314. Anelli, V., et al., *Role of sphingosine kinase-1 in paracrine/transcellular angiogenesis and lymphangiogenesis in vitro.* FASEB J, 2010. **24**(8): p. 2727-38.
315. Chae, S.S., et al., *Requirement for sphingosine 1-phosphate receptor-1 in tumor angiogenesis demonstrated by in vivo RNA interference.* J Clin Invest, 2004. **114**(8): p. 1082-9.
316. Nagahashi, M., et al., *Sphingosine-1-phosphate produced by sphingosine kinase 1 promotes breast cancer progression by stimulating angiogenesis and lymphangiogenesis.* Cancer Res, 2012. **72**(3): p. 726-35.
317. Lahlou, H., et al., *Mammary epithelial-specific disruption of the focal adhesion kinase blocks mammary tumor progression.* Proc Natl Acad Sci U S A, 2007. **104**(51): p. 20302-7.
318. Hao, H.F., et al., *Progress in researches about focal adhesion kinase in gastrointestinal tract.* World J Gastroenterol, 2009. **15**(47): p. 5916-23.
319. Hao, H., et al., *Focal adhesion kinase as potential target for cancer therapy (Review).* Oncol Rep, 2009. **22**(5): p. 973-9.
320. Aust, S., et al., *Ambivalent role of pFAK-Y397 in serous ovarian cancer--a study of the OVCAD consortium.* Mol Cancer, 2014. **13**: p. 67.
321. Stokes, J.B., et al., *Inhibition of focal adhesion kinase by PF-562,271 inhibits the growth and metastasis of pancreatic cancer concomitant with altering the tumor microenvironment.* Mol Cancer Ther, 2011. **10**(11): p. 2135-45.
322. Dia, V.P. and E. Gonzalez de Mejia, *Lunasin potentiates the effect of oxaliplatin preventing outgrowth of colon cancer metastasis, binds to alpha5beta1 integrin and suppresses FAK/ERK/NF-kappaB signaling.* Cancer Lett, 2011. **313**(2): p. 167-80.
323. Megison, M.L., et al., *FAK inhibition abrogates the malignant phenotype in aggressive pediatric renal tumors.* Mol Cancer Res, 2014. **12**(4): p. 514-26.
324. Zhao, J., et al., *Phosphotyrosine protein dynamics in cell membrane rafts of sphingosine-1-phosphate-stimulated human endothelium: role in barrier enhancement.* Cell Signal, 2009. **21**(12): p. 1945-60.

325. Lee, O.H., et al., *Sphingosine 1-phosphate stimulates tyrosine phosphorylation of focal adhesion kinase and chemotactic motility of endothelial cells via the G(i) protein-linked phospholipase C pathway.* Biochem Biophys Res Commun, 2000. **268**(1): p. 47-53.
326. Quint, P., et al., *Sphingosine 1-phosphate (S1P) receptors 1 and 2 coordinately induce mesenchymal cell migration through S1P activation of complementary kinase pathways.* J Biol Chem, 2013. **288**(8): p. 5398-406.
327. Liu, S.Q., et al., *Sphingosine kinase 1 promotes tumor progression and confers malignancy phenotypes of colon cancer by regulating the focal adhesion kinase pathway and adhesion molecules.* Int J Oncol, 2013. **42**(2): p. 617-26.
328. Kim, S., et al., *Silibinin suppresses EGFR ligand-induced CD44 expression through inhibition of EGFR activity in breast cancer cells.* Anticancer Res, 2011. **31**(11): p. 3767-73.
329. Young, N., D.K. Pearl, and J.R. Van Brocklyn, *Sphingosine-1-phosphate regulates glioblastoma cell invasiveness through the urokinase plasminogen activator system and CCN1/Cyr61.* Mol Cancer Res, 2009. **7**(1): p. 23-32.
330. Tamashiro, P.M., et al., *Sphingosine kinase 1 mediates head & neck squamous cell carcinoma invasion through sphingosine 1-phosphate receptor 1.* Cancer Cell Int, 2014. **14**(1): p. 76.
331. Bao, M., et al., *Sphingosine kinase 1 promotes tumour cell migration and invasion via the S1P/EDG1 axis in hepatocellular carcinoma.* Liver Int, 2012. **32**(2): p. 331-8.
332. Donati, C., et al., *Tumor necrosis factor-alpha exerts pro-myogenic action in C2C12 myoblasts via sphingosine kinase/S1P2 signaling.* FEBS Lett, 2007. **581**(23): p. 4384-8.
333. Gandy, K.A., et al., *Sphingosine 1-phosphate induces filopodia formation through S1PR2 activation of ERM proteins.* Biochem J, 2013. **449**(3): p. 661-72.
334. Van Brocklyn, J.R., et al., *Sphingosine kinase-1 expression correlates with poor survival of patients with glioblastoma multiforme: roles of sphingosine kinase isoforms in growth of glioblastoma cell lines.* J Neuropathol Exp Neurol, 2005. **64**(8): p. 695-705.
335. Van Brocklyn, J., et al., *Sphingosine-1-phosphate stimulates human glioma cell proliferation through Gi-coupled receptors: role of ERK MAP kinase and phosphatidylinositol 3-kinase beta.* Cancer Lett, 2002. **181**(2): p. 195-204.
336. Lee, O.H., et al., *Sphingosine 1-phosphate induces angiogenesis: its angiogenic action and signaling mechanism in human umbilical vein endothelial cells.* Biochem Biophys Res Commun, 1999. **264**(3): p. 743-50.

Appendix

A novel role of sphingosine kinase-1 in the invasion and angiogenesis of VHL mutant clear cell renal cell carcinoma

Abstract

Sphingosine kinase 1 (SK1), the enzyme responsible for sphingosine 1-phosphate (S1P) production, is overexpressed in many human solid tumors. However, its role in clear cell renal cell carcinoma (ccRCC) has not been described previously. ccRCC cases are usually associated with mutations in von Hippel-Lindau (VHL) and subsequent normoxic stabilization of hypoxia-inducible factor (HIF). We previously showed that HIF-2a up-regulates SK1 expression during hypoxia in glioma cells. Therefore, we hypothesized that the stabilized HIF in ccRCC cells will be associated with increased SK1 expression. Here, we demonstrate that SK1 is overexpressed in 786-0 renal carcinoma cells lacking functional VHL, with concomitant high S1P levels that appear to be HIF-2a mediated. Moreover, examining the TCGA RNA seq database shows that SK1 expression was 2.7-fold higher in solid tumor tissue from ccRCC patients, and this was associated with less survival. Knockdown of SK1 in 786-0 ccRCC cells had no effect on cell proliferation. On the other hand, this knockdown resulted in an 3.5-fold decrease in invasion, less phosphorylation of focal adhesion kinase (FAK), and an 2-fold decrease in angiogenesis. Moreover, S1P treatment of SK1 knockdown cells resulted in phosphorylation of FAK and invasion, and this was mediated by S1P receptor 2. These results suggest that higher SK1 and S1P levels in VHL-defective ccRCC could induce invasion in an autocrine manner and angiogenesis in a paracrine manner. Accordingly, targeting SK1 could reduce both the invasion and angiogenesis of ccRCC and therefore improve the survival rate of patients.

A.1. Introduction

Clear Cell Renal Cell carcinoma (ccRCC) is the most prevalent type of kidney cancer that accounts for 70–80% of cases [277]. It is usually characterized by inactivation of the von Hippel-Lindau (VHL) protein that is caused by deletion on chromosome 3p [278], gene mutations [279], or hypermethylation of the promoter [280]. The VHL gene product, pVHL, has several functions; however, its main role is to regulate hypoxia-inducible factor (HIF). VHL serves as a recognition element for a ubiquitin ligase that induces proteasomal degradation of the a subunits of HIF following the hydroxylation of one or both prolyl residues of these subunits [281, 282]. Therefore, the lack of functional pVHL is associated with normoxic stabilization of HIFs [283]. HIF-2a is believed to play a key role in VHL-defective renal carcinogenesis as some renal carcinomas produce HIF-2a alone or both HIF-1 and 2a [281]. Moreover, in VHL- defective tumors, ablation of HIF-2a has been shown to be sufficient for tumor growth suppression in vivo [284]. Interestingly, the tumor growth suppressive effect associated with restoration of pVHL was overridden by HIF-2a over-expression [285]. Although both HIF-1a and HIF-2a share some of their biological effects, each of them has a unique ability to regulate particular genes [286]. HIF-1a is mainly involved in regulating enzymes of the glycolytic pathway [287, 288]; conversely, HIF-2a, through its interaction with c- Myc, is mainly involved in tumor cell progression [289]. In addition, we previously showed that HIF-2a transcription- ally up-regulates sphingosine kinase 1 (SK1) expression during hypoxia in glioma cells [290].

SK1 and SK2 are the 2 isoforms of sphingosine kinases that have been identified and cloned in mammals [190, 291]. Although they catalyze the conversion of sphingosine into sphingosine 1-phosphate (S1P), these 2 isoforms have been shown to have different cellular localization and biologic functions [292, 293]. SK1 has pro-survival function and is mainly localized in the cytosol [99, 294]. Conversely, SK2 is important for cellular proliferation, and its inhibition sensitizes cells to apoptotic stimuli [295, 296]. SK2 is localized in nucleus, endoplasmic reticulum, and mitochondria [173]. Overexpression of SK1 has been documented in different cancer types, including breast [297], lung [179], gastric [298, 299], thyroid [299], head and neck [300] and colon cancers [180]. Moreover, SK1 expression and S1P levels could be used as biomarkers of tumor malignancies as both have been shown to be correlated with survival and cancer grade in clinical studies [297, 298]. It is clear now that SK1 plays a role in different cancers; however, such a role has not previously been addressed in ccRCC. There- fore, we aimed to study the potential role of SK1 in ccRCC.

A.2. Experimental Procedures

A.2.1. Materials

RPMI 1640 medium, DMEM, fetal bovine serum (FBS), penicillin- streptomycin, PBS, Lipofectamine 2000, Lipofectamine RNAi- MAX, PureLink RNA Mini Kit, Superscript III first strand synthesis kit, and calcein AM fluorescent dye were purchased from Life Technologies (Grand Island, NY, USA). Monoclonal anti-b-actin antibody and 3-(4, 5-dimethylthiazol-2-yl)-2,5-diphenyltetrazolium bromide (MTT) were from Sigma-Aldrich (St. Louis, MO, USA),

puromycin dihydrochloride, focal adhesion kinase (FAK) inhibitor 14, RIPA lysis buffer system, and horseradish peroxidase- labeled secondary antibodies were from Santa Cruz Biotechnology (Santa Cruz, CA, USA). Anti-phospho-FAK (Tyr397), anti-FAK, anti-VHL, and anti-SK1 were from Cell Signaling Technology (Danvers, MA, USA). Anti-HIF-2a was from Novus Biologicals (Littleton, CO, USA). Anti-HIF-1a was from BD Bio- sciences (San Jose, CA, USA). Corning Biocoat Tumor Invasion Systems (EF8976D) was from Corning (Tewksbury, MA, USA). The chemiluminescence kit and BCA kit were from Thermo Scientific (Suwanee, GA, USA). iTAQ master mix was purchased from Bio-Rad (Hercules, CA, USA). S1P and D-erythro-17-carbon sphingosine (C17-Sph) were from Avanti Polar Lipids (Alabaster, AL, USA). SKi-II (4-[4-(4-chloro-phenyl)- thiazol-2-ylamino]-phenol, VPC23019, and JTE-013 were purchased from Cayman Chemical (Ann Arbor, MI, USA). CYM50358 was from Millipore (Billerica, MA, USA). All plas- mids used for production of lentiviral particles (psPAX2, PLKO.1, and pMD2G) were kindly provided by Dr. Leah Siskind (University of Louisville School of Medicine, Louisville, KY, USA).

A.2.2. Cell culture and small interference RNA

VHL-defective clear cell renal cell carcinoma cells, 786-0, and those expressing wild-type VHL protein, WT-8 cells, were provided by Dr. Harry A. Drabkin (Medical University of South Carolina, Charleston, SC, USA). Cells were cultured in RPMI 1640 medium supplemented with 1% penicillin-streptomycin and 10% FBS. WT-8 cells were grown in the same media supplemented with 1 mg/ml G418 (Invitrogen). HEK-239T cells were purchased originally from American Type Culture Collection (Manassas, VA, USA) and were grown in DMEM supplemented with 1% penicillin-streptomycin and 10% FBS. All cell lines were incubated in standard culture conditions: 37°C and 5% CO_2. Gene silencing was carried out using siRNA directed against human HIF-2a (Silencer Pre-Designed siRNA, siRNA ID:106447; Life Technologies), S1PR2, Hs_EDG5_6 FlexiTube siRNA SI02663227 (FlexiTube siRNA, experimentally verified; Qiagen, Valencia, CA, USA), and with AllStar negative control siRNA (Qiagen). Transfections were carried out using Lipofectamine RNAiMAX according to the manufacturer's protocol. For siRNA experiments, 786-0 cells were seeded into 6-well plates at 100,000 cells per well and transfected with 20 nM siRNA for 48 hours, followed by RNA and protein extraction to validate target gene knockdown. S1PR2 siRNA transfections were con- ducted as described previously [301], and cells were serum starved 48 hours after transfection and then treated with S1P.

A.2.3. Immunoblot analysis

Cells were washed with ice-cold PBS and then directly lysed in cold RIPA buffer containing 1 mM sodium orthovanadate, 2 mM PMSF, and protease inhibitor cocktail (Santa Cruz Biotechnology). Equal amounts of protein (10 mg) were boiled in Laemmli buffer (Bio-Rad), and separated by SDS-PAGE (4–15%, Tris-HCl) using the Bio-Rad Criterion system. Separated proteins were then transferred onto nitrocellulose membranes (Bio-Rad) and blocked with 5% nonfat milk in PBS-0.1% Tween-20 for at 1 hour at room temperature. Primary antibodies diluted 1:1000 or 1:20,000 for b-actin were then added to membranes and incubated at 4°C overnight. Membranes were washed 3 times with PBS-0.1% Tween 20 and then incubated

with diluted 1:5000 horseradish peroxidase- conjugated secondary antibodies for 1 hour at room temperature. Membranes were then incubated with Pierce ECL Western Blotting Substrate (ThermoScientific, Suwanee, GA, USA) and exposed to X-ray films that were then processed and scanned.

A.2.4. Short-hairpin RNA constructs and lentiviral infections

Lentivirus particles were produced in HEK-293T cells transfected with 500 ng psPAX2, 50 ng PMD2G, and 500 ng lentiviral plasmid (pLKO.1) containing either SK1 or a nontargeted sequence using Lipofectamine 2000. 786-0 cells were then infected with the lentiviral particles with polybrene (8 mg/ml) and selected for puro- mycin resistance (5 mg/ml) for 1 week, followed by RNA and protein extraction to validate gene silencing by quantitative PCR and Western blotting, respectively.

A.2.5. Cell proliferation assay

Cell proliferation was determined by colorimetric assay using MTT (Sigma-Aldrich). In brief, cells were seeded in 6-well plates at 50,000 cells per well. The next morning, for the zero time point, the medium was replaced with 1 ml fresh medium plus 1 ml MTT solution (5 mg/ml), and cells were incubated for 3 hours. The solution was then carefully removed, followed by addition of 2 ml DMSO (Invitrogen) to each well to solubilize crystals. The absorbance of each sample was measured at 550 nm. The same was performed after 24, 48, and 72 hours. Triplicate measurements were performed for each time point.

A.2.6. Plasmid constructs and transient transfections

Human SK1 (GenBank accession no. AF200328) cDNA was subcloned into NheI and NotI sites of pcDNA3.1-mCherry.Zeo [302]. 786-0 cells were seeded in 6-well plates at 100,000 cells per well in antibiotic-free RPMI 1640 medium 1 day before transfection. On the next day, the cells were transfected with 1 mg pcDNA3.1-mCherry.SK1 or empty vector using Lipofectamine 2000 transfection reagent according to the manufacturer's instructions. Cells were incubated for 48 hours followed by protein extraction and Western blot analysis.

A.2.7. C17-Sph labeling

786-0, WT-8, or short-hairpin RNA (shRNA) stably expressing cells were plated at 150,000 cells per 60 mm dish. Once 90% confluent, cells were incubated with 1 mM C17 sphingosine for 20 minutes. The cells were washed with PBS; 2 ml cell extraction mixture (2:3 70% isopropanol/ethyl acetate) then was directly added to the cells. The cells were then gently scraped, and extracts were sent for analysis at the Lipidomics Core Facility of Stony Brook University Medical Center.

A.2.8. Mass spectrometry to measure sphingolipid levels

For extracellular S1P levels, media were aspirated and transferred to glass tubes, and an equal volume of medium extraction mixture (15:85 isopropanol/ethyl acetate) was added. For lipid extraction, cells were washed with PBS, the cells were then directly lysed with 2 ml cell extraction mixture (2:3 70% isopropanol/ethyl acetate) followed by gentle scraping of the cell from the culture plate, and the lysate then was transferred to 15 ml Falcon tubes. The lipid extracts were then sent for analysis at the Lipidomics Core Facility at Stony Brook University Medical Center. Data were normalized by total inorganic phosphate (Pi) present in the sample [303] after a Bligh and Dyer extraction [304]. Cellular sphingolipid levels were expressed as picomoles per nmoles Pi.

A.2.9. Cellular invasion assays

Cell invasion experiments were performed using Corning Bio- coat Tumor Invasion Systems according to the manufacturer's protocol with slight modifications as previously described (30). In brief, after 4 h of serum starvation, cells were trypsinized and resuspended at 150,000 cells/ml. These cells were then placed in the apical chamber of the transwell insert at a volume of 500 ml. Inhibitors such as JTE-013, VPC 23019, SKi-II, or the FAK inhibitor were mixed with the cells at this stage. Media containing serum or S1P were added to the bottom well of the insert at a volume of 750 ml. Cells were allowed to invade for 48 hours under normal cell culture conditions. Cells were washed twice with PBS and then stained with 4mg/ml calcein AM (Invitrogen) for 1 hour. Invading cells were then quantified by measuring their fluorescence using a Spectra- Max M5 plate reader (Molecular Devices, Sunnyvale, CA, USA).

A.2.10. Survival analysis

The patient survival data were obtained from the TCGA ccRCC project. On the basis of the expression levels of SK1 in TCGA RNA-seq data, patients were ranked into upper half (SK1 expression median) and lower half (SK1 expression median) groups. Kaplan-Meier survival analysis was performed on 2 patient groups, followed by a log-rank test for statistical significance.

A.2.11. Chorioallantoic membrane assay

Specific pathogen-free chicken eggs were purchased from Charles River Laboratories (North Franklin, CT, USA). In brief, eggs were incubated at 37°C and 65% relative humidity with rocking for 3 days. After the initial incubation, eggs were cracked, and chicken embryos were placed into sterile Petri dishes and allowed to develop further for maturation of the chorioallantoic membrane (CAM) for another 7 days. For each sponge, 500,000 cells were resuspended in 20 ml PBS, supplemented with 0.5 mM both Calcium and Magnesium. The resuspended cells were treated with the indicated inhibitors and incubated with sterile gelatin sponges for 30 minutes at 37°C. Next, 2–3 sponges were placed on each chicken, which were then allowed to incubate for 4 days at 37°C and 65% relative humidity. The sponges were imaged on the fourth day of incubation with the sponges. Angiogenesis was assessed by counting the number of vessels that grew toward the sponge.

A.2.12. Statistical analysis

The data are represented as means SE. Two-tailed unpaired Student t test and 1-way ANOVA with Bonferroni posttest statistical analyses were performed using GraphPad Prism software (GraphPad Software, Incorporated, La Jolla, CA, USA).

A.3. Results

A.3.1. VHL-defective ccRCC 786-0 cells showed higher SK1 expression and higher S1P levels

To examine the effect of stabilized HIF in VHL-defective renal carcinoma cells on SK1 expression, protein extracts and cDNA from VHL-defective, 786-0, and those stably expressing VHL, WT-8, cells were subjected to Western blot and quantitative PCR analysis. As shown in **Fig. 19A**, 786-0 cells showed higher levels of HIF-2a compared with WT-8 cells, with undetectable HIF-1a protein in both cell lines, consistent with results showing that this cell type expresses HIF-2a and not HIF-1a [282]. SK1 mRNA and protein expressions were significantly higher in 786-0 cells, with no difference in SK2 message level **(Fig. 19B, C)**. To determine whether the observed increase in SK1 protein expression in VHL-defective cells results in increased output of the enzyme, we measured cellular levels of its lipid product S1P, which were found to be elevated in the 786-0 cells **(Fig. 19D)**. In further evaluation of cellular SK1 activity, C17-sphingosine labeling was performed (1 mM C17-Sph for 20 min), followed by measurement of acute conversion of C17-Sph to C17-S1P. As shown in **Fig. 19E**, 786-0 cells showed higher levels of C17-S1P than WT-8 cells, indicating ongoing higher activity of the enzyme.

A.3.2. Effect of HIF-2a down-regulation on SK1 expression in 786-0 cells

We previously showed that HIF-2a regulates SK1 transcriptionally in response to hypoxia in glioma cells [290]. To examine whether stabilized HIF-2a protein in VHL-defective 786-0 cells is responsible for higher SK1 expression, HIF-2a was down-regulated using siRNA technology. Cells were transfected with AllStars negative control or HIF-2a siRNA for 48 hours. As shown in **Fig. 20A, B,** HIF-2a was efficiently down-regulated by siRNA at message and protein levels. It is noteworthy that SK1 message and protein levels were decreased with HIF-2a siRNA treatment. These data suggest that stabilized HIF-2a is involved in SK1 up-regulation in VHL-defective renal carcinoma cells.

A.3.3. SK1 is up-regulated in ccRCC patients and correlates with clinical outcome

To assess expression of SK1 in ccRCC patients, TCGA RNA seq datasets were analyzed from 72 paired normal and ccRCC tumor samples. As shown in **Fig. 21A**, SK1 mRNA expression is 2.7-fold higher in the primary tumor than in normal tissue. Moreover, the survival rates of patients with the top 50% SK1 expression were significantly lower than those with the bottom 50% SK1 expression **(Fig. 21B)**. These data demonstrate a clear correlation between high SK1 expression in ccRCC and poor clinical outcome.

A.3.4. SK1 down-regulation is associated with less invasive phenotype in ccRCC 786-0 cells

To explore the role of the high SK1 expression in ccRCC biology, SK1 was down-regulated using shRNA technology. Cells stably expressing scrambled (scr) or SK1 shRNA were selected using puromycin followed by validation of gene knockdown using quantitative PCR and Western blot analysis. As shown in **Fig. 22A, B**, SK1 was efficiently down-regulated in SK1 shRNA-expressing compared with scr shRNA- expressing cells at protein and message levels, with no difference in SK2 message level. Moreover, cellular and extracellular S1P levels were decreased with SK1 knockdown **(Fig. 22C, D)**. SK1 activity, assessed by C17-sphingosine labeling, was also decreased with SK1 down-regulation **(Fig. 22E).** SK1 has previously been shown to be involved in different biologic processes, including cell proliferation, survival, progression, and metastasis [305, 306]. To examine the biological consequences of SK1 down-regulation, cell proliferation was assessed by MTT assay in cells stably expressing scr or SK1 shRNA. As shown in **Fig. 22F**, no differences were observed in proliferation between the 2 cell lines. The invasiveness of shRNA expressing cells was then determined by cell invasion assays using transwell chambers. Both cells were allowed to invade toward complete growth medium for 48 hours **(Fig. 22G).** Knocking down SK1 resulted in 3-fold reduction in the invasion of 786-0 cells, suggesting that SK1 plays an important role in cellular invasion.

A.3.5. SK1 induces FAK phosphorylation in an S1P-S1PR2–dependent manner

To further explore the mechanism of SK1-induced cell invasion, the levels of FAK phosphorylation, which has been reported to be an important modulator of cellular invasion [307], were assessed in cells expressing scr and SK1 shRNA. As shown in **Fig. 23A**, SK1 down-regulation was associated with reduced phosphorylation of FAK. In addition, to solidify the role of SK1 in FAK phosphorylation, we next assessed the impact of transfection-mediated up-regulation of the SK1 gene on FAK phosphorylation in 786-0 cells. As shown in **Fig. 23B**, SK1 up-regulation was associated with increased FAK phosphorylation, with no difference in total FAK protein levels. Next, to further confirm the role of SK1 in FAK phosphorylation, a pharmacological approach was applied by using a nonlipid SK inhibitor, SKi-II [308], as well as an inhibitor for FAK phosphorylation (FAKi) [309] as a positive control. 786-0 cells were treated with DMSO vehicle, FAKi 14 (5 and 10 mM), or SKi-II (5 and 10 mM) for 24 hours. FAK phosphorylation then was examined **(Fig. 23C)** and found to be decreased in response to inhibition of FAK or SK1. It is worth mentioning that SKi-II has recently been reported to have an off-target effect on ceramide desaturase [310]; however, by use of that inhibitor, we observed a similar effect on biology and FAK phosphorylation as shown by knocking down SK1 in ccRCC 786-0 cells. These findings further support the role of SK1, probably through the production of S1P, in inducing FAK phosphorylation.

Next, to further define the mechanism of SK1 regulation of FAK phosphorylation, pFAK levels were examined in response to S1P treatment. As shown in **Fig. 23D**, treatment of SK1 shRNA-expressing cells with 100 nM S1P for 10 minutes was sufficient to induce phosphorylation of FAK. We were interested to understand the mechanism by which S1P induces FAK phosphorylation. As S1P can signal either extracellularly through G protein-

coupled receptors or intracellularly [311], we evaluated the possible role of S1P receptors in FAK phosphorylation by using pharmacologic antagonists for S1P receptors. Cells were treated with the S1PR1/3 antagonist VPC 23019; the S1PR2-specific antagonist JTE-013; or the S1PR4-specific antagonist CYM50358. Cells were pretreated for 1 hour with vehicle or 10 mM from each S1PR antagonist followed by 10 minutes of S1P treatment. S1P maintained its ability to induce FAK phosphorylation in the presence of the S1PR1/3 and S1PR4 antagonists, indicating that S1PR1, S1PR3, and S1PR4 are not involved in S1P-mediated FAK phosphorylation **(Fig. 23D)**. On the other hand, JTE-013, a specific S1PR2 antagonist, inhibited S1P-stimulated FAK phosphorylation, indicating that S1PR2 plays an important role in FAK phosphorylation in response to S1P. JTE-013 also inhibited S1P-induced FAK phosphorylation in scr shRNA stable cells (**Supplemental Fig S9).** In addition, a similar effect on S1P-induced FAK phosphorylation was observed following S1PR2 knockdown using siRNA **(Fig. 23E).**

A.3.6. SK1-mediated cell invasion occurs via S1PR2- dependent FAK phosphorylation and a FAK- independent mechanism through S1PR1/3

We showed that FAK phosphorylation in ccRCC cells is dependent on the S1P/S1PR2 axis. Next, we wanted to assess the role of this pathway on cellular invasion. To this end, we used pharmacologic inhibitors against SK1 and S1PR2 to check their effect on cellular invasion. As shown in **Fig. 24A,** treatment with SK inhibitor and S1PR2 antagonist significantly reduced the cellular invasion toward complete medium (+serum). In addition, treatment of cells with S1P reversed the inhibitory effect of SKi-II on cell invasion **(Supplemental Fig. S10)**. These results demonstrate that SK1/S1PR2 axis is essential for the invasion of ccRCC cells. Furthermore, we wanted to examine whether S1P/S1PR2-mediated cellular invasion is FAK dependent. To this end, we used a pharmacologic inhibitor of FAK phosphorylation and assessed its role in cellular invasion. As shown in **Fig. 24A**, inhibition of FAK phosphorylation markedly reduced cellular invasion. Therefore, these results suggest that FAK-mediated invasion of ccRCC cells is dependent on the S1P/S1PR2 axis. To further support the role of S1P/S1PR2 axis in invasion of ccRCC cells, SK1 shRNA-expressing cells were allowed to invade toward serum-free medium or serum-free media containing 500 nM S1P in the presence or absence of JTE-013. As shown in **Fig. 24B**, cells invaded toward serum-free media containing S1P, and this was significantly inhibited by JTE-013, suggesting that S1P activation of FAK could play a role in cellular invasion that is mediated by S1PR2. Moreover, treating cells with the S1PR1/3 antagonist VPC 23019 also decreased the cellular invasion **(Supplemental Fig. S11);** however, this effect is not mediated via FAK activation (as shown in Fig. 24D). These data together with the previously presented data provide insight into the mechanism by which SK1/S1P could play an important role in cellular invasion of ccRCC cells through a S1PR2/FAK-dependent mechanism and a FAK-independent mechanism through S1PR1/3.

A.3.7. SK1 down-regulation is associated with less angiogenesis in ccRCC 786-0 cells

ccRCC is well known to be an angiogenic tumor [312]; moreover, SK1 and S1P have been shown previously to be involved in tumor angiogenesis [313-315]. Therefore, we aimed

to examine whether SK1 is also involved in the increased angiogenesis of ccRCC using an in vivo CAM assay. CAMs were incubated for 4 days with cells stably expressing scr or SK1 shRNA. To determine whether the effect on angiogenesis by SK1 is due to S1P, we used the S1PR1/3-specific antagonist VPC23019 and the S1PR2 antagonist JTE-013. In addition, a pharmacologic inhibitor of SK, SKi-II, was also used to confirm the role of SK1 in angiogenesis. As shown in **Fig. 25** and **Supplemental Fig. S12** cells expressing scr shRNA were more angiogenic, as assessed by the number of vessels that grew toward the sponge, than those expressing SK1 shRNA, and their angiogenesis was inhibited by VPC23019 and SKi-II but not by JTE-013. These results suggest that SK1 plays an important role in angiogenesis in VHL- deficient ccRCC cells that is mediated by S1P/S1PR1/3.

A.4. DISCUSSION

In the present study, a novel role of SK1/S1P-induced invasion and angiogenesis of 786-0 ccRCC cells has been identified. First, the data showed that lack of functional VHL in 786-0 ccRCC cells results in higher SK1 expression at both the protein and message level, as well as higher S1P levels, which seem to be HIF-2a dependent. Moreover, S1P treatment of SK1 knockdown cells, which exhibited a less invasive phenotype, resulted in S1PR2-mediated phosphorylation of FAK and invasion. Moreover, down regulation of SK1 was also associated with less angiogenesis in vivo that appears to be mediated by S1PR1/3. These findings suggest that higher S1P levels in VHL-defective ccRCC could induce invasion and angiogenesis. Together, these results have important implications for the role of the SK1/S1P pathway in the invasion and angiogenesis of ccRCC, which has not been addressed previously.

SK1 has been suggested as a potential therapeutic target as its expression is increased in many cancer types. Previous studies suggested that it plays important roles in proliferation, angiogenesis, survival, and invasion of tumor cells [99, 316]. However, its role in ccRCC has not been addressed previously. Therefore, we aimed to study the potential role of SK1 in renal carcinoma. We showed that VHL-defective ccRCC cells showed higher SK1 and S1P levels that seem to be HIF-2a dependent. These results support the previously reported findings by our group that HIF-2a binds to the SK1 promoter, inducing its over-expression during hypoxia in glioma cells [290]. We also demonstrated that SK1 is required for activation of FAK through S1P/S1PR2. FAK is a nonreceptor tyrosine kinase that has been reported to modulate cell migration and invasion [307]. Several previous reports have shown that FAK is overexpressed in different tumors such as gastrointestinal and breast cancer and correlated with tumor progression and malignancy [317, 318]. Increased FAK activity has been shown previously to be associated with malignancy in different types of cancer cells, suggesting that FAK could play an important role in cancer progression and metastasis [319]. Likewise, high pFAK abundance was recently reported to be associated with distant and lymph node metastases in serous ovarian cancer [320]. In the mouse model of pancreatic cancer, inhibition of FAK phosphorylation reduced tumor growth, invasion, and metastasis [321]. Moreover, suppression of FAK signaling prevented the metastasis of human colon cancer cells [322]. Recently, FAK inhibition has been reported to abrogate the invasion of aggressive pediatric renal tumor [323], suggesting that FAK could play a role in invasion of kidney cancer. By studying S1P activation of FAK, we were able to implicate the S1P/S1PR2

pathway in an SK1-mediated invasive biology in ccRCC cells. We showed that SK1 is important for phosphorylation of FAK through a mechanism involving S1P and S1PR2. Previous studies have shown that S1P is able to induce FAK phosphorylation and motility of human endothelial cells [324, 325]. However, here we describe the mechanism by which such induction occurs and its implication in invasion biology. Targeting FAK phosphorylation directly by FAK-specific inhibitor or indirectly by SK inhibitor and S1PR2 antagonist significantly reduced the invasion of ccRCC cells, suggesting that SK1-induced FAK activation is important for promoting cellular invasion. Moreover, targeting S1PR1/3 by a specific antagonist also reduced the cellular invasion; however, that effect occurs through a FAK-independent mechanism. It was recently shown that S1PR1 and S1PR2 coordinately mediate S1P-induced migration through activation of different kinase pathways [326]. A link between SK1, FAK, and invasion has been described recently in colon cancer [327]. The authors showed that SK1 is involved in the regulation of FAK expression and invasion in colon cancer cells. However, our results clearly demonstrate that SK1 is only required for phosphorylation of FAK and has no effect on the expression of FAK.S1P has previously been shown to induce the invasion of MCF10A breast cancer cells [328]. Moreover, SK/S1P has been implicated in invasive behavior of glioma cells via S1PR2 and up-regulation of urokinase-type plasminogen activator [329]. S1PR2 has also recently been shown by our group to mediate epidermal growth factor-induced cellular invasion of HeLa cervical cancer cells [301]

There are multiple lines of evidence that highlight the role of S1P and S1PRs in the induction of cancer cell invasion and migration. However, many of the cancer-promoting roles of the SK/S1P pathway are mediated by S1P receptors other than S1PR2. SK1 has recently been shown to mediate the invasion of head and neck squamous cell carcinoma [330] and metastasis of hepatocellular carcinoma cells through S1PR1 [331]. Furthermore, S1PR3 has been reported to mediate invasion of MCF10A breast cancer cells [328]. In contrast, S1PR2 has been shown to prevent migration of hematopoietic stem cells [332] and invasion of cervical cancer cells [333]. However, other studies have provided evidence that S1PR2 has a cancer- promoting effect. S1PR2 has been shown to induce the invasion of glioma cells [334, 335] and to mediate EGF-induced invasion of cervical cancer cells (30). The findings presented in the current study provide additional evidence supporting the role of S1PRs in cancer cell invasion through S1P/S1PR2-mediated ac- tivation of FAK and a FAK-independent role of S1PR1/3. Angiogenesis is one of the hallmarks of ccRCC [312], and there is much evidence suggesting that both SK1 and S1P are involved in tumor angiogenesis [313-315]. Here we clearly demonstrated that angiogenesis observed in ccRCC is mediated by S1PR1/3. The role of S1P and S1PR in angiogenesis has been shown previously by other reports. S1P has been shown to promote angiogenesis in vivo using Matrigel plug assay [336] and to induce angiogenesis and lymphangiogenesis in mouse model of breast cancer metastasis [316]. The effect of S1P has been shown to be mediated by S1PR1 in vivo [315]and in vitro [290, 314]. A previous study by our group reported that the modulation of SK1 expression in glioma and breast cancer cells affected exogenous S1P levels that induce angiogenesis and lymphangiogenesis in vitro [314].

From our results presented herein, we propose that SK1-generated S1P could have autocrine and paracrine effects in ccRCC. The autocrine effect involves invasion that is mediated by 2 mechanisms: the first involves S1PR2- dependent FAK activation and the other one is S1PR1/3-mediated. Conversely, the paracrine effect involves S1P/ S1PR1/3-mediated angiogenesis.

In summary, our data indicate for the first time that SK1 is overexpressed and essential for cellular invasion and angiogenesis of ccRCC cells. Therefore, targeting SK1 could hinder the invasiveness and angiogenesis of ccRCC, thus resulting in improved survival rate of patients.